

Fall 2018

# EVALUATION OF CONTINUOUS, LOW-INTENSITY ULTRAVIOLET IRRADIATION FOR BIOFILM PREVENTION

Stephanie Conrad

Follow this and additional works at: [https://digitalcommons.mtech.edu/grad\\_rsch](https://digitalcommons.mtech.edu/grad_rsch)



Part of the [Environmental Engineering Commons](#)

---

## Recommended Citation

Conrad, Stephanie, "EVALUATION OF CONTINUOUS, LOW-INTENSITY ULTRAVIOLET IRRADIATION FOR BIOFILM PREVENTION" (2018). *Graduate Theses & Non-Theses*. 194.  
[https://digitalcommons.mtech.edu/grad\\_rsch/194](https://digitalcommons.mtech.edu/grad_rsch/194)

This Thesis is brought to you for free and open access by the Student Scholarship at Digital Commons @ Montana Tech. It has been accepted for inclusion in Graduate Theses & Non-Theses by an authorized administrator of Digital Commons @ Montana Tech. For more information, please contact [sjuskiewicz@mtech.edu](mailto:sjuskiewicz@mtech.edu).

# EVALUATION OF CONTINUOUS, LOW-INTENSITY ULTRAVIOLET IRRADIATION FOR BIOFILM PREVENTION

By  
Stephanie Conrad

A proposal submitted in partial fulfillment of the  
requirements for the degree of

Masters of Science in Environmental Engineering

Montana Technological University

2019



## Abstract

Biofilms occur when planktonic bacteria attach to a surface, forming a sticky, extracellular matrix that makes them difficult to remove. Biofilms are especially troublesome in water filtration membrane systems due to their strong adhesive properties. Once attached, biofilms cause a decrease in water production (biofouling) and an increase in membrane degradation. Traditional cleaning methods use harsh chemicals and require modules being taken offline, which reduces water production rates. Moreover, despite current cleaning efforts, irreversible biofouling inevitably leads to membrane module replacement. The implementation of low-intensity UV irradiation for biofilm prevention could decrease waste and increase production. However, while much is known about the effects of high-intensity UV on planktonic bacteria death, we know little about the impact of low-intensity UV on biofilm formation.

This study evaluated the effects of low-intensity UV on biofilm formation. To accomplish this task, this thesis also evaluated the effect of low-intensity UV irradiation on planktonic bacteria under stagnant growth conditions, identified a relevant disinfection kinetics model, and determined the effect of UV on bacterial motility.

This study investigated the model bacterium *E. coli* in three media: a newly designed medium referred to as HT medium (publishing pending by Clemson University), tryptic soy broth (TSB), and M9 minimal medium. Both M9 medium and TSB medium are commonly utilized in bacterial cultivation. HT medium is specially formulated to augment biofilm growth while minimizing UV absorbance encountered with TSB medium.

Overall, no statistically significant decrease in biofilm formation was observed under sub-lethal irradiation with UVC in the three media tested. For *E. coli* in HT medium, biofilm growth was only reduced at the highest, lethal applied dose ( $p = 0.001$ ). At all intensities studied (12.96 to 240.5 mJcm<sup>-2</sup>), biofilm growth in TSB ( $p \geq 0.989$ ) and M9 ( $p \geq 0.366$ ) was not significantly reduced.

It was observed, however, that low-intensity UVC irradiation may reduce bacterial motility. Swimming motility of *E. coli* was significantly reduced ( $p \leq 0.003$ ) at all intensities studied. Similarly, swarming motility was significantly reduced ( $p \leq 0.046$ ) at all intensities above 53.64 mJcm<sup>-2</sup>. Therefore, while sub-lethal irradiation by UVC may significantly reduce swimming and swarming motility in *E. coli*, there was no evidence that biofilm formation is significantly affected.

Keywords: Ultraviolet Irradiation, Biofilm prevention, *E. coli*, Swimming Motility, Swarming Motility

## Dedication

For Donna and Paul Conrad who have supported me in innumerable ways the last two years. For Curtis and Maddie Conrad, Brenna Andrews, and the rest of the Clan all of whom have been an endless support system and source of great laughs. For Hans, Mort, and Sarah, who were always there to snuggle through the good and bad days. Lastly, to my grandma, Ruth Ann Frederick, the most un-ironically excited and all-around amazing person I have had the pleasure of knowing. I strive to be even half as remarkable as you were.

## Acknowledgements

First and foremost, I'd like to thank my primary advisor Dr. Katherine Zodrow and my secondary advisor Dr. Daqian "D.J." Jiang. I'd also like to thank the rest of my committee, Dr. Joel Graff and Dr. Akua Oppong-Anane. To Dr. Ezra Cates and Hamed Torkzadeh thank you both for providing the recipe for HT medium and lending us your radiometer. To Jeanne Larson, who has been a tremendous resource both in and out of the lab thank you for all the supplies and kind words. To my great-grandfather, Wilfred Conrad, whose in-depth study of the distillation process paved the way for me to achieve a B.S. in Chemical Engineering.

Finally, I would like to thank a man, who though I have read all of his published works will never read mine. Thank you for your fearless honesty about pursuing your dreams in spite of your anxiety and OCD. Your works have helped me get through the darkest days of university. After all "We need never be hopeless because we can never be irreparably broken."-John Green

## Table of Contents

<b>ABSTRACT .....</b>	<b>II</b>
<b>DEDICATION .....</b>	<b>III</b>
<b>ACKNOWLEDGEMENTS .....</b>	<b>IV</b>
<b>LIST OF FIGURES.....</b>	<b>VII</b>
<b>LIST OF TABLES.....</b>	<b>XIII</b>
<b>LIST OF EQUATIONS .....</b>	<b>XIV</b>
 1. OVERVIEW .....	 1
2. BACKGROUND.....	5
2.1. <i>Membrane and Reverse Osmosis Systems</i> .....	5
2.2. <i>Biofouling and Biofilms</i> .....	7
2.3. <i>Mechanism of Biofilm Formation</i> .....	8
2.4. <i>UV for Disinfection and Biofilm Prevention</i> .....	10
3. RESEARCH HYPOTHESIS.....	14
3.1. <i>There is a Critical, Non-Lethal Dose for Prevention of Biofilm Attachment.</i> .....	14
3.2. <i>Non-Lethal UV Irradiation Prevents Biofilm Formation by Suppressing Motility</i> .....	14
4. MATERIALS AND METHODS .....	17
4.1. <i>Experimental Apparatus</i> .....	17
4.2. <i>Bacterial Cultivation and Culture Preparation</i> .....	19
4.3. <i>Ultraviolet Irradiation</i> .....	21
4.4. <i>Planktonic Death UV model</i> .....	21
4.5. <i>Biofilm Formation and Bacterial Growth</i> .....	22
4.6. <i>Motility Assays</i> .....	22
4.6.1. <i>Swimming Motility</i> .....	23

4.6.2.	Swarming Motility .....	24
4.6.3.	Twitching Motility .....	25
4.7.	<i>Statistical Analysis</i> .....	26
5.	RESULTS AND DISCUSSION .....	27
5.1.	<i>Apparatus Verification</i> .....	27
5.2.	<i>Planktonic Death</i> .....	30
5.2.1.	Log Removal .....	30
5.2.1.	Chick-Watson Model .....	35
5.3.	<i>Bacterial Replication Results</i> .....	39
5.4.	<i>Biofilm Formation</i> .....	46
5.5.	<i>Motility Analysis</i> .....	50
5.5.1.	Swimming Motility .....	50
5.5.2.	Swarming Motility .....	51
6.	FUTURE WORK AND RECOMMENDATIONS .....	54
7.	CONCLUSIONS.....	56
8.	BIBLIOGRAPHY .....	60
9.	APPENDIX A – BIOFILM GROWTH ANOVA CODE .....	70
10.	APPENDIX B- BACTERIAL GROWTH ANOVA CODE.....	76
11.	APPENDIX C- SWIM PLATE ANOVA CODE .....	89
12.	APPENDIX D- SWARM PLATE ANOVA CODE .....	92
13.	APPENDIX E- AVERAGE AND STANDARD DEVIATION USED FOR NORMALIZATION.....	95
13.1.	<i>E.1- Bacterial Growth</i> .....	95
13.2.	<i>E.2- Biofilm Growth</i> .....	96
13.3.	<i>E.3-Swimming Motility</i> .....	96
13.4.	<i>E.4-Swarming Motility</i> .....	97

## List of Figures

Figure 1: Overview of membrane and reverse osmosis filtration including the types of materials that are retained and pass through the membrane [21]. Figure courtesy of Dr. Katherine Zodrow.....	5
Figure 2: Removal mechanisms in membrane filtration [14] .....	7
Figure 3: Biofilms formed by <i>B. subtilis</i> showing EPS channels used to convey nutrients, water, and waste.....	8
Figure 4: Biofilm attachment, maturation, and dispersion. Top row, from left to right: the attachment of a protobiofilm [30], the attachment of planktonic bacteria [25], and the attachment of polymers, colloids, and planktonic bacteria to a conditioning film [21]. .....	9
Figure 5: Preliminary testing using <i>B. subtilis</i> in 1:1000 TSB. Complete death occurred at 4.5 mJcm <sup>-2</sup> which corresponds to 30 seconds of irradiation .....	18
Figure 6: Final iteration of the experimental apparatus.....	19
Figure 7: <i>E. coli</i> -K12 growth curve in TSB. Absorbance was measured at a wavelength of 600 nm. ....	20
Figure 8: Example of an image taken for a dark control swim plate result where the white circles are the area of disturbance. ....	24
Figure 9: Example of an image taken for a dark control swarm plate result where the white circles are the area of disturbance.....	25
Figure 10: Variation of intensity as a function of both height and filter usage. Height was varied using a chemical stand and a clamp. Filters were Safeway brand white paper coffee	



filters. Standard deviation does not exist for these test as replicates were not conducted.	
.....	27
Figure 11: Evaluation of the inverse squares law in correlation to the experimental apparatus.	
Intensity decreases with the inverse square of the height. ....	28
Figure 12: Intensity displays little variation across the irradiation area. Each box represents a	
3.39 cm high and 4.06 cm wide sample area. Irradiation was measured at the center of	
each box. ....	29
Figure 13: Consistent intensity over 24 hours. Both tests occurred at 33 cm above the collimator	
and with a coffee filter in place. The first test was conducted with the light source	
pointed directly down while the second test was conducted with the light source pointed	
to the right side.....	30
Figure 14: Log removal of <i>E. coli</i> as a function of UVC dose in HT medium. The dotted line	
shows a linear least squares regression. Starting <i>E. coli</i> concentration was $4.73 \pm 2.73 \times$	
$10^8$ CFU/mL <sup>-1</sup> , and bacteria were irradiated at the appropriate intensity for 24 hr.	31
Figure 15: Log removal of <i>E. coli</i> as a function of UVC dose in TSB medium. The dotted line	
shows a linear least squares regression. Starting <i>E. coli</i> concentration was $1.77 \pm 0.427 \times$	
$10^9$ CFU/mL <sup>-1</sup> , and bacteria were irradiated at the appropriate intensity for 24 hr.	32
Figure 16: Log removal of <i>E. coli</i> as a function of UVC dose in M9 medium. The dotted line	
shows a linear least squares regression. Starting <i>E. coli</i> concentration was $1.33 \pm 0.326 \times$	
$10^8$ CFU/mL <sup>-1</sup> , and bacteria were irradiated at the appropriate intensity for 24 hr.	33
Figure 17: Log removal of <i>E. coli</i> as a function of UVC dose in all three media. Dotted lines	
show linear least squares regressions. This figure is a combination of Figures 14-16.	
.....	34

Figure 18: Wavelength scan for the three media evaluated during experimentation. Absorbance was measured at 50 nm intervals between 200 and 650 nm with DI water as a blank. The red line represents a wavelength of 254 nm, or biocidal UV.....35

Figure 19: Removal of *E. coli* as a function of UVC dose in HT medium fit to the Chick-Watson model. The dotted line shows a linear least squares regression. Starting *E. coli* concentration was  $4.73 \pm 2.73 \times 10^8$  CFU/mL<sup>-1</sup>, and bacteria were irradiated at the appropriate intensity for 24 hr.....36

Figure 20: Log removal of *E. coli* as a function of UVC dose in TSB medium. The dotted line shows a linear least squares regression. Starting *E. coli* concentration was  $1.77 \pm 0.427 \times 10^9$  CFU/mL<sup>-1</sup>, and bacteria were irradiated at the appropriate intensity for 24 hr.37

Figure 21: Log removal of *E. coli* as a function of UVC dose in M9 medium. The dotted line shows a linear least squares regression. Starting *E. coli* concentration was  $1.33 \pm 0.326 \times 10^8$  CFU/mL<sup>-1</sup>, and bacteria were irradiated at the appropriate intensity for 24 hr.38

Figure 22: Log removal of *E. coli* as a function of UVC dose in all media. The dotted line shows a linear least squares regression. This figure is a combination of Figures 19-21. .39

Figure 26: Normalized Bacterial Growth as a function of dose for irradiated *E. coli* grown in HT medium. A starting *E. coli* concentration of  $4.73 \pm 2.37 \times 10^8$  CFU/mL<sup>-1</sup> was used, and bacterial growth was calculated from an OD<sub>620</sub> measurement. A normalized value of 1.0 represents zero growth difference between irradiated and dark, and bacteria were irradiated for 24 hr. ....41

Figure 27: Normalized Bacterial Growth as a function of dose for irradiated *E. coli* grown in TSB medium. A starting *E. coli* concentration of  $1.77 \pm 0.427 \times 10^9$  CFU/mL<sup>-1</sup> was used, and bacterial growth was calculated from an OD<sub>620</sub> measurement. Irradiated values were

normalized to the dark controls for the same experiment, and bacteria were irradiated for 24 hr. ....42

Figure 28: Normalized Bacterial Growth as a function of dose for irradiated *E. coli* grown in M9 medium. A starting *E. coli* concentration of  $1.33 \pm 0.326 \times 10^8$  CFU mL<sup>-1</sup> was used, and bacterial growth was calculated from an OD<sub>620</sub> measurement. A normalized value of 1.0 represents zero growth difference between irradiated and dark, and bacteria were irradiated for 24 hr. ....43

Figure 29: Normalized Bacterial Growth as a function of dose for irradiated *E. coli* grown in all media. A starting *E. coli* concentrations of  $4.73 \pm 0.237 \times 10^8$ ,  $1.77 \pm 0.427 \times 10^9$ , and  $1.33 \pm 0.326 \times 10^8$  CFU mL<sup>-1</sup> were used for HT, TSB, and M9 media respectively. Bacterial growth was calculated from an OD<sub>620</sub> measurement. A normalized value of 1.0 represents zero growth difference between irradiated and dark, and bacteria were irradiated for 24 hr. ....44

Figure 30: Normalized Bacterial Growth as a function of dose for irradiated *E. coli* grown in all media. ....45

Figure 31: Normalized biofilm growth as a function of dose for irradiated *E. coli* grown in HT medium. A starting *E. coli* concentration of  $4.73 \pm 2.37 \times 10^8$  CFU mL<sup>-1</sup> was used, and biofilm growth was quantified using a safranin stain read at 450 nm. A normalized value of 1.0 represents zero growth difference between irradiated and dark, and bacteria were irradiated for 24 hr. ....46

Figure 32: Normalized biofilm growth as a function of dose for irradiated *E. coli* grown in TSB medium. A starting *E. coli* concentration of  $1.77 \pm 0.427 \times 10^9$  CFU mL<sup>-1</sup> was used, and biofilm growth was quantified using a safranin stain read at 450 nm. A normalized value

of 1.0 represents zero growth difference between irradiated and dark, and bacteria were irradiated for 24 hr. ....47

Figure 33: Normalized Biofilm Growth as a function of dose for irradiated *E. coli* grown in M9 medium. A starting *E. coli* concentration of  $1.33 \pm 0.326 \times 10^9$  CFU mL<sup>-1</sup> was used, and biofilm growth was quantified using a safranin stain read at 450 nm. A normalized value of 1.0 represents zero growth difference between irradiated and dark, and bacteria were irradiated for 24 hr. ....48

Figure 34: Normalized biofilm growth as a function of dose for irradiated *E. coli* grown in all media. Starting *E. coli* concentrations of  $4.73 \pm 0.237 \times 10^8$ ,  $1.77 \pm 0.427 \times 10^9$ , and  $1.33 \pm 0.326 \times 10^8$  CFU mL<sup>-1</sup> were used for HT, TSB, and M9 media respectively. Biofilm growth was quantified using a safranin stain read at 450 nm. A normalized value of 1.0 represents zero growth difference between irradiated and dark controls, and bacteria were irradiated for 24 hr. This Figure is a combination of Figures 31 to 33. ....49

Figure 35: Normalized Biofilm Growth as a function of dose for irradiated *E. coli* grown in all media. Dotted lines represent linear regressions. Starting *E. coli* concentrations of  $4.73 \pm 0.237 \times 10^8$ ,  $1.77 \pm 0.427 \times 10^9$ , and  $1.33 \pm 0.326 \times 10^8$  CFU mL<sup>-1</sup> were used for HT, TSB, and M9 media respectively. Biofilm growth was quantified using a safranin stain read at 450 nm. A normalized value of 1.0 represents zero growth difference between irradiated and dark, and bacteria were irradiated for 24 hr. ....50

Figure 36: Normalized swim plate growth area results for *E. coli*. (1% tryptone, 0.5% NaCl, and 0.3% agar). Irradiation occurred over 24 hr. Error bars represent the combined standard error of the dark and irradiated values. ....51

Figure 37: Normalized swarm plate growth area results for <i>E. coli</i> (0.5% agar, 8 g/L nutrient broth, and 8 g/L dextrose). Irradiation occurred over 48 hr.....	52
----------------------------------------------------------------------------------------------------------------------------------------------------------------------	----

## List of Tables

Table I: Averages and standard deviations for bacterial growth normalization. ....	95
Table II: Averages and standard deviations for biofilm growth normalization.....	96
Table III: Averages and standard deviations for swimming motility normalization. ....	96
Table IV: Averages and standard deviations for swarming motility normalization. ....	97

## List of Equations

Equation 1: Applied Biocide Dose Equation: .....	12
Equation 2: Chick-Watson Disinfection Model.....	12
Equation 3: Log Removal Equation.....	12
Equation 4: Rennecker-Mariñas Disinfection Model .....	12

## 1. Overview

The exponential growth of the world's population in the last 200 years [1] has strained freshwater resources. Today, it is estimated that approximately 66% of the global population endure severe water scarcity at least one month every year [2], and the situation is only expected to worsen. For example, in late 2017, 3.81 million residents [3] of Cape Town, South Africa were limited to a water usage rate of 6.6 gallons of water per day due to a projected complete water outage by February 2018 [4]. As a comparison, the United States Environmental Protection Agency estimates that the average American family utilizes 300 gallons of water a day [5]. Of those 300 gallons, almost 45% percent (135 gallons per day) used for showering and flushing toilets. In fact, flushing a standard toilet just four times uses 6.4 gallons of water, nearly the same volume that Cape Town residents were allotted per day. By reducing water usage and receiving much-needed precipitation, the city never ran out of water and is in the process of building a seawater desalination plant [4].

Desalination, or the conversion saltwater into freshwater, is a promising solution for today's water crisis because seawater is the most abundant water source on earth, making up 96.5% of earth's total available water. Saltwater is 88.9 times more abundant than freshwater [6] and 1.3 million times the current global freshwater demand [7]. Desalination can either be performed by thermal separation such as distillation or physical separation such as reverse osmosis [8].

Reverse osmosis (RO) is a promising desalination technology [9]. Accounting for 66% of the online capacity, RO removes salt from water by applying pressure to a semi-permeable membrane. The applied pressure works to overcome osmotic pressure and drive a separation between clean water and a concentrated salt solution, or brine. RO is particularly reliable and



scalable technology for desalination. For instance, Tampa Bay, Florida has an RO system that produces 25 million gallons of drinking water per day [10]. Similarly, a plant in Algiers, Algeria was completed in 2016 that produces 53 million gallons of clean water per day [9]. Additionally, Israel acquires half of all their drinking water by desalination [11].

Despite the apparent advantages of RO technology, operational detriments exist making a new operating approach essential. One such issue is biofouling, or the formation of biofilms on a membrane surface [12]. While biofilms are helpful in wastewater treatment and mammalian digestion, excessive biofilm formation is particularly troublesome in membrane operations for multiple reasons. First, biofouling decreases system productivity as it increases energy use. Second, biofouling leads to accelerated membrane degradation, as biofilms produce acids that degrade membrane surfaces. Additionally, biofilms are extremely difficult to remove [12], and they can self-replicate. Therefore, a single bacterium surviving a physical or chemical pre-treatment can cause biofouling [12].

Within membrane systems specifically, the sticky extracellular polymeric substance (EPS) produced by bacteria prevents penetration of biocides, causes biofilms to be difficult to remove, and contributes to irreversible fouling [14] [15]. One traditional foulant removal technique is physical cleaning. Physical cleaning on micro-and ultrafiltration membranes normally occurs in the form of backwashing whereby clean water is pushed backwards through the membrane, dislodging loosely adhered material [16]. Chemical cleaning is also utilized for foulant removal. Chemical cleaning occurs when a chemical agent, such as chlorine, is used to break down materials not removed during backwashing [16] [15]. Due to the nature of reverse osmosis membranes, they can be neither backwashed nor cleaned with chlorine, therefore turbulence is the primary physical cleaning method [15]. Chemical cleaning in RO systems is

done using surfactants and ethylenediaminetetraacetic acid (EDTA). Traditional cleaning methods, however, are inefficient as they tend to waste clean process water and create an abundance of chemicals that are released to the environment [14]. In addition to cleaning mechanisms, antifouling methods can be utilized including the addition of biocides into influent water to reduce bacteria concentration. Not all bacteria are susceptible to the same biocides, however, and chemical additions can be costly or lead to membrane destruction [15]. Therefore it is desired to identify an innovative biofilm prevention method that reduces chemical use.

Recently, researchers have focused on biofilm prevention instead of cleaning. While high-intensity ultraviolet (UV) light may damage the polyamide layer on the RO membrane, it may not be as susceptible to low-intensity UV. In the proposed process, UV irradiation of the membrane surface would occur at a low intensity for an extended time. Traditional UV irradiation, which is used in water treatment, wastewater treatment, and meat sterilization [17], operates at a high intensity for a short time. Because UV sterilization is commonly used, the efficacy of lethal dosages of ultraviolet irradiation for inactivation of planktonic bacteria has been widely studied. By applying low-intensity UV, less energy, and therefore less cost, is associated with this method. Additionally, with emerging technology such as up-conversion phosphors [18], membranes could have a coating that produces biocidal UV upon irradiation with direct sunlight.

Currently, there are significant knowledge gaps surrounding the application of low-intensity UV as a biofilm prevention technique, including the mechanisms by which UV influences bacterial motility. This thesis addresses these knowledge gaps by 1) verifying a quantitative model that predicts the intensity of a lethal dose of UV, 2) evaluating the hypothesis that low-intensity UV suppresses biofilm formation, and 3) determining if UV suppresses of

bacterial motility. A custom-built apparatus was made to qualitatively analyze the effect of low-intensity UV on *Escherichia coli* biofilm formation and motility.

## 2. Background

### 2.1. Membrane and Reverse Osmosis Systems

Membrane filtration became a relevant technology in the United States as recently as the 1990s [18]. The Safe Drinking Water Act in the United States mandated that all surface water be treated using a filtration treatment system to remove coliform bacteria and control other parameters [20]. The first American membrane water treatment plant was built in California in 1993 [18], and new plants continue to be built.

Membrane filtration removes suspended materials—including particles and microbes—by size selection, a process where water and particles less than a certain diameter pass through pores into the permeate stream while larger particles are trapped in the retentate or concentrate stream. Membrane technologies are classified into four types based on the size of particles they remove: microfiltration, ultrafiltration, nanofiltration, and reverse osmosis (Figure 1).

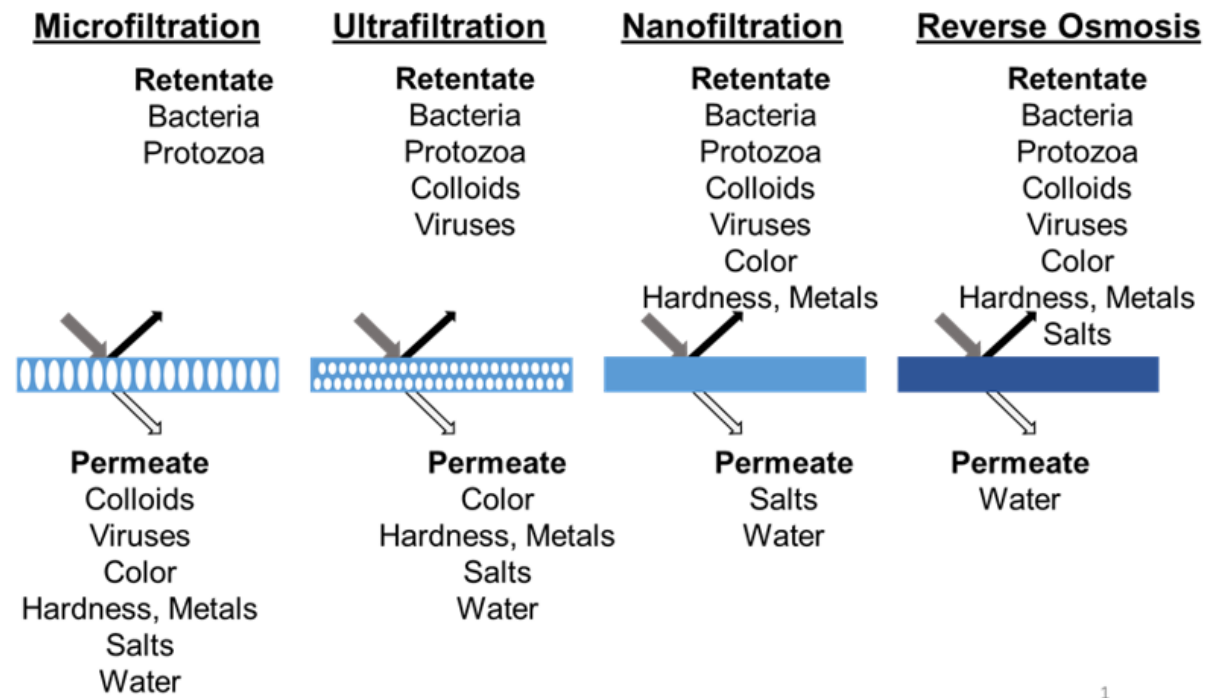


Figure 1: Overview of membrane and reverse osmosis filtration including the types of materials that are retained and pass through the membrane [21]. Figure courtesy of Dr. Katherine Zodrow.

Microfiltration has the largest pore sizes and removes larger particles such as suspended solids and most living organisms, including protozoa and bacteria. Ultrafiltration operates with the second largest pore sizes and removes small colloids and viruses, and nanofiltration removes most divalent salts. Non-porous reverse osmosis membranes are the most restrictive membrane type, and they remove monovalent salts, such as sodium chloride. As membrane pore size decreases, particles that are removed by membranes with larger pores are also removed. For example, nanofiltration removes large molecules, suspended solids, and small colloids. While membranes with smaller pores remove the largest variety of contaminants, these membranes also require higher pressures and yield a lower recovery. Recovery is the percent of the feed water that is recovered as treated permeate [14]. When treating fresh surface water, microfiltration and ultrafiltration are used most often, as they can remove surface water contaminants of concern, such as suspended solids, bacteria, and protozoa. Nanofiltration and reverse osmosis, however, are most useful for softening well water and desalinating saltwater.

In porous membrane filtration, removal of particles occurs by one of three mechanisms (Figure 2). Particles can be strained when they are removed by the pores at the membrane surface, adsorbed when they stick to the pore wall, or removed by cake filtration. In cake filtration, large particles form a layer over the membrane that traps smaller particles that would otherwise pass through the membrane.

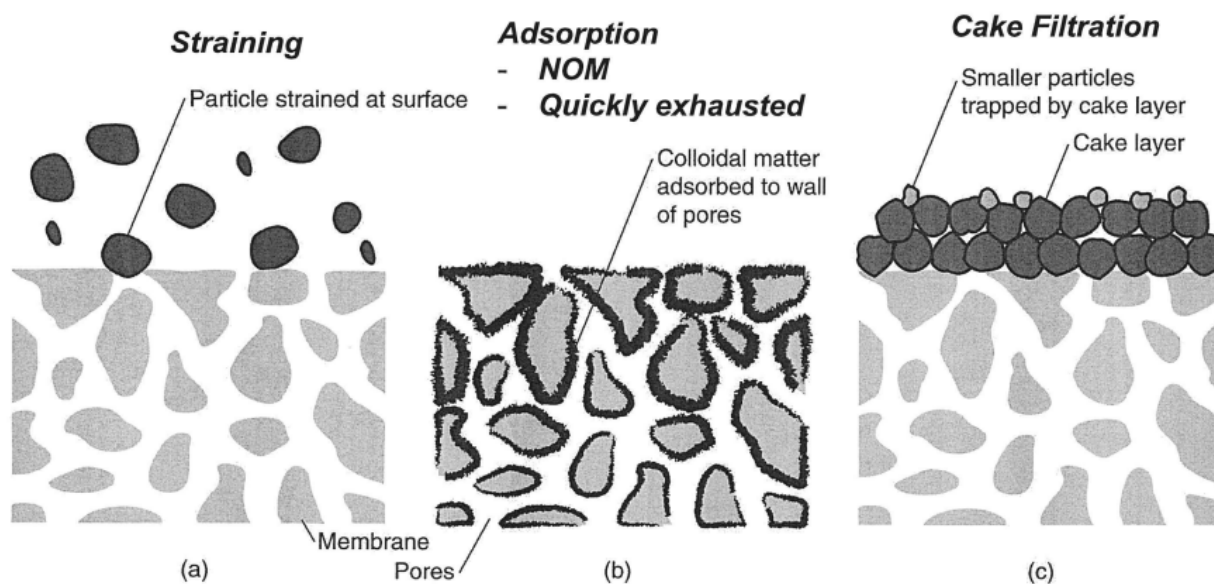


Figure 2: Removal mechanisms in membrane filtration [14]

## 2.2. Biofouling and Biofilms

In membrane technologies, fouling is categorized by a 15-30% pressure drop across the membrane or a 10% decrease in flux at constant temperature and pressure [21] [22]. Fouling leads to decreased productivity, increased energy consumption, and ultimately membrane degradation and replacement [15].

Biofouling is fouling due to bacterial growth on the membrane. Most commonly, biofouling occurs due to biofilms [12] and is known to contribute to at least 45% of membrane fouling [15]. Biofouling occurs almost under any conditions, e.g., high dissolved organic carbon, [15] and very low calcium concentrations [22].

Biofilms are scientifically described as communities of bacteria, surrounded by sticky extracellular polymeric substances, or EPS [24] [25]. EPS is a complex substance composed of polysaccharides, proteins, humic substances, and nucleic acids [26]. EPS protects bacteria from bactericides, aids in surface attachment, and forms hollow channels. These channels convey

water, nutrients, and waste throughout the system [24]. Figure 3 shows a *Bacillus subtilis* biofilm formed on an agar plate where hollow channels formed from the EPS are clearly visible.



**Figure 3: Biofilms formed by *B. subtilis* showing EPS channels used to convey nutrients, water, and waste.**

### **2.3. Mechanism of Biofilm Formation**

A key step in biofilm formation is initial bacterial/biofilm attachment. Initial biofilm attachment occurs by any of three methods, (Figure 4). The first method occurs when a conditioning film forms on the surface, altering the physical-chemical interactions between the bacteria and the surface [21]. These interactions include surface charge, hydrophobicity, and other bacterium-specific characteristics [26]. For example, a lithophilic conditioning film containing both hydrophobic and hydrophilic sites can increase bacterial attachment to hydrophilic surfaces [15]. These films may also augment attachment by increasing surface roughness. The increased surface roughness is caused by micro-scale cavities or other low-turbulence zones where bacteria can more easily attach without being affected water flow or other washing mechanisms [28] [22]. Avila *et al.* estimated that a surface threshold roughness of  $0.2\ \mu\text{m}$  can augment initial biofilm attachment while an increase in surface roughness beyond

that is correlated with an exponential increase in bacterial accumulation at the surface [28]. It is important to note, however, that some surface patterns can decrease biofilm attachment, such as sharkskin which utilizes a protruding micro-patterned surface to reduce bacterial attachment [28]. Conditioning films also allow for attachment of polymers, colloids, and planktonic bacteria, which eventually mature into a biofilm [30].

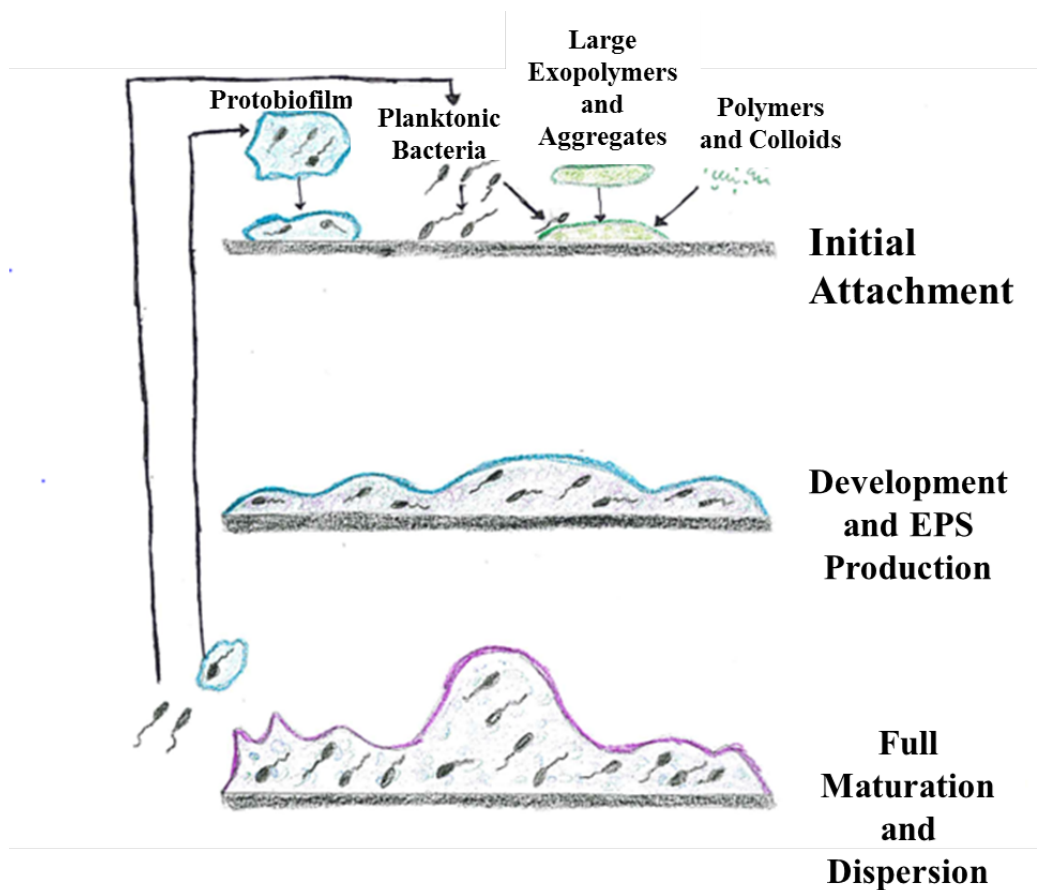


**Figure 4: Biofilm attachment, maturation, and dispersion. Top row, from left to right: the attachment of a protobiofilm [30], the attachment of planktonic bacteria [25], and the attachment of polymers, colloids, and planktonic bacteria to a conditioning film [21].**

The second method of attachment occurs when a biofilm precursor, or protobiofilm, attaches to a surface. Because the protobiofilm already contains EPS precursors, called transparent exopolymer particles (TEP), it allows for streamlined attachment and more rapid



biofilm maturation [30]. In addition, TEP acts in the same way as a conditioning film, allowing for easier attachment of additional bacteria [30]. The last attachment regime occurs when a single bacteria bacterium attaches to a surface and begins to grow, following the same maturation process [25].

Once attached, bacteria continue to grow and produce EPS [25]. This growth and EPS production continue until the biofilm thickens and matures [25]. Once matured, the biofilm enters a phase known as dispersion where it releases protobiofilms and planktonic bacteria back into the aqueous environment [25].

In membrane systems, fluid dynamics play a major role in initial interactions between both motile and non-motile bacteria and surfaces [30]. This is in part because elements designed to promote turbulent flow at the membrane surface create laminar flow conditions in other locations. In areas of laminar flow, bacteria and particles accumulate, allowing for more surface contact time [15]. Additionally, EPS at the membrane surface reduces turbulence, exacerbating bacterial attachment [15]. Finally, RO membranes reject nutrients, increasing nutrient concentration at the membrane surface, and encouraging motile bacteria to utilize chemotaxis to move towards the nutrients at the surface [30] [32]. Because motility is so important for bacterial attachment, this thesis will evaluate the effect UV has on motility.

## **2.4. UV for Disinfection and Biofilm Prevention**

Ultraviolet irradiation potentially offers an innovative way to prevent biofouling. UV light has wavelengths between 200 and 400 nm, and it can be further broken down into UVA, UVB, and UVC [33]. UVA has the longest wavelengths (315-400 nm) and is primarily responsible for dermal cancers in humans [33], while UVB (290-320 nm) contributes to epidermal cancers [33]. Naturally occurring UVC (100-280 nm) is absorbed within the

atmosphere [33], but artificial UVC is often used for disinfection purposes [18]. At 254 nm, biocidal UVC is the most effective for disinfection [18] [34]. Under UVB disinfection, the primary mode of action is DNA damage [34]. This damage occurs when UV causes dimerization of pyrimidines. Dimerization is an additive process where two identical compounds combine to create a new compound [32]. Pyrimidines are single ring bases in deoxyribose nucleic acid (DNA), cytosine and thymine [32]. Secondary modes of action include hormone inactivation, protein destruction, cellular membrane damage, and oxidative damage [34]. Once damaged, DNA cannot be transcribed, and daughter cells cannot be formed [36] or are unable to replicate [34]. In addition to damaging DNA, UV can also break down polysaccharides and cause oxidative injury [37].

While traditional UV disinfection is beneficial for reducing the number of colony forming units (CFU) in the feed water of membrane processes, it is not currently utilized for biofilm prevention at the membrane surface [15] nor does it have much effect on the EPS of established biofilm [38]. This minimal effect is most likely due to the nature of EPS, which adheres strongly to surfaces via Van der Waals forces, electrostatic forces, and chemical bonding with other polymers [15]. These processes are not easily interrupted by UV. Any damage occurs due to protein oxidation [26].

Disinfection kinetics were initially characterized by Dr. Harriet Chick and Herbert Watson, whose combined kinetic model, called the Chick-Watson model, is the simplest and most widely used disinfection kinetic model for UV disinfection [14]. By assuming a system under UV irradiation is modeled as a pseudo-first order reaction, a reaction that is linearly dependent on UV dose (Equation 1) in a completely mixed batch reactor (CMBR), Equation 2 was derived.

$$\text{Dose} = It \quad \text{Equation 1}$$

$$-k_c It = \ln\left(\frac{N}{N_o}\right) \quad \text{Equation 2}$$

Here,  $I$  is UV intensity in  $\text{mWcm}^{-2}$ ,  $t$  is irradiation time in seconds,  $N_o$  is the initial bacterial concentration ( $\text{CFUmL}^{-1}$ ),  $N$  is final concentration ( $\text{CFUmL}^{-1}$ ), and  $k_c$  is a reaction rate constant called the coefficient of specific lethality ( $\text{cm}^2\text{mJ}^{-1}$ ) [14]. Literature reports that *E. coli* have a  $k_c$  of  $8.3\text{cm}^2\text{mJ}^{-1}$  for high-intensity UV disinfection [14].

Disinfection is commonly characterized using a log removal value (LRV). The LRV allows for the quantification of logarithmic changes in CFU, a count of active bacteria in a culture (Equation 3).

$$\text{LRV} = -\log\left(\frac{N}{N_o}\right) \quad \text{Equation 3}$$

Where all variables have previously been defined.

In theory, the same LRV is achieved at the same applied dose even if the intensity and time are not the same. Therefore, low-intensity UV could be applied for a long time to achieve the same applied dose as a high-intensity for a short period of time.

In some cases, low doses of a disinfectant have no effect on bacterial viability. This led to the development of the Rennecker-Mariñas disinfection model (Equation 4) [14]. The Rennecker-Mariñas model assumes that once this minimum dose ( $b$ ) is achieved, disinfection follows first-order kinetics according to the Chick-Watson model, described below.

$$\text{For } It < b \quad 0 = \ln\left(\frac{N}{N_o}\right) \quad \text{Equation 4}$$

$$It > b \qquad -k_c(It - b) = \ln\left(\frac{N}{N_o}\right)$$

Where all variables have previously been defined.

While traditional UV disinfection can reduce suspended (or planktonic) bacteria in the feed water of membrane processes, it is not currently utilized for biofilm prevention at the membrane surface [15]. While little is known about the effect of UV on biofilm formation, it is known that UV has minimal effect on the EPS of established biofilm [38]. This is most likely due to the nature of EPS, which adheres strongly to surfaces via Van der Waals forces, electrostatic forces, and chemical bonding with other polymers [15]. These processes are not easily interrupted by UV, although some damage could occur due to oxidative degradation [26].

The EPS of established biofilms provides several protective measures against UV. For instance, physical protection occurs when EPS absorbs UV that would otherwise splice bacterial DNA [37]. The bacteria within the film have also developed protection methods including the emission of free radicals that intercept UV, usage of motility to avoid UV (phototaxis), and the use of quorum sensing [37]. While the extent of UV-induced protein and polysaccharide degradation depends on the type of bacteria [37] [26], it is postulated that with time, biofilms can repair themselves after irradiation has ended [37] [26]. Even with a UV dose of  $86.4 \text{ kJcm}^{-2}$ , biofilms are still able to recover [26]. Because it is difficult to remove established biofilms using UV, it is better to prevent biofilms from growing in the first place. If UV could be supplied at a sufficient dose to cause non-lethal oxidative injury to bacteria, then UV could potentially reduce both the initial attachment and further development of biofilms.

### 3. Research Hypothesis

This research was designed to validate two hypotheses:

#### 3.1. There is a Critical, Non-Lethal Dose for Prevention of Biofilm Attachment.

Previously, most studies focused on bacterial inactivation with high-intensity UV. For example, Tingpej *et al.* [13] found that 20 minutes of irradiation under a biosafety cabinet UV light (intensity not reported) killed both planktonic and biofilm-associated *E. coli* [13] Redman *et al.* [39], who studied the effect of UV on slime-forming bacteria, found that a minimum dose of  $45 \text{ mJcm}^{-2}$  reduced the concentration of bacteria in raw water to less than 1500 CFU per 1 mL (no starting concentration given). Cates *et al.* [18] found that *B. subtilis* spores experienced a 90% reduction in viability after a UVC applied dose of  $12 \text{ mJcm}^{-2}$ . Zenoff *et al.* [40] discovered that for four different bacterial strains, a 50% or higher reduction was experienced after an applied UVB dose of  $393 \text{ mJcm}^{-2}$ .

This study hypothesized that a critical, or minimum dose of UV needed to prevent biofilm attachment to a surface without killing bacteria exists. If this hypothesis is found to be valid, then low-intensity UVC could be applied at an infinite time throughout a system to prevent biofouling. Within membrane systems, this application would decrease waste, both freshwater and chemical, and increase the production of freshwater.

#### 3.2. Non-Lethal UV Irradiation Prevents Biofilm Formation by Suppressing Motility

The effect of UV on motility is most often studied in correlation with the effect of increasing UVB in the atmosphere due to the depletion of the ozone layer [41]. In algae, flagellated species are more susceptible to the effects of UVB than non-motile species [41].

Flagellated algae species were also found to experience flagella loss at an applied dose of 0.6 kJm<sup>-2</sup> [41]. In addition, UVB damages flagella proteins [42].

Motility, including the categories of swimming, swarming, and twitching, is directly linked to biofilm formation under stagnant conditions [43]. By allowing bacteria to swim through a fluid, motility facilitates bacterial colonization, or initial reversible attachment [43]. Primarily, swimming motility in relation to biofilm formation occurs due to chemotaxis where bacteria are attracted to an increased concentration of nutrients [43]. In RO systems, nutrients are concentrated at the membrane surface because they are rejected by the membrane. Swarming and twitching motility, both of which are characterized as movement across a surface, aid in permanent attachment [43]. Because non-motile bacteria are limited in their interaction with the surface, they have more difficulty colonizing it [43]. Additionally, motility plays a role in biofilm architecture [43]. For example, *Aeromonas* species display major defects in biofilm architecture in mutations that are unable to perform swarming motility [43]. Non-flagellated mutants are also found to produce patchy biofilms [43]. However, bacterial adhesion to a surface is complicated under flow conditions, and less of a correlation between motility and adhesion exists because other factors play a role in bacterial colonization [43]. For example, under flow conditions, biofilm growth of *A. tumefaciens* is not possible unless chemotaxis is utilized [44]. Motility is commonly divided into three categories—swimming, swarming, and twitching.

Swimming motility occurs in aqueous environments where rotating flagella propels the bacteria forward [45] and is most likely to aid in initial surface interaction [45]. It was hypothesized that similar to previous research [17] [46], a reduction in swimming ability with increased irradiation doses would be found due in part to flagella motor damage.

Similar to swimming, swarming motility occurs due to flagella movement, however, while swimming occurs in a fluid, swarming occurs at a wetted surface [47]. Furthermore, it is a coordinated movement amongst a group of mobile bacteria and is believed to play a role in biofilm attachment [48]. Due to swimming and swarming motility utilizing the same mechanism of transport, the flagella, it is hypothesized that swimming and swarming effects under irradiation will be the same.

Unlike the two previous forms of motility, twitching is not performed by flagella. Instead, twitching is facilitated by small hair-like structures known as type IV pili [45]. Once a bacterium has made contact with a surface, pili extend and retract, [49] causing movement. Research suggests that type IV pili might aid in attachment to a surface [45]. Likewise, most motility studies have been conducted using high-intensity UV and focused solely on swimming motility [17] [46].

## 4. Materials and Methods

### 4.1. Experimental Apparatus

Prior to experimentation, an apparatus was built following the standard protocol for bench top UV irradiation [50]. The apparatus included a 0.305 (1 ft) collimator made of 10.14 cm (4 in) PVC painted black internally. The collimator absorbs any UV that is not pointed orthogonally to the sample surface [50]. The sample area of the apparatus was created by nailing together three 0.305 m<sup>2</sup> pieces of particle board and supporting them in the front with a 3.8 cm × 9 cm × 30 cm wood piece. The top of the apparatus was created by drilling a 10.14 cm hole in a 0.305 m<sup>2</sup> piece of particle board. Both the sample holding area, as well as the top of the apparatus, were attached with metal brackets. After the apparatus was created, an initial reading was taken with a radiometer, and it was determined that this apparatus produced an intensity of 0.150 mWcm<sup>-2</sup>.

Preliminary tests utilizing *B. subtilis* in 1:1000 TSB determined that complete death occurred after just 30 seconds (a dose of 4.500 mJcm<sup>-2</sup>) in this apparatus (Figure 5).



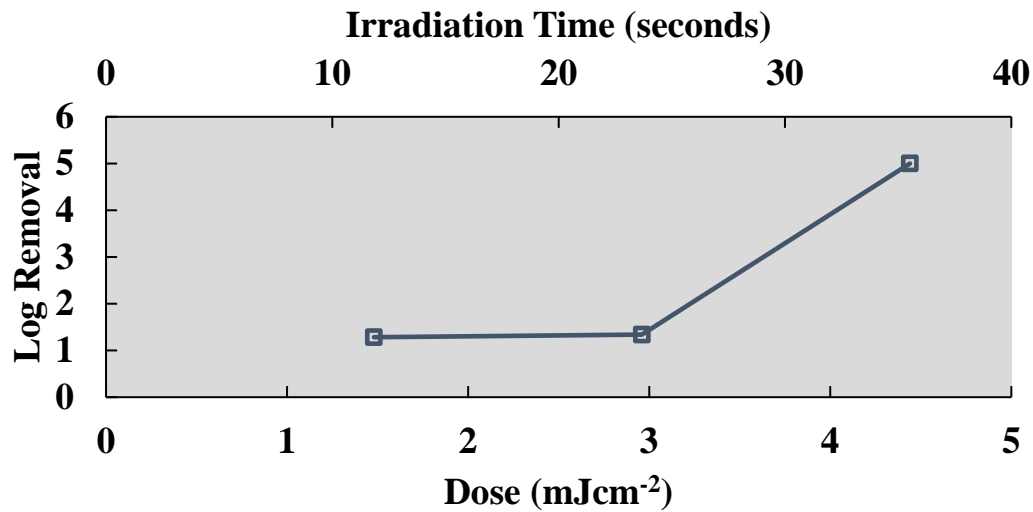


**Figure 5: Preliminary testing using *B. subtilis* in 1:1000 TSB. Complete death occurred at 4.5 mJcm<sup>-2</sup> which corresponds to 30 seconds of irradiation**

Because an irradiation time of 8 hours was desired, alterations were needed to enable low-intensity irradiation. A target intensity was determined by rearranging Equation 1 ( $\text{Dose} = \text{Intensity} \times \text{time}$ ) for intensity, estimating an 8-hour experiment, and setting dose equal to 4,500 mJcm<sup>-2</sup>. From this, it was determined that a target intensity of 0.156  $\mu\text{Wcm}^{-2}$  was required to facilitate low-intensity irradiation. Thus, the distance between the light and the top of the collimated beam was increased to four feet using a chemistry lab stand (Figure 6). The chemistry stand allowed for variation of height between the UVC source and the collimator, thus allowing for variation of intensity as a function of height. Ultimately, the added height resulted in an intensity of 2.36  $\mu\text{Wcm}^{-2}$ , which was still greater than the target intensity.

To further reduce intensity, several filter materials were tested including borosilicate glass, polypropylene plastic, and acrylic plastic. Eventually, a Safeway brand standard paper coffee filter (less than 1mm in thickness) was chosen to reduce intensity to 0.13  $\mu\text{Wcm}^{-2}$ .

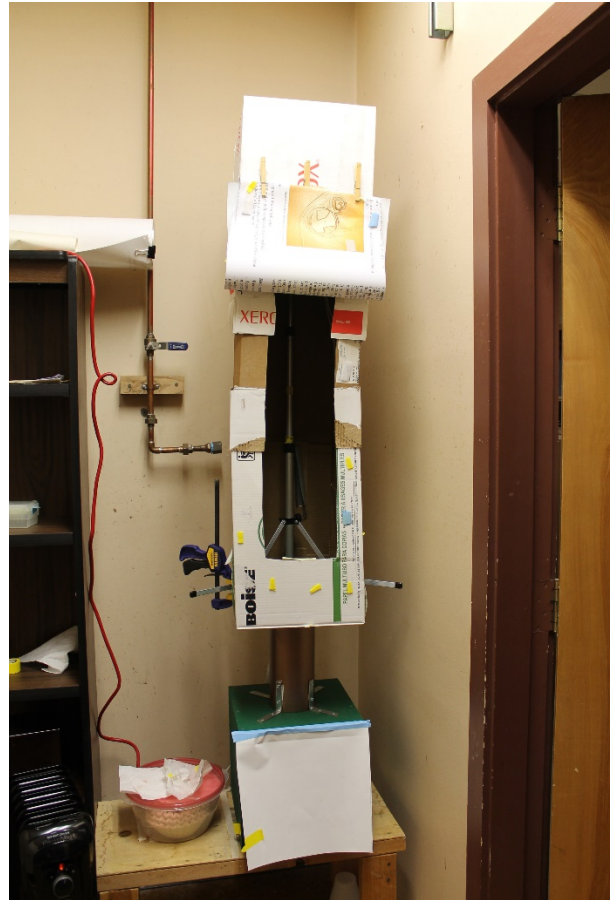
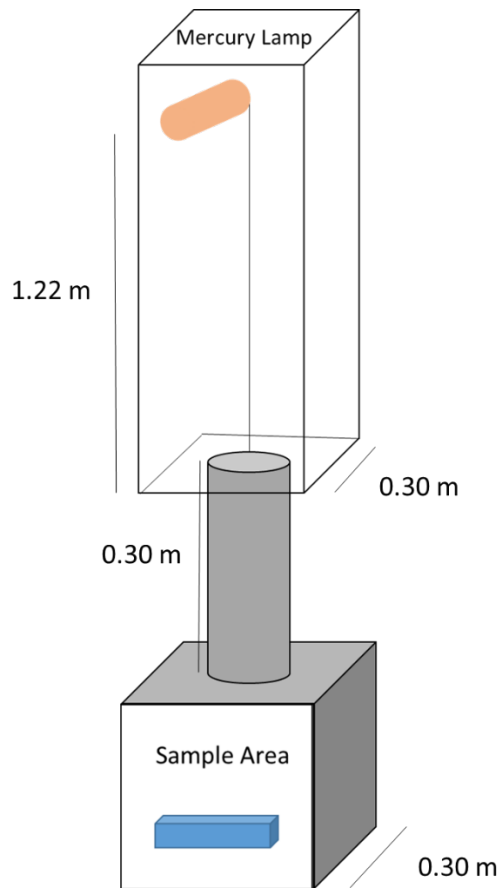


Figure 6: Final iteration of the experimental apparatus.

## 4.2. Bacterial Cultivation and Culture Preparation

The model bacteria *E. coli*, a facultative anaerobe [51], was studied. *E. coli* K-12 was kindly provided by Dr. Ezra Cates. Three media types were also used. The first was Tryptic Soy Broth (TSB) (Sigma-Aldrich) [51], a standard medium for bacterial growth. The second medium was M9 minimal medium (12.8 g  $\text{Na}_2\text{HPO}_4 \cdot 7\text{H}_2\text{O}$ , 3 g  $\text{KH}_2\text{PO}_4$ , 0.5 g  $\text{NaCl}$ , 1 g  $\text{NH}_4\text{Cl}$ , 10 mL 20% D-glucose solution, 1 mL 1.0 M  $\text{MgSO}_4$  solution, and 0.05 mL 1.0 M  $\text{CaCl}$  in 1 L deionized, DI, water) [25] which is also commonly used in microbiology as a medium that contains the minimum concentrations of nutrients necessary to facilitate bacterial growth. M9 medium is most similar to surface water. Finally, HT medium was utilized. HT medium was

specially formulated by Clemson University student Hamed Torkzadeh in order to promote biofilm growth without inhibiting UVC penetration [52].

Bacterial colonies were maintained on tryptic soy agar (TSA) (Sigma-Aldrich) plates. An overnight bacterial culture was created by inoculating 10 mL of TSB medium with a single colony and incubating at 37 °C for 12-24 hours. 250 µL of the overnight culture was then pipetted into 5 mL of fresh TSB and cultivated at 37 °C for an additional 3 hours, yielding a culture in log phase growth [53]. Log phase growth time was verified by a growth curve (Figure 7). Next, an experimental culture was created in one of three media: HT, TSB, and M9.

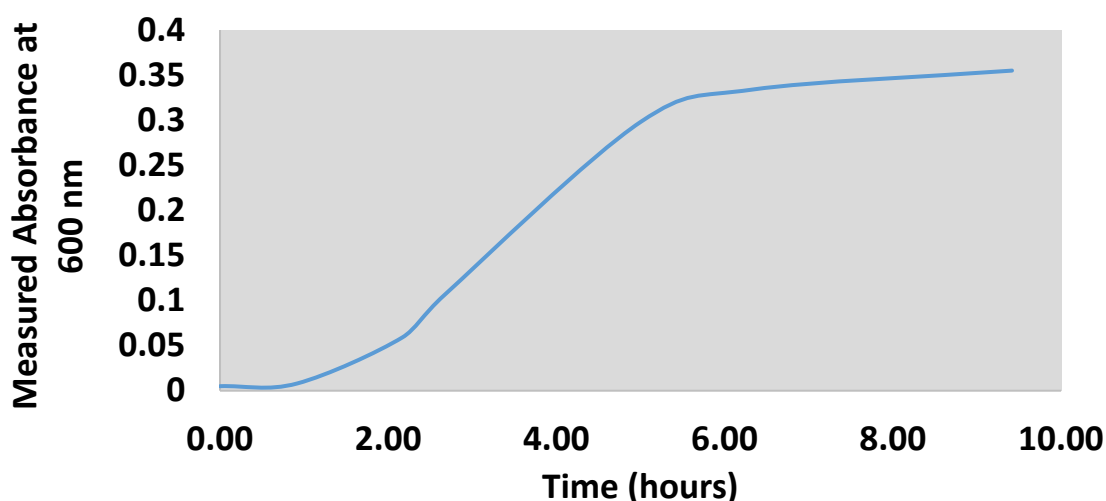


**Figure 7: *E. coli*-K12 growth curve in TSB. Absorbance was measured at a wavelength of 600 nm.**

Both M9 and HT Media experimental cultures were created by a process where a log phase culture was centrifuged for 10 minutes at 3600 rpm in an angle centrifuge (Hamilton Bell 1550), decanted, and re-filled with 5 mL fresh medium. This process was repeated three times. After dilution, the sample was sonicated in a bath sonicator (Branson 3510) for 15 seconds to ensure a homogenous sample and the experimental culture was adjusted to an optical density of 0.075 (corresponding to  $4.73 \times 10^8$  CFU/mL<sup>-1</sup> for HT medium,  $1.77 \times 10^9$  CFU/mL<sup>-1</sup> for TSB

medium and  $1.33 \times 10^8$  CFU mL<sup>-1</sup> for M9 medium) as measured on a UV-Vis spectrophotometer (HACH DR 6000).

### 4.3. Ultraviolet Irradiation

Irradiation was conducted in a custom-built apparatus with a 15 W Florence tube bulb IN-0HV41 (Technical Precision) as the UV source. Intensity was measured by placing a radiometer (PMA2200, Solar Light) in the center of the sample area, allowing the radiometer to stabilize for 15 minutes, and then recording the value. Irradiation of biofilms occurred between 20-23 °C, the room temperature of the lab during the experimentation. Motility assays were irradiated at 25 °C, a temperature that was achieved by heating the lab with a space heater (Mainstays HO-02708).

### 4.4. Planktonic Death UV model

Disinfection kinetics modeling was accomplished by studying planktonic death in correlation to applied dose for *E. coli*. To do this, 175 µL of experimental sample ( $4.73 \pm 2.73 \times 10^8$  CFU mL<sup>-1</sup> for HT medium,  $1.33 \pm 0.326 \times 10^8$  CFU mL<sup>-1</sup> for M9 medium, and  $1.77 \pm 0.427 \times 10^9$  CFU mL<sup>-1</sup> for TSB medium) was placed in eight replicates in wells of a 96-well plate. In addition to experimental samples, negative controls were also plated in quadruplicate in the form of non-inoculated medium. The plate was then irradiated at 20-23 °C for 24 hours. A second, identical plate was set next to the apparatus, serving as a dark control. Plate counts were performed post-irradiation to determine final bacterial counts while starting bacterial counts were estimated using optical density [17]. Plate counts were performed by pipetting 50 µL of the irradiated sample onto an agar plate, spreading with a spread bar 10 times, rotating the plate 45°, spreading and rotating two more times, and then incubating 12-24 hours at 37 °C. Colonies were then counted to determine the number of colony forming units in the sample. Both final and

initial counts were then used to determine LRV by utilizing Equation 3 ( $LRV = -\log(\frac{N}{N_o})$ ).

Height above the collimator was used to set experimental intensity while irradiation time was 24 hours for all experiments. Eight different doses were studied: 12.96 mJcm<sup>-2</sup>, 26.82 mJcm<sup>-2</sup>, 86.40 mJcm<sup>-2</sup>, 121.0 mJcm<sup>-2</sup>, 204.0 mJcm<sup>-2</sup>, 240.4 mJcm<sup>-2</sup>, and 360.0 mJcm<sup>-2</sup>. Using data from the planktonic death experiments, both the Chick-Watson and Rennecker-Mariñas disinfection models were evaluated for the best fit.

#### **4.5. Biofilm Formation and Bacterial Growth**

In order to quantify bacterial growth, absorbance was measured post-irradiation on a 96-well plate reader (Multiskan™ FC Microplate Photometer) at 620 nm. After spread plating, the remaining liquid was removed from each well, the wells were gently rinsed with phosphate-buffered saline (PSB) ( 8g NaCl, 0.2 g KCl, 1.44 g Na<sub>2</sub>HPO<sub>4</sub>, dissolved in 1 L DI water, pH adjusted to 7.4), and attached biofilms fixed with 95% ethanol (Alfa Aesar). After fixing, the ethanol was evaporated at room temperature overnight before staining with 0.1% safranin (Fischer Scientific) [53]. Once stained, the sample was rinsed four times with PBS and the stained biofilm was suspended with 1% sodium dodecyl sulfate (SDS) (Fisher Scientific). A blank was also created by staining empty wells in quadruplicate and the resulting average was subtracted from other results to account for a blank. Absorbance was then measured on a 96-well plate reader (Multiskan™ FC Microplate Photometer) at 450 nm.

#### **4.6. Motility Assays**

Swimming and swarming motility of *E. coli* were tested upon irradiation by UV. Twitching motility assays were also attempted but were ultimately unsuccessful.

#### **4.6.1. Swimming Motility**

Swimming motility plates (1% tryptone, 0.5% NaCl, and 0.3% agar in DI water) were inoculated with a sterile 100  $\mu$ L pipette tip in two locations using the stab inoculation method [45]. The stab inoculation method is as follows: a sterile pipette tip was dipped twice into overnight culture (optical density of 0.30) and then used to stab the agar plate. The plate was then irradiated for 24 hours at the same intensities studied in the biofilm tests. Post-irradiation, images of the plates were taken using a Canon Rebel T3 and the area of disturbance was analyzed using ImageJ [54]. The area of disturbance is described as the white, cloudy area as shown in Figure 8. To evaluate results in Image J, the image was uploaded to the program and the scale was set with a known distance in the image. After setting the scale, the image was turned into a black and white image and cropped to include only the areas of disturbance. Then, the particle size was analyzed and recorded in  $\text{cm}^2$ . Particle size was normalized to a dark control.

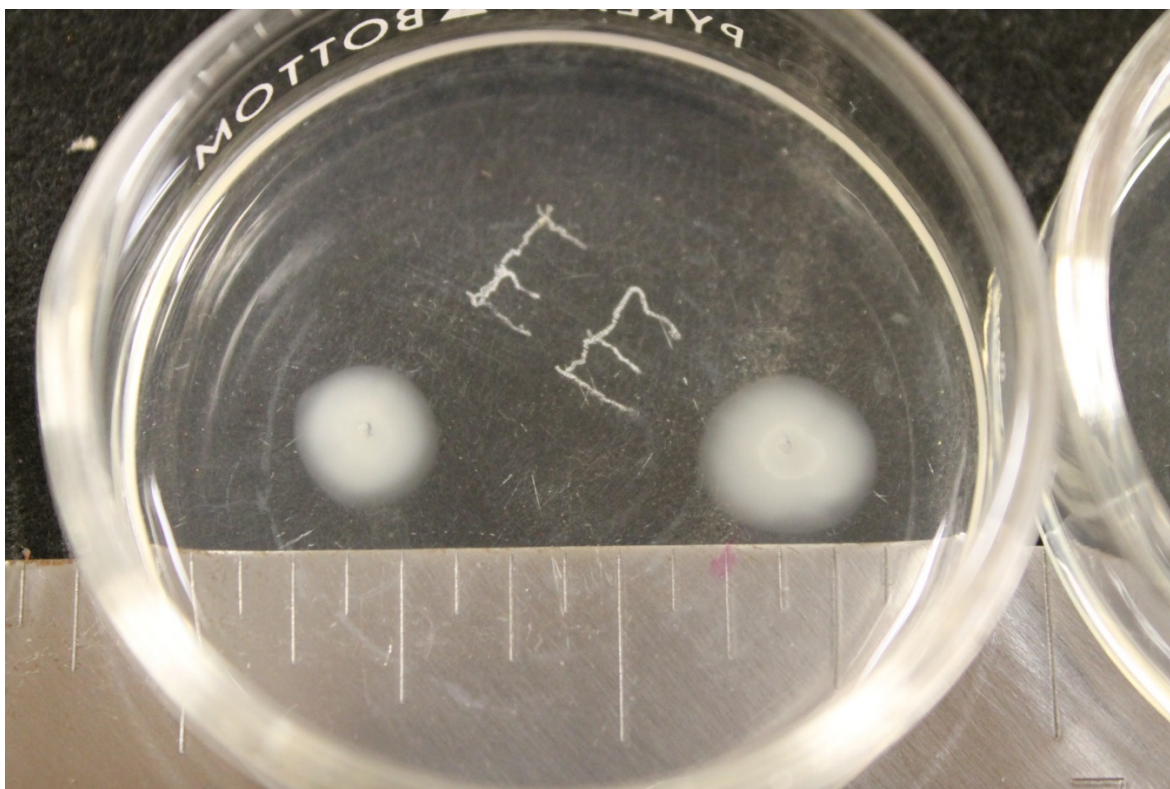


**Figure 8: Example of an image taken for a dark control swim plate result where the white circles are the area of disturbance.**

#### **4.6.2. Swarming Motility**

Similarly, swarming motility analysis was performed by inoculating a soft agar plate (0.5% agar, 8 g/L nutrient broth, and 8 g/L dextrose in DI water) [48] using the stab inoculation technique. The plate was then irradiated for 48 hours at the same intensities studied in the biofilm tests. Post Irradiation, a picture of the plate was taken using a Canon Rebel T3. ImageJ [54] was also used to evaluate the swarm area, as determined by the cloudy areas shown in Figure 9.



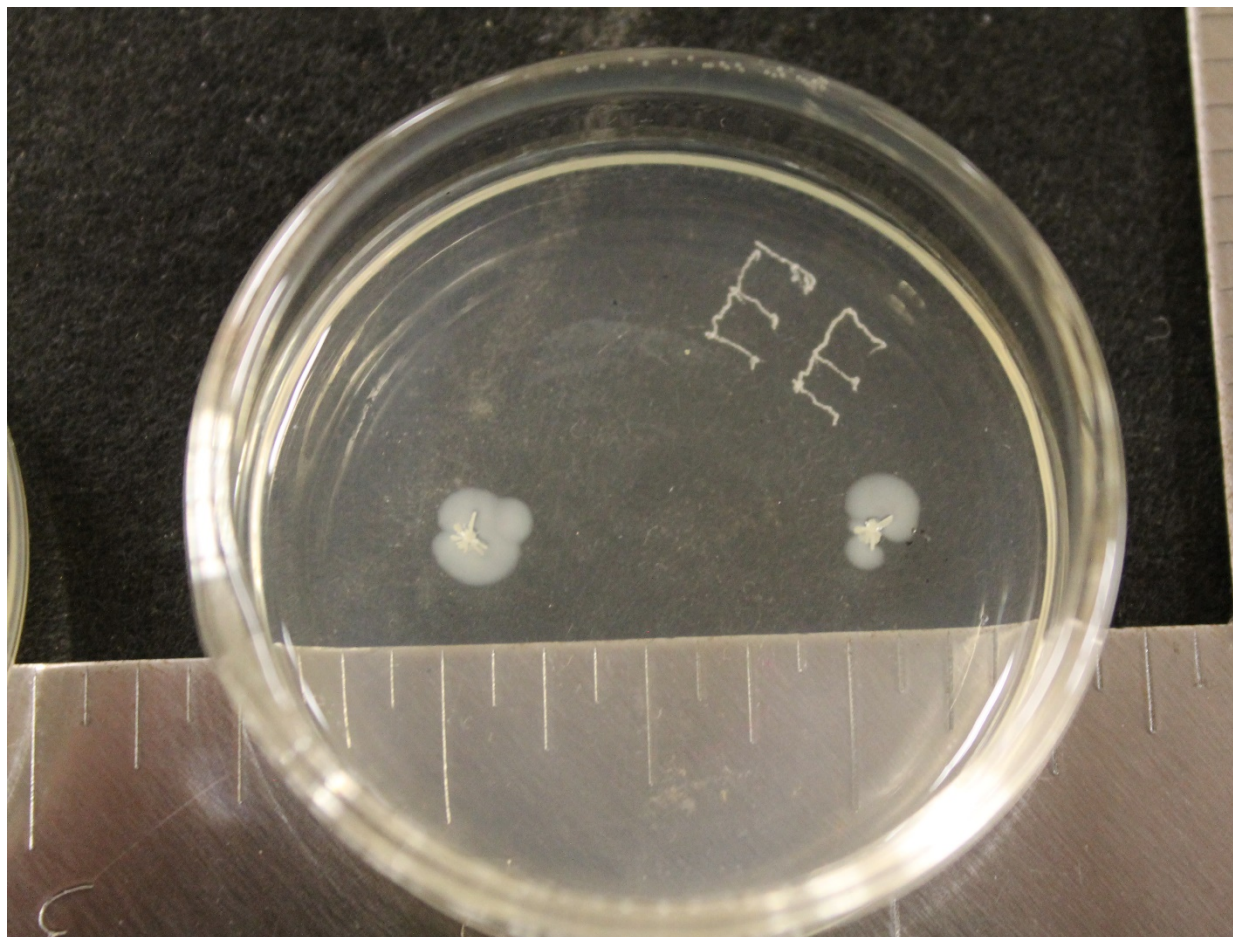


**Figure 9:** Example of an image taken for a dark control swarm plate result where the white circles are the area of disturbance.

#### **4.6.3. Twitching Motility**

Twitching motility assays were attempted by inoculating a 3 mm LB agar plate (1% agar) with a sterile pipette similarly to the stab technique, however, the tip was stabbed through the agar, between the plate and the agar, and then removed [45]. After the assays came back with no disturbance area, a further literature review confirmed that in a laboratory setting, *E. coli* may not express the genes that are responsible for creating type IV pili [55] and therefore do not utilize twitching motility.



#### **4.7. Statistical Analysis**

Analysis of variances (ANOVA) [56] was used to determine if there is significant evidence to suggest that motility is statistically affected by UV irradiation and if biofilm growth is statistically reduced. By utilizing coding with R [56], all data was input into a code. For each medium, a dark control data set was created which included all dark results. For irradiated results, however, a set was created for each individual applied dose. R codes for bacteria growth, biofilm formation, swimming motility, and swarming motility are contained in appendix A, B, C, and D respectively. After the code was written, it was carried out, with the results being pasted into a section of the code. P-values were considered to denote statistical significance if the reported value was greater than the assumed  $\alpha$  of 0.05.

## 5. Results and Discussion

### 5.1. Apparatus Verification

Irradiation intensity was varied by changing the height of the light above the collimator and incorporating a paper coffee filter (Safeway). For instance, when setting a height of 117 cm between the lamp and the collimator, the intensity was  $2.36 \mu\text{Wcm}^{-2}$ . By maintaining the same height of 1.17 m, and placing a coffee filter at the top of the collimator, irradiation intensity was reduced to  $0.13 \mu\text{Wcm}^{-2}$ . Figure 10 shows that as the distance between the bulb and the collimator increases from 0.35 to 1.17 m, the intensity without a filter decreases from  $6.72 \mu\text{Wcm}^{-2}$  to  $2.36 \mu\text{Wcm}^{-2}$ . Likewise, the addition of a filter reduced the intensity at 46 inches above the collimator from  $2.36 \mu\text{Wcm}^{-2}$  to  $0.13 \mu\text{Wcm}^{-2}$ , the target intensity.

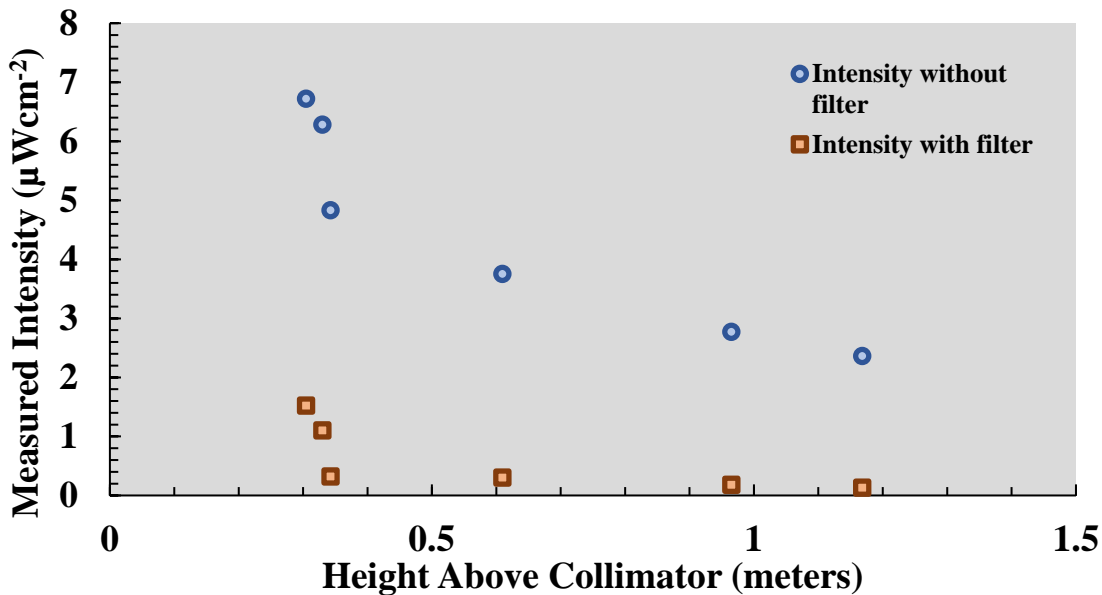


**Figure 10: Variation of intensity as a function of both height and filter usage. Height was varied using a chemical stand and a clamp. Filters were Safeway brand white paper coffee filters. Standard deviation does not exist for these test as replicates were not conducted.**

The correlation between height above the collimator and measured intensity were then compared to the inverse-square law [57]. This law states that as the distance away from a point source of light increases, the intensity is proportional to the inverse of the distance squared (

$I \propto \frac{1}{d^2}$  [57]. To evaluate this, the measured intensity was plotted as a function of the inverse square of height (Figure 11). It was determined that both with and without a filter, the change as a function height fits the inverse-square law. It is important to note however that the  $R^2$  value of the line decreases with a filter in place. This decrease in fit is most likely due to inhomogeneous light refraction through a medium. When a light ray enters a new medium, such as a filter, the angle of the ray is altered [57], and because the filter is heterogeneous, it introduces more variation in the light that reaches the sample.

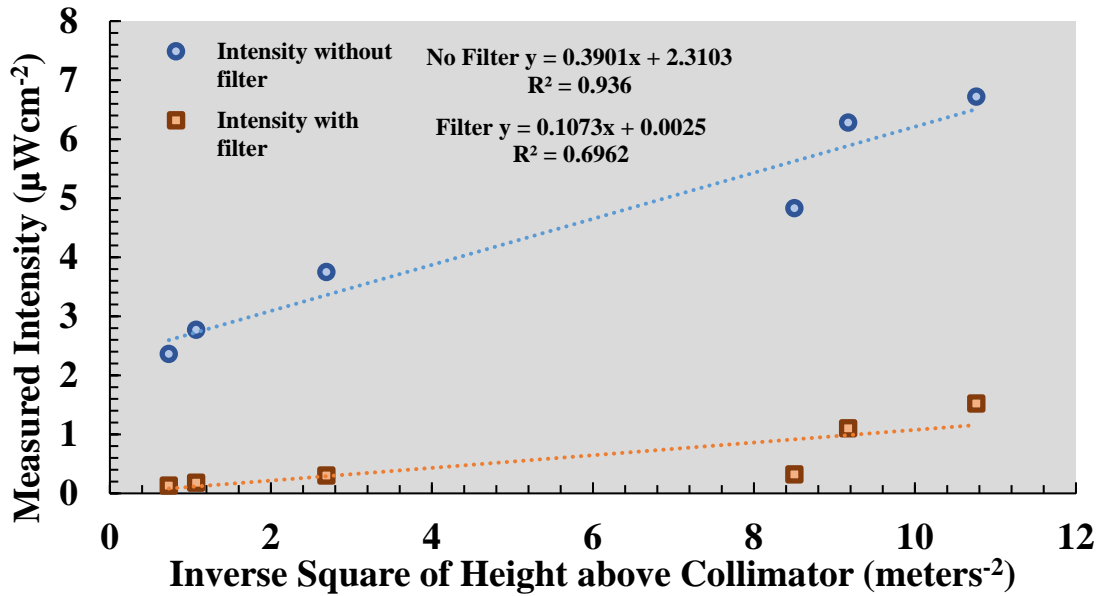


Figure 11: Evaluation of the inverse squares law in correlation to the experimental apparatus. Intensity decreases with the inverse square of the height.

Once the final apparatus and filter material were determined, testing was conducted to ensure uniform intensity across the sample area. Figure 12 shows that for a 10.16 cm by 12.17 cm sample area, the intensity is fairly constant when irradiated at 0.33 m above the collimator with a filter in place. Within the sample area, an average intensity of  $0.994 \pm 0.052 \mu\text{Wcm}^{-2}$  was measured. The lowest measured intensity ( $0.92 \mu\text{Wcm}^{-2}$ ) occurred in the upper-right hand corner

while the highest intensity ( $1.07 \mu\text{Wcm}^{-2}$ ) occurred in the top, center. The corresponding areas on the 96-well plate contained non-inoculated media controls.

0.96	1.07	0.92
1.03	0.94	0.97
1.04	1.04	0.98

**Figure 12: Intensity displays little variation across the irradiation area. Each box represents a 3.39 cm high and 4.06 cm wide sample area. Irradiation was measured at the center of each box.**

Additionally, consistent intensity over a 24-hour irradiation time was verified at two different intensities (Figure 13). The first test was conducted with a filter when the light was 33 cm above the collimator and the bulb was pointed parallel to the chemistry stand. The second test occurred at the same height and with a filter, but with the light bulb positioned perpendicular to the chemistry stand. In the first test, the intensity was originally measured at  $0.94 \mu\text{Wcm}^{-2}$ , and within fifteen minutes, the intensity increased to  $1.12 \mu\text{Wcm}^{-2}$ . In the second test, the initial intensity reading was  $0.68 \mu\text{Wcm}^{-2}$ , however, by 17 hours the intensity had decreased to  $0.61 \mu\text{Wcm}^{-2}$ . Based on similar results with the radiometer in a different apparatus by a different graduate student, it was concluded that the radiometer takes about 15 minutes to stabilize. After the initial readings, all intensity results for the 24-hour test were within  $0.02 \mu\text{Wcm}^{-2}$ , verifying that within the period experiments were conducted, the apparatus produced a consistent intensity.

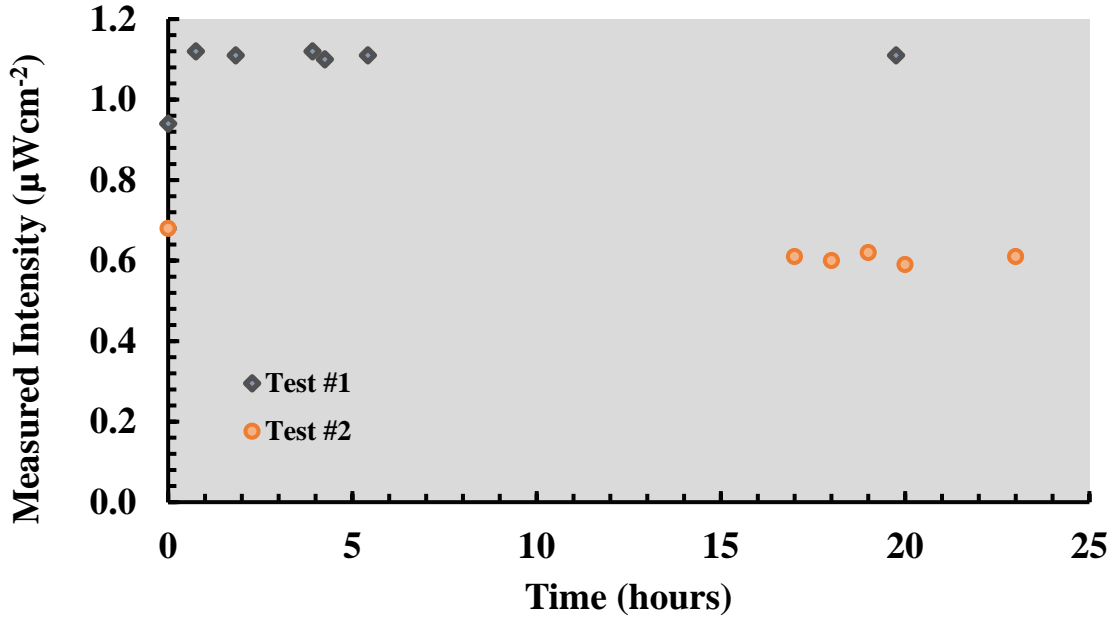


Figure 13: Consistent intensity over 24 hours. Both tests occurred at 33 cm above the collimator and with a coffee filter in place. The first test was conducted with the light source pointed directly down while the second test was conducted with the light source pointed to the right side.

## 5.2. Planktonic Death

### 5.2.1. Log Removal

Planktonic death was evaluated using Equation 3,  $LRV = -\log\left(\frac{N}{N_0}\right)$ . Plate counts were used to determine  $N$  while  $N_0$  was estimated using starting  $OD_{600}$ . Best practices available during experimentation did not allow for quantification of LRV at zero applied dose, so no intercept was set for trend lines produced.

For *E. coli* in HT medium (Figure 14), log removal decreased linearly between 1.752 at 0 mJcm<sup>-2</sup> applied dose and  $10.14 \pm 0.34$  at an applied dose of 203.9 mJcm<sup>-2</sup>. In these experiments, a log removal of 11 represents near complete death, where the majority of the ending plate counts had zero colonies.

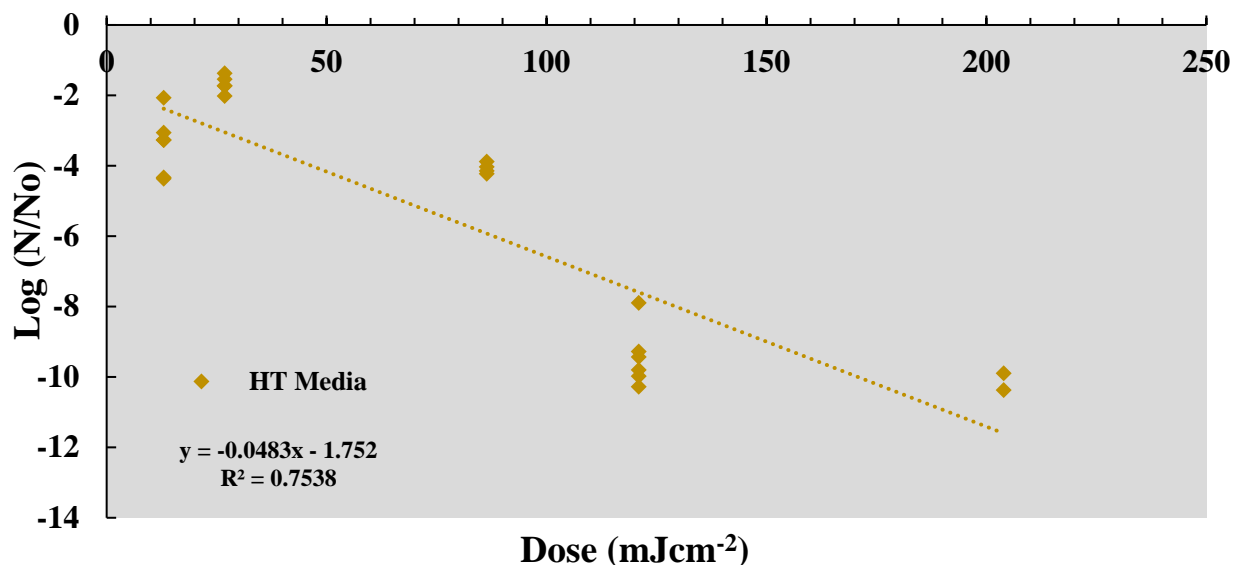


**Figure 14: Log removal of *E. coli* as a function of UVC dose in HT medium. The dotted line shows a linear least squares regression. Starting *E. coli* concentration was  $4.73 \pm 2.73 \times 10^8$  CFU mL<sup>-1</sup>, and bacteria were irradiated at the appropriate intensity for 24 hr.**

Planktonic death of *E. coli* in TSB is reported in Figure 15 where LRV again decreases linearly as a function of applied dose. The highest LRV value was calculated at  $6.93 \pm 1.54$  at an applied dose of  $121.0 \text{ mJcm}^{-2}$ . At the lowest applied dose studied,  $12.96 \text{ mJcm}^{-2}$ , LRV was  $-0.23 \pm 0.38$ , meaning that over the course of the experiment, more bacteria replicated than was inactivated by UVC. In fact, the intercept of the trend line suggests that if no dose is applied, the colony forming units experience a log increase of 1.02. This increase at very low intensities in TSB makes sense for two reasons. First, TSB absorbs some UV at 254 nm, discussed below. Second, TSB has a very high nutrient density relative to the other medium studied. Because of this, *E. coli* were exposed to ample nutrients to facilitate replication and results indicate that replication was greater than the effect coming from low-intensity UV.

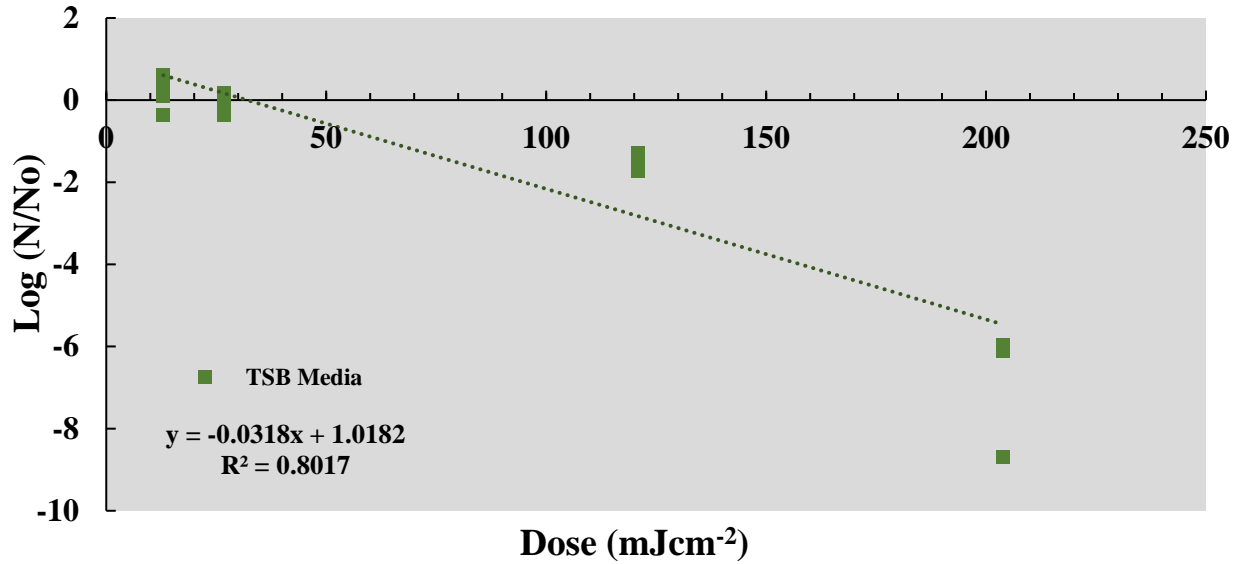


**Figure 15: Log removal of *E. coli* as a function of UVC dose in TSB medium. The dotted line shows a linear least squares regression. Starting *E. coli* concentration was  $1.77 \pm 0.427 \times 10^9$  CFUmL<sup>-1</sup>, and bacteria were irradiated at the appropriate intensity for 24 hr.**

Planktonic death of *E. coli* in M9 medium is reported in Figure 16 where the log removal value increases linearly from the y-intercept of 2.58 to  $9.09 \pm 0.50$  at an applied dose of 203.9 mJcm<sup>-2</sup>. In these experiments, an LRV of 11 represents near complete death, where the majority of the ending plate counts had zero colonies.

Log removal appears to jump to 4.63 at an applied dose of 26.82 mJcm<sup>-2</sup>. While the exact cause of the discontinuity is unknown, the increase may have been due to humidity, which was problematic throughout experimentation. At this specific point there appeared to be more of an influence in liquid bacteria level at the end of the experiment than in other experiments.

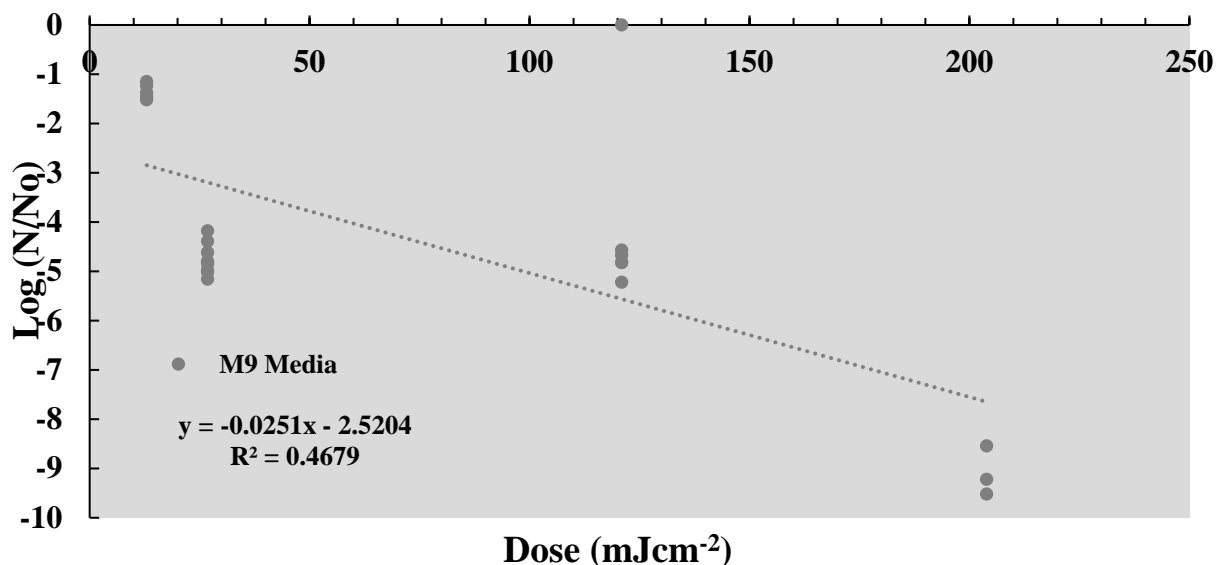


**Figure 16: Log removal of *E. coli* as a function of UVC dose in M9 medium. The dotted line shows a linear least squares regression. Starting *E. coli* concentration was  $1.33 \pm 0.326 \times 10^8$  CFUmL<sup>-1</sup>, and bacteria were irradiated at the appropriate intensity for 24 hr.**

LRV results for *E. coli* in all media is displayed in Figure 17. It was to be expected that log removal in all media would follow a linear trend as Severin *et al* determined that *E. coli* experienced a linear increase in log removal as a function of irradiation time when utilizing a mercury vapor lamp at 254 nm [58].

For all media, it was determined that while log removal fits a linear trend, the fit ( $R^2$ ) of the linear regression suggests that the data has a high variance. In M9 medium specifically, there is a much higher variance, which, as discussed previously may be due to a higher temperature during one of the tests. The variance of all media was also likely due to evaporation due to low humidity as well as not quantifying the exact starting concentration.



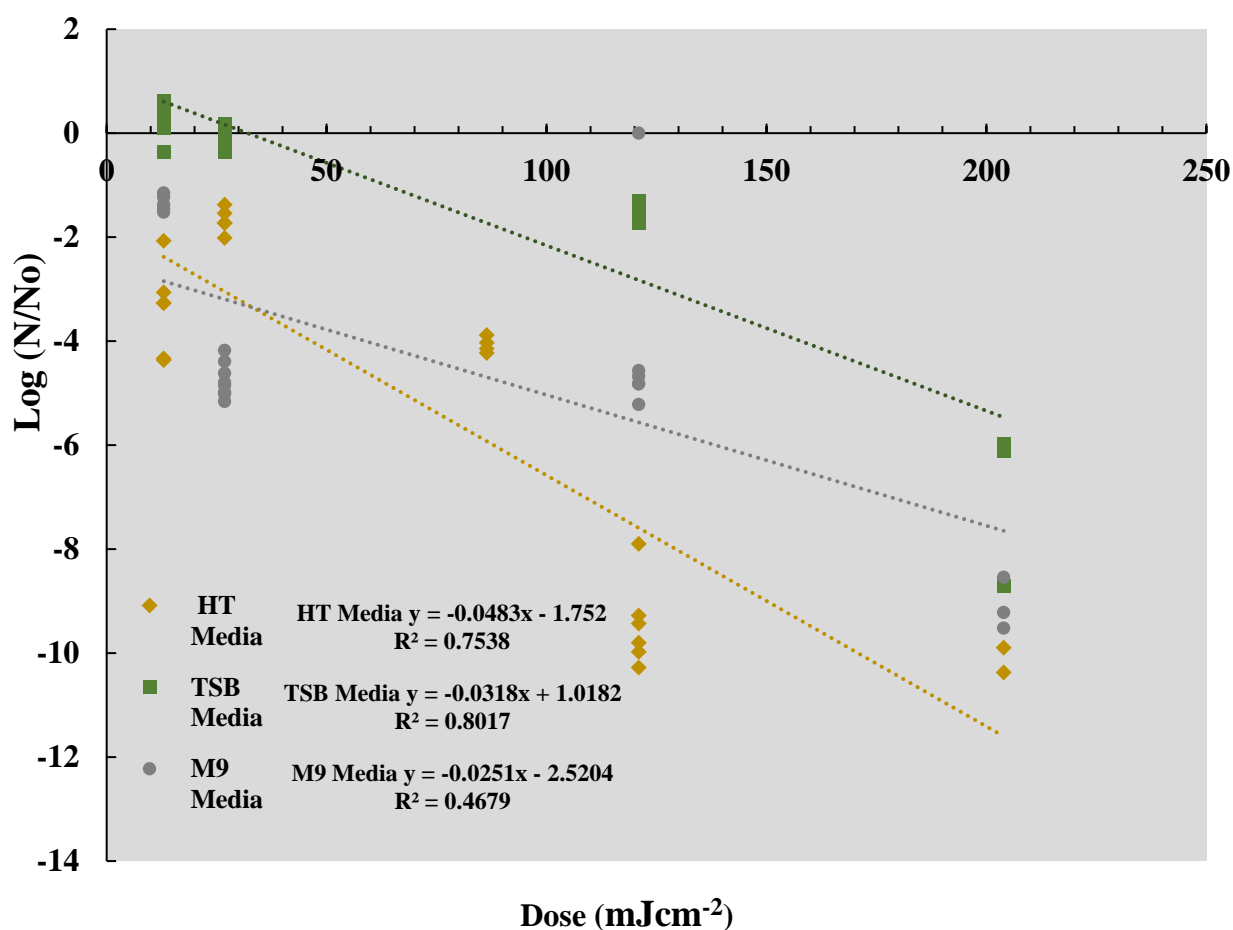


Figure 17: Log removal of *E. coli* as a function of UVC dose in all three media. Dotted lines show linear least squares regressions. This figure is a combination of Figures 14-16.

In addition to a large variance, the y-intercept for M9 medium is also twice that of HT medium. While variance may have played a role in the significant changes between the y-intercept for all media, it is more likely that this is a function of medium type on the absorbance of UV at 254 nm and the amount of nutrients available (and therefore the growth rate) in each media. Figure 18 shows a wavelength scan for all three media tested. TSB medium experienced the highest absorbance of any medium, most likely contributing to a lower removal of bacteria. HT medium experiences the second highest UV absorbance, however, has the highest removal. M9 medium has approximately zero absorbance in comparison to DI water and had medium

removal compared to other media. The removal in M9 may have been more a function of low nutrient availability, leading to the bacteria not being able to replicate at the same rate seen in the other two media. This concept will be further discussed in the bacterial replication results section.

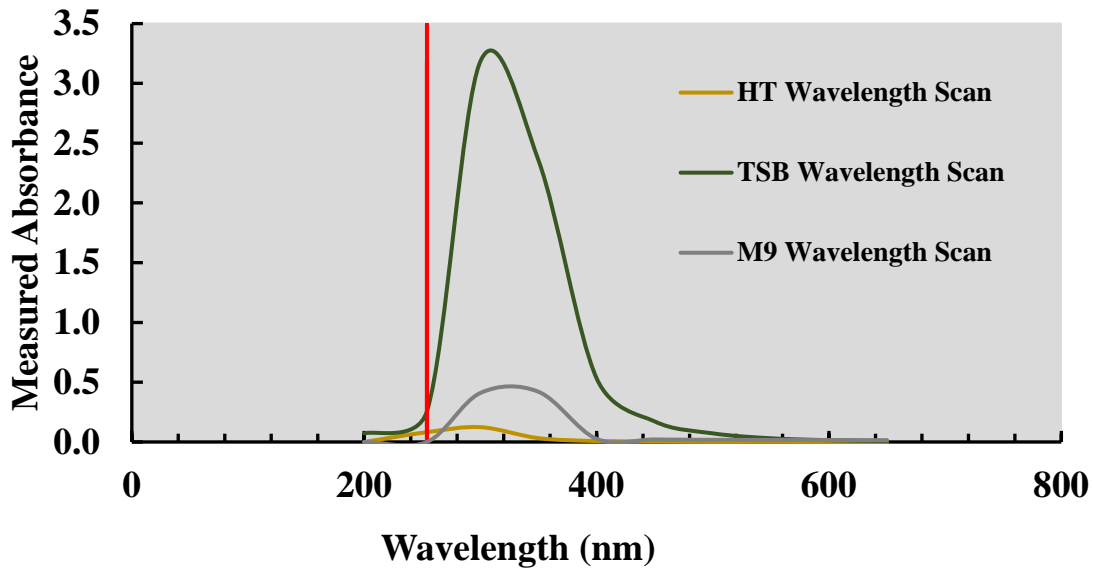


Figure 18: Wavelength scan for the three media evaluated during experimentation. Absorbance was measured at 50 nm intervals between 200 and 650 nm with DI water as a blank. The red line represents a wavelength of 254 nm, or biocidal UV.

### 5.2.1. Chick-Watson Model

Death kinetics were analyzed by fitting the final plate counts to the Chick-Watson disinfection model from Equation 4 ( $-k_c I t = \ln(\frac{N}{N_o})$ ). This model is known to accurately quantify bacterial death during high-intensity UVC biocidal treatment [14].

For *E. coli* grown in HT medium (Figure 19), the death kinetics were found to follow the Chick-Watson model where the natural log of the surviving fraction was found to linearly decrease from  $-7.81 \pm 1.99$  at an applied dose of  $12.96 \text{ mJcm}^{-2}$  to  $-23.33 \pm 0.78$  at an applied

dose of 203.9 mJcm<sup>-2</sup>. The coefficient of specific lethality was determined to be 0.1444 for *E. coli* in HT medium.

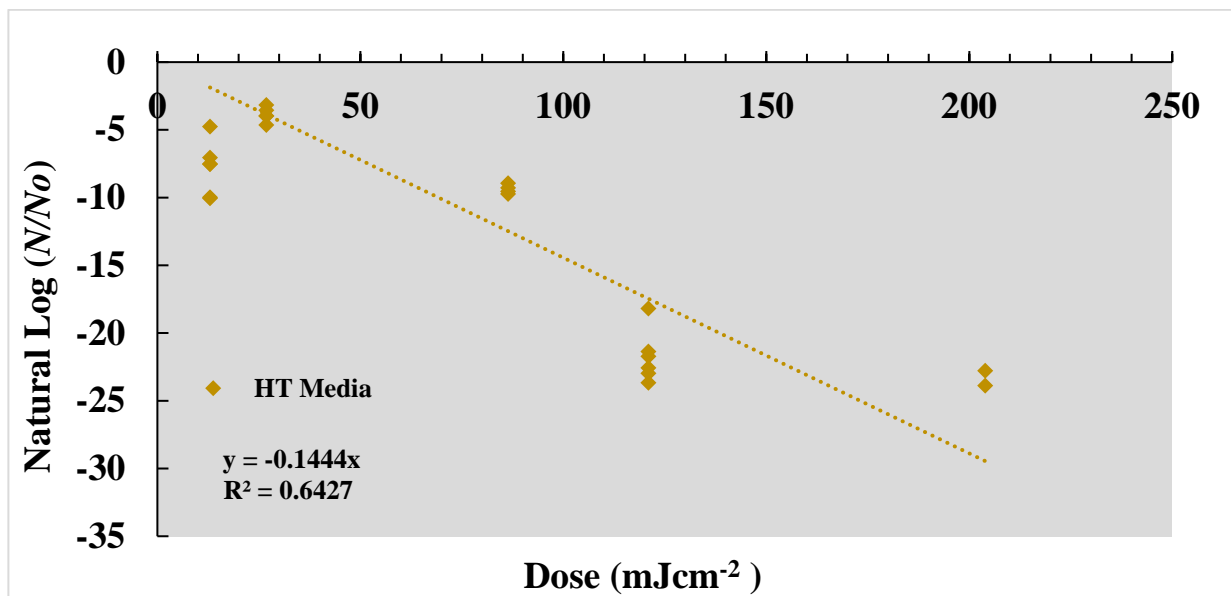


**Figure 19: Removal of *E. coli* as a function of UVC dose in HT medium fit to the Chick-Watson model. The dotted line shows a linear least squares regression. Starting *E. coli* concentration was  $4.73 \pm 2.73 \times 10^8$  CFUmL<sup>-1</sup>, and bacteria were irradiated at the appropriate intensity for 24 hr.**

Death kinetics for *E. coli* grown in TSB were also evaluated using the Chick-Watson model (Figure 20), but it was determined that the kinetics did not follow this model. Again, these results are most likely due to the fact that TSB absorbs UVC, therefore the applied dose is not actually the dose that reached the bacteria. The natural log of the surviving fraction was found to linearly decrease from  $-0.53 \pm 0.88$  at an applied dose of 12.96 mJcm<sup>-2</sup> to  $-15.54 \pm 3.01$  at an applied dose of 203.9 mJcm<sup>-2</sup>. The coefficient of specific lethality was determined to be 0.059 for *E. coli* in TSB medium.

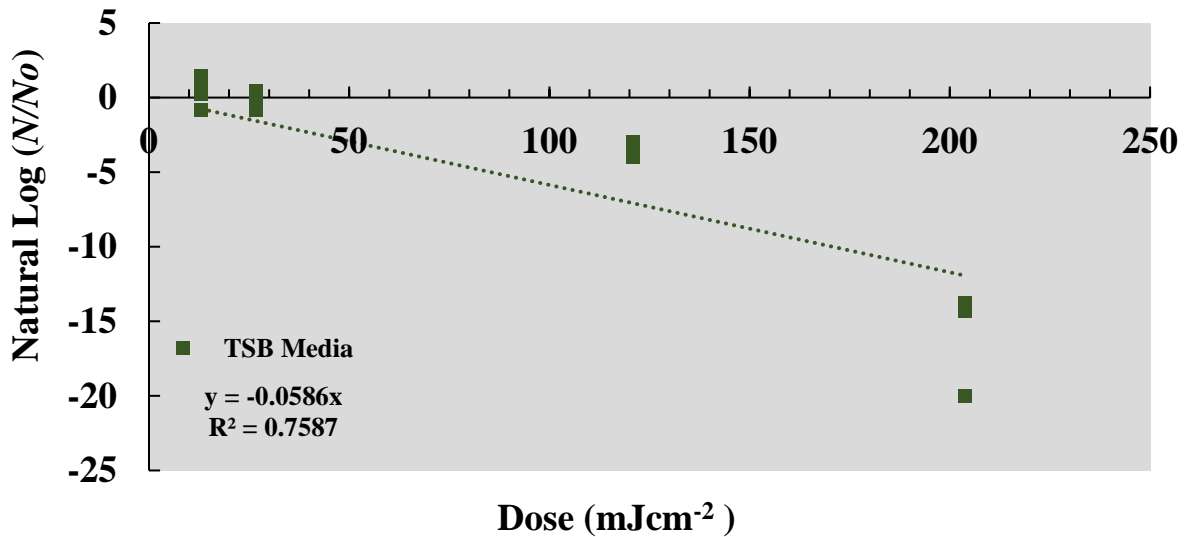


**Figure 20: Log removal of *E. coli* as a function of UVC dose in TSB medium. The dotted line shows a linear least squares regression. Starting *E. coli* concentration was  $1.77 \pm 0.427 \times 10^9$  CFU mL<sup>-1</sup>, and bacteria were irradiated at the appropriate intensity for 24 hr.**

Figure 21 shows the Chick-Watson death kinetics model of death kinetics for *E. coli* in M9 medium where natural log removal was found to linearly decrease as a function of applied dose. Natural log removal was found to be  $-3.10 \pm 0.36$  at an applied dose of  $12.96 \text{ mJcm}^{-2}$  to  $-20.94 \pm 1.15$  at an applied dose of  $203.9 \text{ mJcm}^{-2}$ . The coefficient of specific lethality was determined to be 0.1079 for *E. coli* in M9 medium.

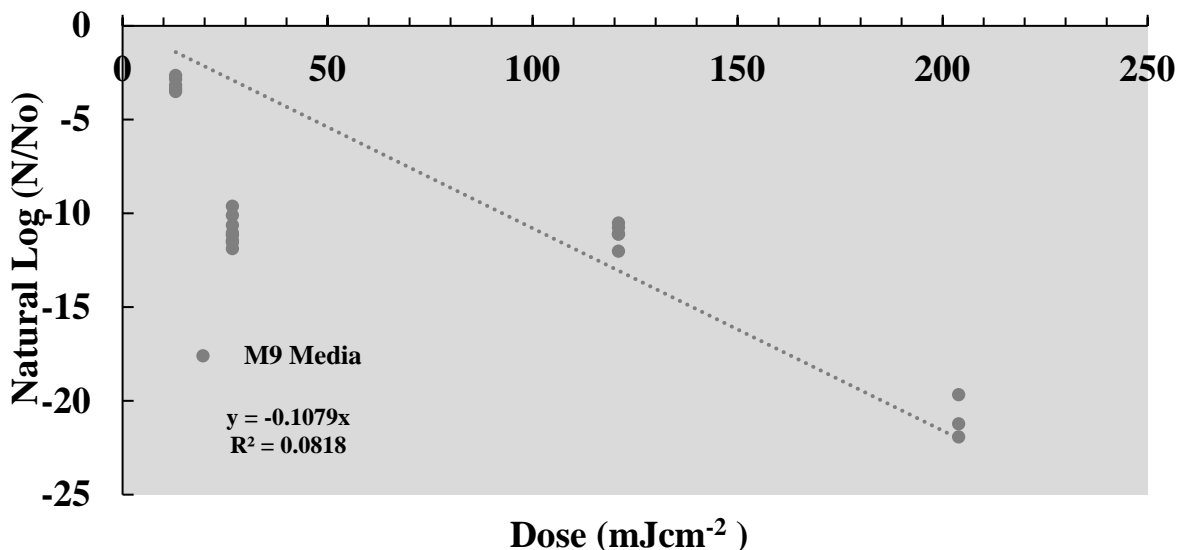


**Figure 21: Log removal of *E. coli* as a function of UVC dose in M9 medium. The dotted line shows a linear least squares regression. Starting *E. coli* concentration was  $1.33 \pm 0.326 \times 10^8$  CFU mL<sup>-1</sup>, and bacteria were irradiated at the appropriate intensity for 24 hr.**

While textbooks cite the coefficient of specific lethality of *E. coli* undergoing high-intensity UV irradiation to be  $8.3 \text{ cm}^2 \text{ mJ}^{-1}$  [14], this thesis found it to be much lower. In fact, the coefficient of specific lethality was found to be 0.1444, 0.0586, and  $0.1079 \text{ cm}^2 \text{ mJ}^{-1}$  in HT, TSB, and M9 media respectively. Gilba *et al.* [59] found that the coefficient of specific lethality for *E. coli* in greywater is  $0.88 \text{ cm}^2 \text{ mJ}^{-1}$ . While greywater typically is most similar to TSB, having an absorbance at 254 nm of 0.28 [59], the medium studied by Severin *et al.* was more similar to HT and M9 media, with an absorbance at 254 nm of 0.032 [58]. Thus, the media plays a major role in the effectiveness of UV as a disinfectant.

As mentioned above in the section about log removal, while all media follow a linear trend, the fit of the lines ( $R^2$ ) is poor. This again is most likely due to the variance of the growth conditions including temperature and humidity. Figure 22 shows a combined graph of all three

media types studied. According to the Chick-Watson model, as the coefficient of specific lethality increases, so does the susceptibility of bacteria to UVC [59]. Because of this fact, the results of this thesis support that as absorbance of the medium decreases, the susceptibility of the bacteria being treated increases. From a processing standpoint, this determination means that as the water being treated increases in quality, a low-intensity UVC treatment will be more effective at killing bacteria.

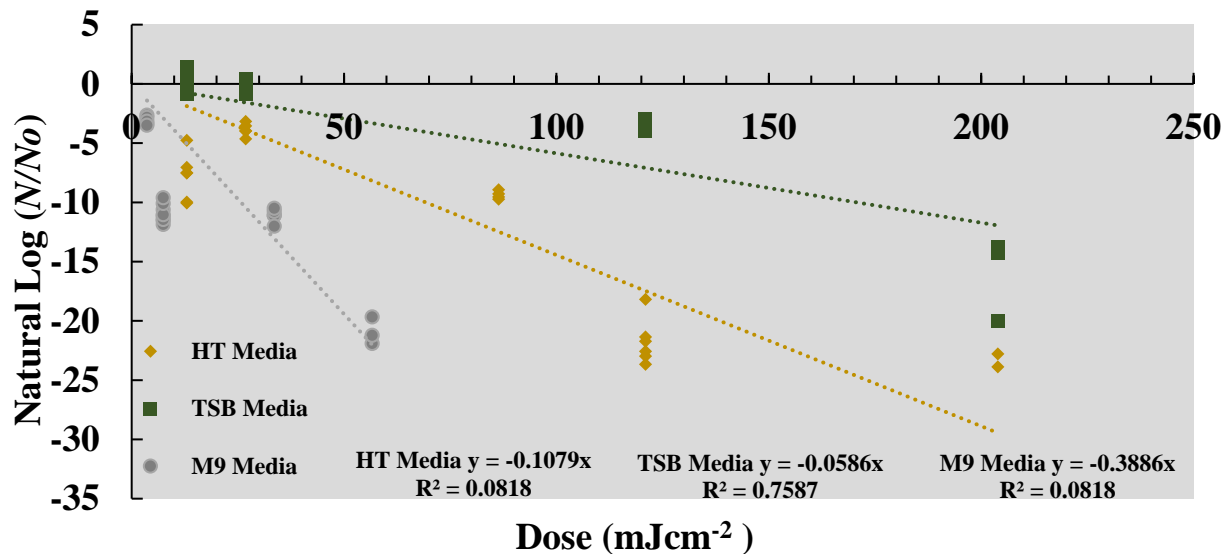


Figure 22: Log removal of *E. coli* as a function of UVC dose in all media. The dotted line shows a linear least squares regression. This figure is a combination of Figures 19-21.

While the hypothesis for this thesis stated that under low-intensity UVC would follow the Rennecker-Mariñas kinetics model, it was determined based on the fit of the Chick-Watson testing that this hypothesis was not determined to be accurate.

### 5.3. Bacterial Replication Results

Traditional UV irradiation, which occurs over short time periods (generally < 30 minutes) and therefore does not account for bacterial growth, or replication. The *E. coli* used for this

thesis, however, had a doubling time of 68 minutes. Therefore, for 24-hour experiments, bacteria was expected to double more than 21 times, and it was important to determine how bacterial growth changes with increasing UVC irradiation. Figure 26 shows the normalized growth results for *E. coli* in HT medium, and a value of one denotes equal irradiated and dark bacterial growth. Due to UV's ability to inhibit replication, it is important to evaluate this figure to determine if an applied dose exists that does not significantly affect bacterial growth. For *E. coli* in HT medium, bacterial growth increased to  $0.568 \pm 0.018$  at a dose of  $12.96 \text{ mWcm}^{-2}$  ( $p = 0.000$ ). Otherwise, sub-lethal UVC irradiation did not statistically affect bacterial growth until complete death occurred at  $203.90 \text{ mWcm}^{-2}$  ( $p = 0.020$ ). After complete death occurred, normalized bacterial growth was  $0.798 \pm 0.055$ . Thus, apart from the anomaly at  $12.96 \text{ mWcm}^{-2}$ , no significant decreases in bacterial growth occurred in HT media until the highest irradiation dose, which is somewhat at odds with the inactivation observed in HT (Figure 23). The difference between these two results is likely due to the complicated interaction between bacterial replication and inactivation, and  $\text{OD}_{620}$  measurements (reported in Figure 26) do not account for the viability of the bacterial cells.

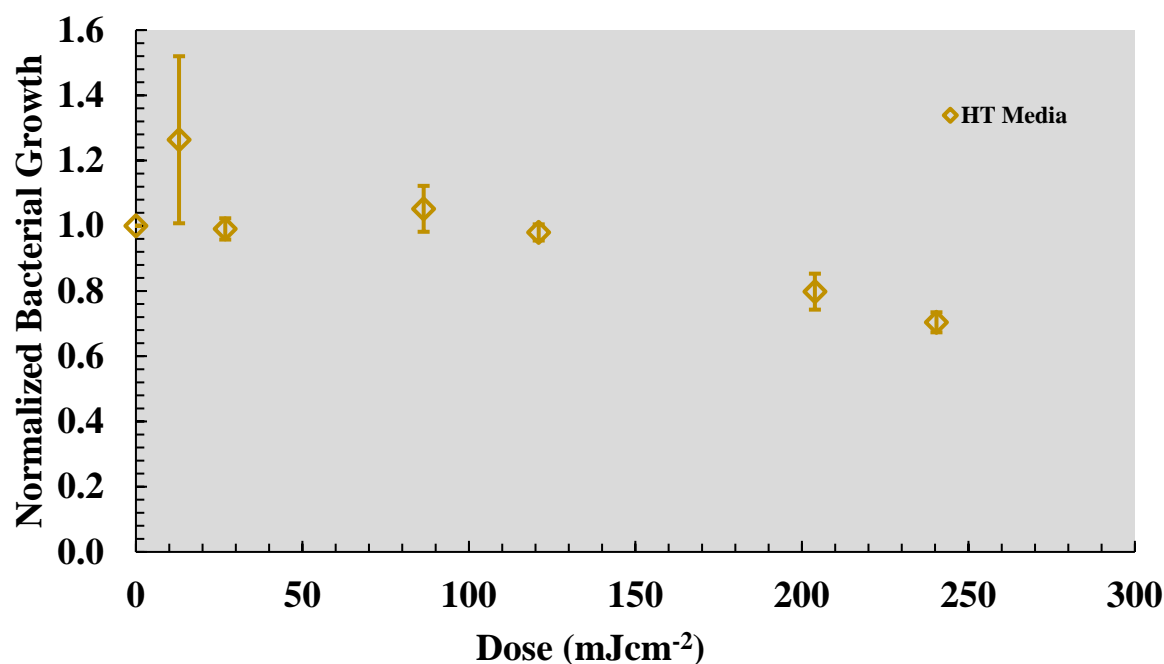


**Figure 23: Normalized Bacterial Growth as a function of dose for irradiated *E. coli* grown in HT medium. A starting *E. coli* concentration of  $4.73 \pm 2.37 \times 10^8$  CFUmL<sup>-1</sup> was used, and bacterial growth was calculated from an OD<sub>620</sub> measurement. A normalized value of 1.0 represents zero growth difference between irradiated and dark, and bacteria were irradiated for 24 hr.**

*E. coli* grown in TSB (Figure 27) experienced little change in bacterial growth as a function of applied dose. The lowest calculated normalized bacterial growth result was  $0.928 \pm 0.009$  at  $240.4 \text{ mJcm}^{-2}$  while the highest calculated value,  $1.024 \pm 0.029$ , occurred at  $86.4 \text{ mJcm}^{-2}$ . Two applied doses experienced a significantly significant change,  $12.96$  and  $203.9 \text{ mJcm}^{-2}$  ( $p < 0.001$ ). Overall, TSB growth shows less of a downward trend than HT growth, as TSB absorbs some of the UVC (Figure 18), experiences slower disinfection kinetics (Figure 20), and contains more nutrients for growth.



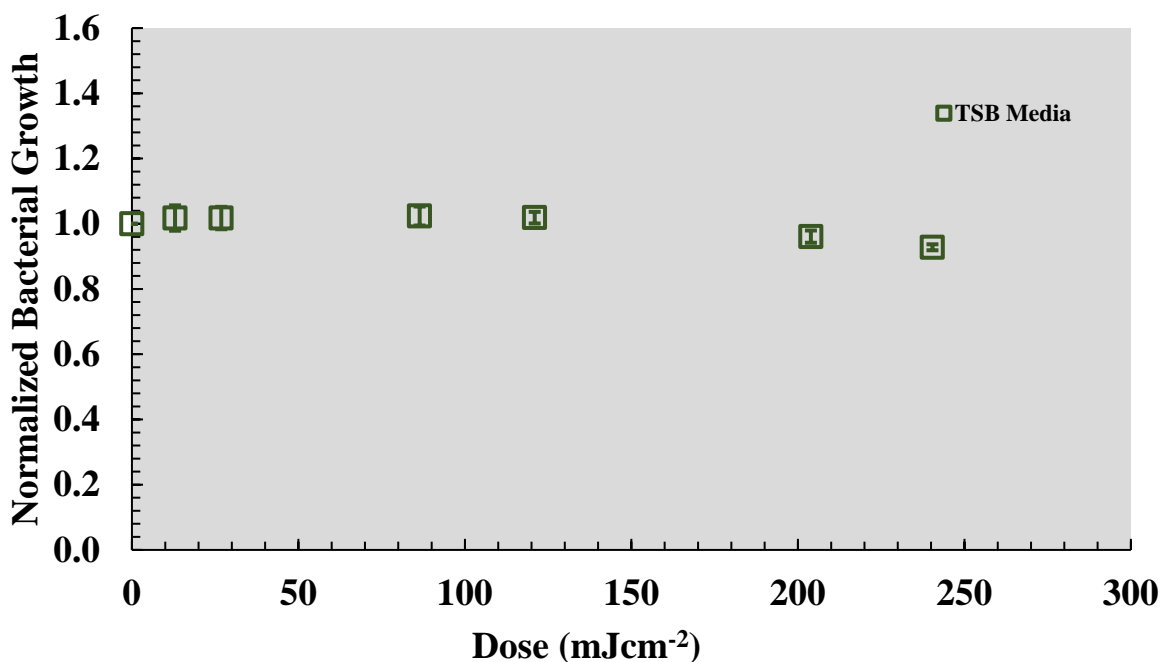


**Figure 24: Normalized Bacterial Growth as a function of dose for irradiated *E. coli* grown in TSB medium. A starting *E. coli* concentration of  $1.77 \pm 0.427 \times 10^9$  CFU mL<sup>-1</sup> was used, and bacterial growth was calculated from an OD<sub>620</sub> measurement. Irradiated values were normalized to the dark controls for the same experiment, and bacteria were irradiated for 24 hr.**

Similar to TSB, M9 saw only small changes in bacterial growth with increasing UVC dose. Results for normalized bacterial growth are shown in Figure 28. The lowest calculated normalized bacterial growth result was  $0.654 \pm 0.066$  at 203.9 mJcm<sup>-2</sup> while the highest calculated value,  $0.776 \pm 0.048$ , occurred at 240.4 mJcm<sup>-2</sup>. In all cases, there were no statistically significant differences between growth in the irradiated and control samples ( $p > 0.447$ ).

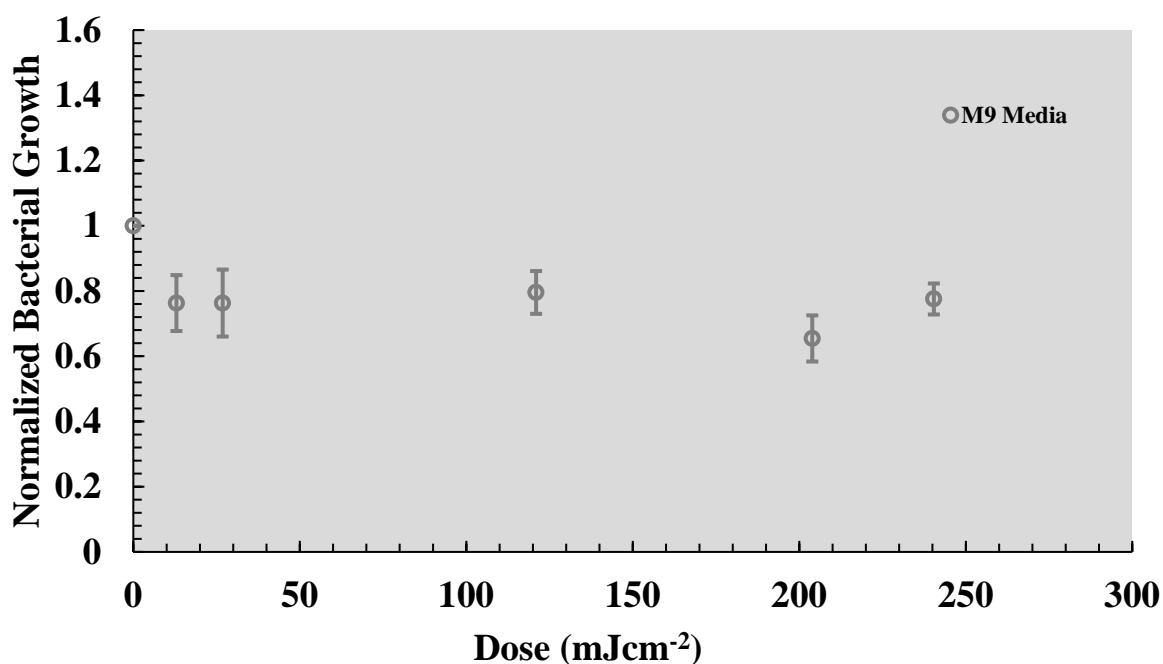


**Figure 25: Normalized Bacterial Growth as a function of dose for irradiated *E. coli* grown in M9 medium. A starting *E. coli* concentration of  $1.33 \pm 0.326 \times 10^8$  CFU mL<sup>-1</sup> was used, and bacterial growth was calculated from an OD<sub>620</sub> measurement. A normalized value of 1.0 represents zero growth difference between irradiated and dark, and bacteria were irradiated for 24 hr.**

In general, bacteria grown in all media (Figure 29) experienced minimal changes in bacterial growth at low-intensity UVC irradiation. It is curious that these results differ so greatly from the results obtained using plate counts (Figure 22). The difference between these results likely lies in the methods used. First, OD<sub>620</sub> measurements will account for all cells—dead or alive—in the sample, whereas plate counts will account only for those bacteria that are able to replicate on incubated plates. It appears that UVC makes it more difficult for bacteria to replicate on plates after irradiation; however, it seems that bacteria can still replicate in media under these exposure conditions.

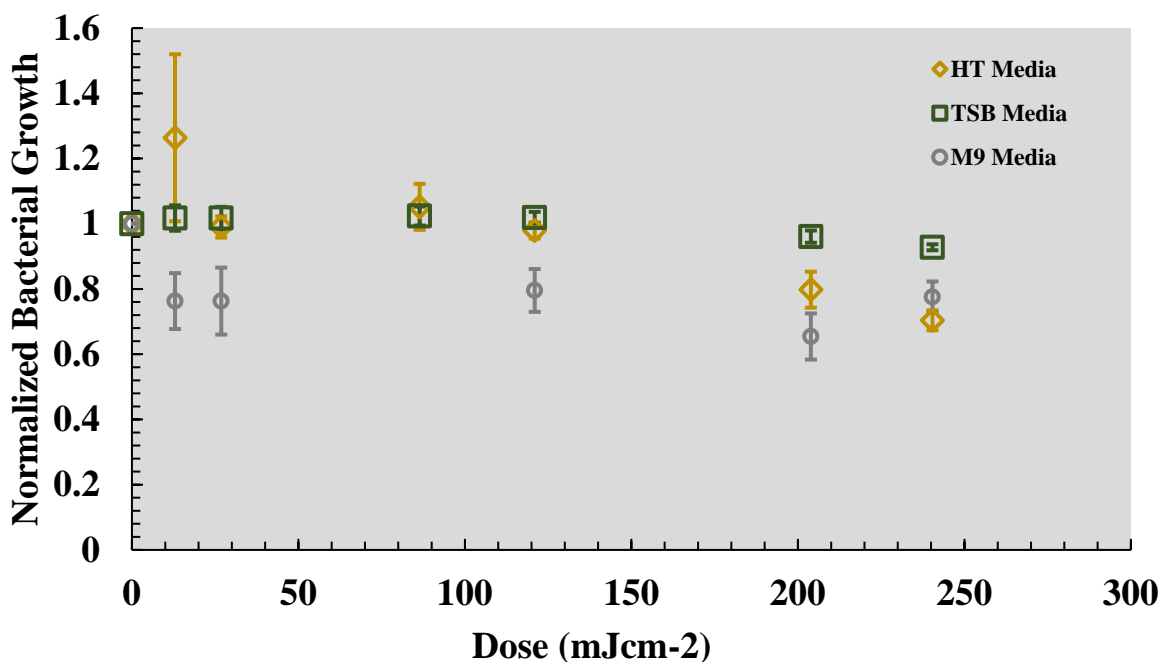


**Figure 26: Normalized Bacterial Growth as a function of dose for irradiated *E. coli* grown in all media. A starting *E. coli* concentrations of  $4.73 \pm 0.237 \times 10^8$ ,  $1.77 \pm 0.427 \times 10^9$ , and  $1.33 \pm 0.326 \times 10^8$  CFU mL<sup>-1</sup> were used for HT, TSB, and M9 media respectively. Bacterial growth was calculated from an OD<sub>620</sub> measurement. A normalized value of 1.0 represents zero growth difference between irradiated and dark, and bacteria were irradiated for 24 hr.**

In addition to evaluating the average of the normalized biofilm growth, overall trends were studied by normalizing each irradiated biofilm growth result to an overall dark control average of  $0.549 \pm 0.062$  in HT medium,  $1.536 \pm 0.293$  in TSB medium, and  $0.594 \pm 0.103$  in M9 medium (Figure 30). When fit to linear least sums regressions, all three slopes are less than 0.0021, suggesting what has been verified statistically above, that there is minimal change in bacterial growth as a function of applied low-intensity UVC dose.

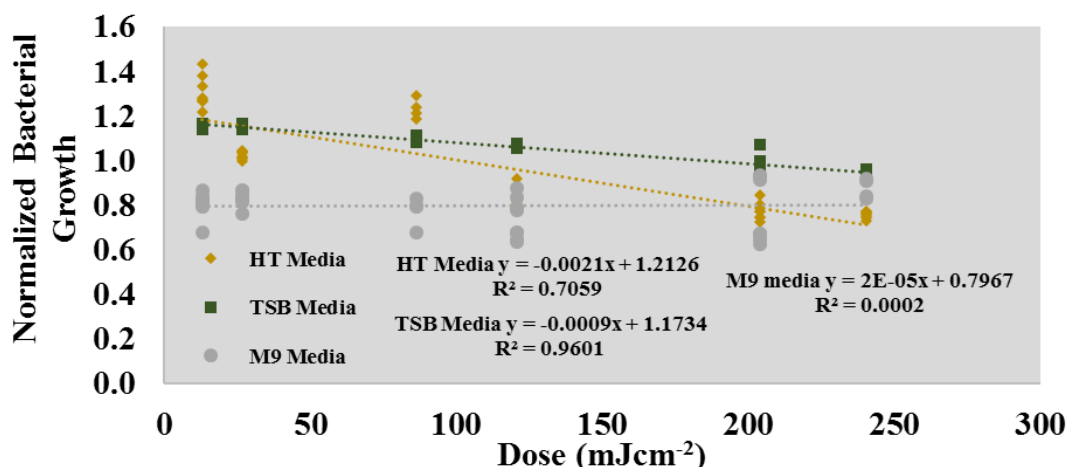


Figure 27: Normalized Bacterial Growth as a function of dose for irradiated *E. coli* grown in all media. Dotted lines represent linear regression. A starting *E. coli* concentrations of  $4.73 \pm 0.237 \times 10^8$ ,  $1.77 \pm 0.427 \times 10^9$ , and  $1.33 \pm 0.326 \times 10^8$  CFU mL<sup>-1</sup> were used for HT, TSB, and M9 media respectively. Bacterial growth was calculated from an OD<sub>620</sub> measurement. A normalized value of 1.0 represents zero growth difference between irradiated and dark, and bacteria were irradiated for 24 hr.

In general, bacteria grown in all media (Figure 29, 30) experienced minimal changes in bacterial growth at low-intensity UVC irradiation. It is curious that these results differ so greatly from the results obtained using plate counts (Figure 22). The difference between these results likely lies in the methods used. First, OD<sub>620</sub> measurements will account for all cells—dead or alive—in the sample, whereas plate counts will account only for those bacteria that are able to replicate on incubated plates. It appears that UVC makes it more difficult for bacteria to replicate on incubated agar plates after irradiation; however, it seems that bacteria can still replicate in media under these exposure conditions. That is, if the bacteria were mostly inactivated (as results in Figure 22 indicate), they would not be able to grow (as results in Figure 29 indicates). These contradicting results make it somewhat difficult to make conclusions concerning the overall health of irradiated planktonic bacteria.

## 5.4. Biofilm Formation

Biofilm growth was quantified by utilizing a colorimetric assay with safranin stain. Measured results were then normalized to the dark control for the same experiment. Figure 31 shows the normalized biofilm growth in HT medium as a function of applied dose. A value of one denotes no change in growth compared to the dark control. Standard deviation is a function of both irradiated and dark samples' standard deviation by using the propagation of error. For HT medium, normalized biofilm growth appeared to be reduced to  $0.585 \pm 0.477$  after an applied dose of  $12.96 \text{ mJcm}^{-2}$ . Little further change in biofilm growth was observed until a lethal dose of  $240.5 \text{ mJcm}^{-2}$  was applied, and normalized biofilm growth was  $0.324 \pm 0.124$ . It was only at this lethal dose where there was evidence to suggest a difference between irradiated samples and dark controls ( $p < 0.001$ ).

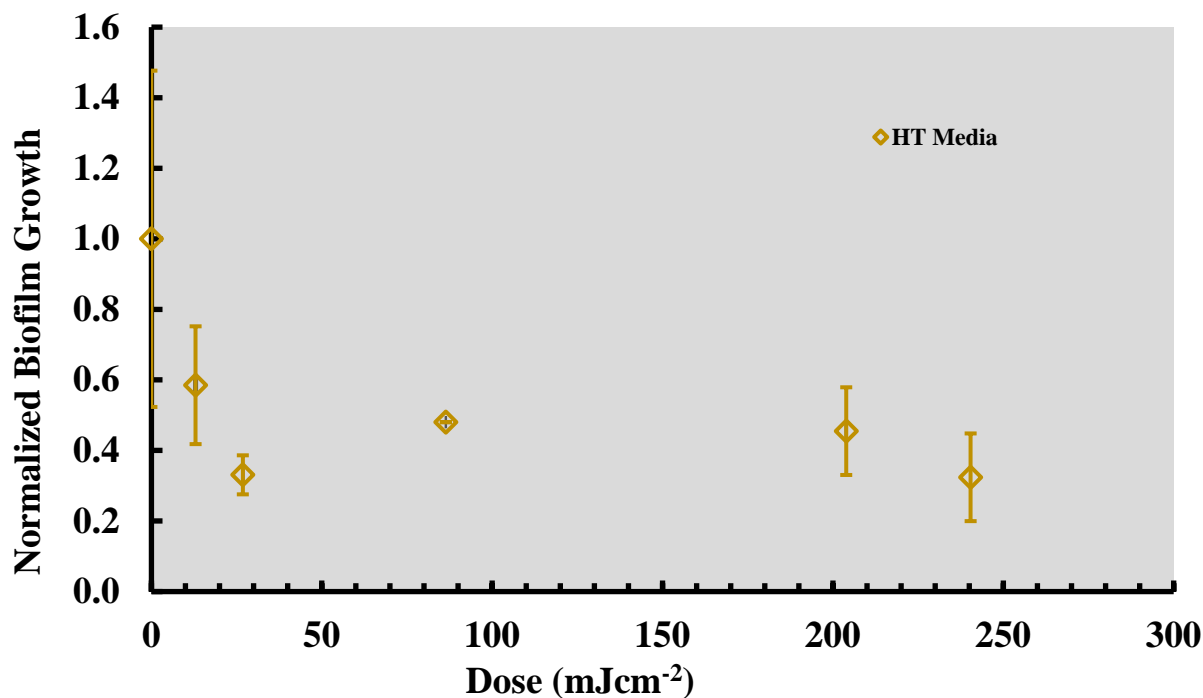
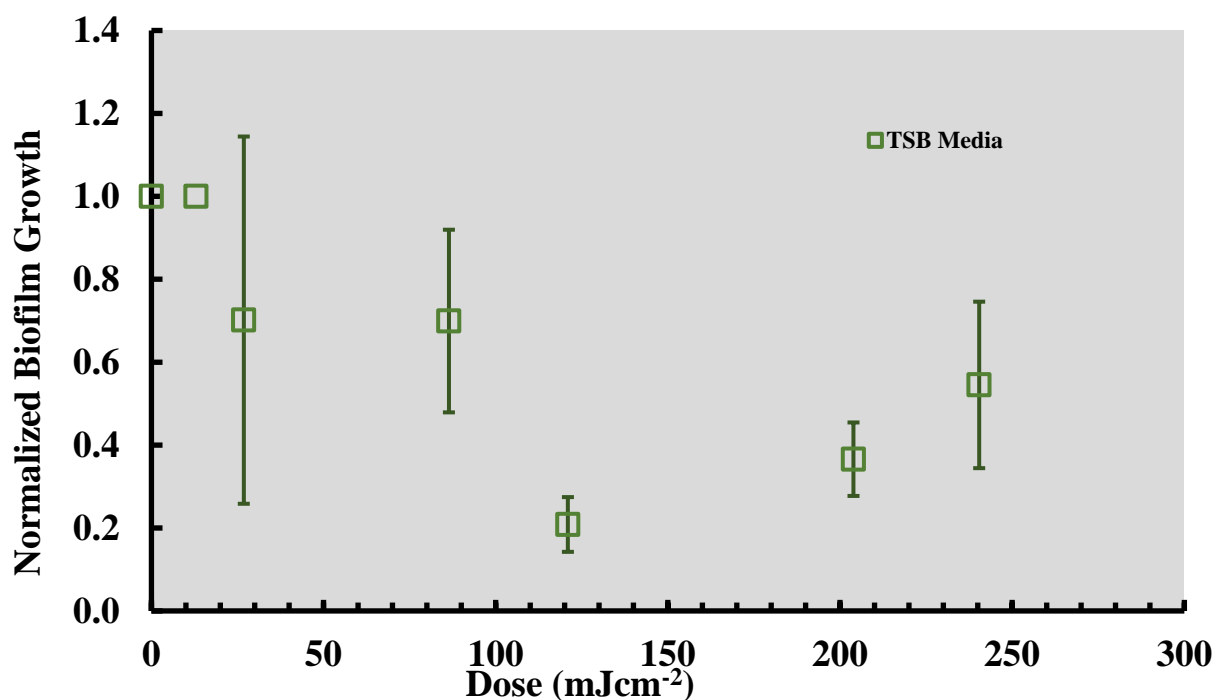


Figure 28: Normalized biofilm growth as a function of dose for irradiated *E. coli* grown in HT medium. A starting *E. coli* concentration of  $4.73 \pm 2.37 \times 10^8 \text{ CFU mL}^{-1}$  was used, and biofilm growth was quantified using a safranin stain read at 450 nm. A normalized value of 1.0 represents zero growth difference between irradiated and dark, and bacteria were irradiated for 24 hr.

For *E. coli* grown in TSB (Figure 32), normalized biofilm growth ranged between  $0.208 \pm 0.066$  at an applied dose of  $120.96 \text{ mJcm}^{-2}$  and  $1.00 \pm 3.07$  at an applied dose of  $12.96 \text{ mJcm}^{-2}$ . There is not sufficient evidence to suggest that biofilm growth is significantly affected at applied UV doses ranging from  $12.96 \text{ mJcm}^{-2}$  to  $240.5 \text{ mJcm}^{-2}$  ( $p > 0.989$ ).



**Figure 29: Normalized biofilm growth as a function of dose for irradiated *E. coli* grown in TSB medium. A starting *E. coli* concentration of  $1.77 \pm 0.427 \times 10^9 \text{ CFUmL}^{-1}$  was used, and biofilm growth was quantified using a safranin stain read at 450 nm. A normalized value of 1.0 represents zero growth difference between irradiated and dark, and bacteria were irradiated for 24 hr.**

For bacteria grown in M9 medium, normalized bacterial growth shows slight decreases from  $0.879 \pm 0.325$  at  $12.96 \text{ mJcm}^{-2}$  to  $0.378 \pm 0.261$  at  $240.4 \text{ mJcm}^{-2}$ . However, these differences are not significant ( $p > 0.366$ ). Figure 34 shows a combination of all trends.

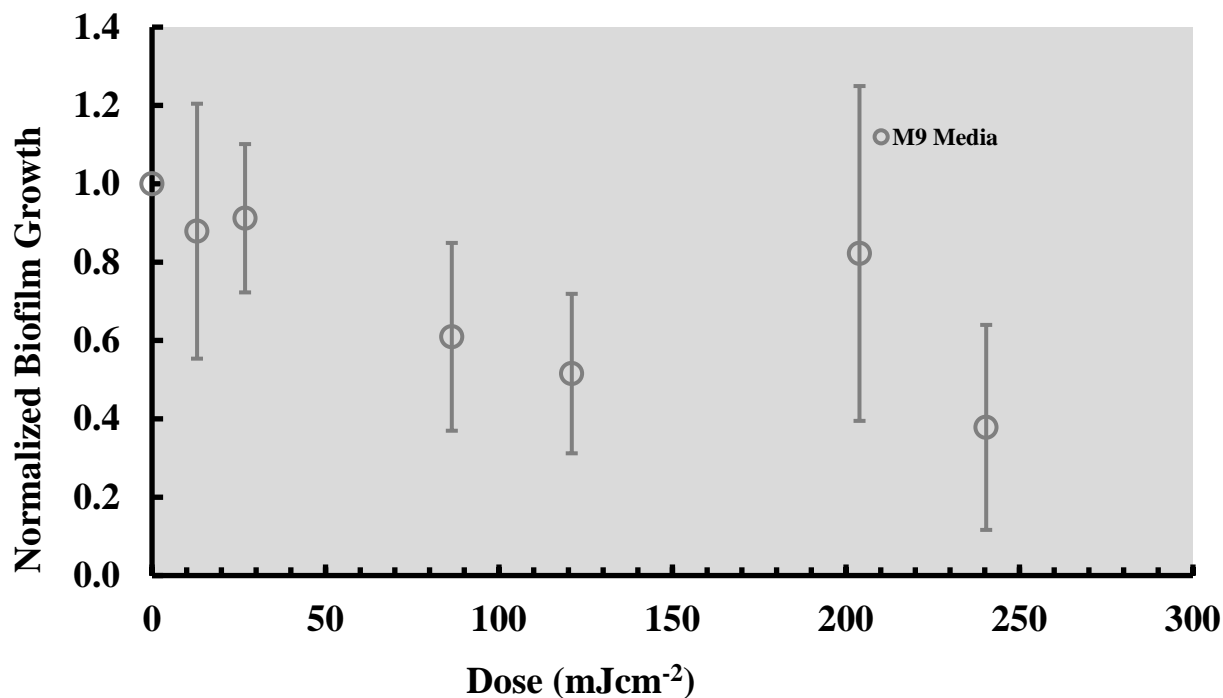


**Figure 30:** Normalized Biofilm Growth as a function of dose for irradiated *E. coli* grown in M9 medium. A starting *E. coli* concentration of  $1.33 \pm 0.326 \times 10^9 \text{ CFUmL}^{-1}$  was used, and biofilm growth was quantified using a safranin stain read at 450 nm. A normalized value of 1.0 represents zero growth difference between irradiated and dark, and bacteria were irradiated for 24 hr.

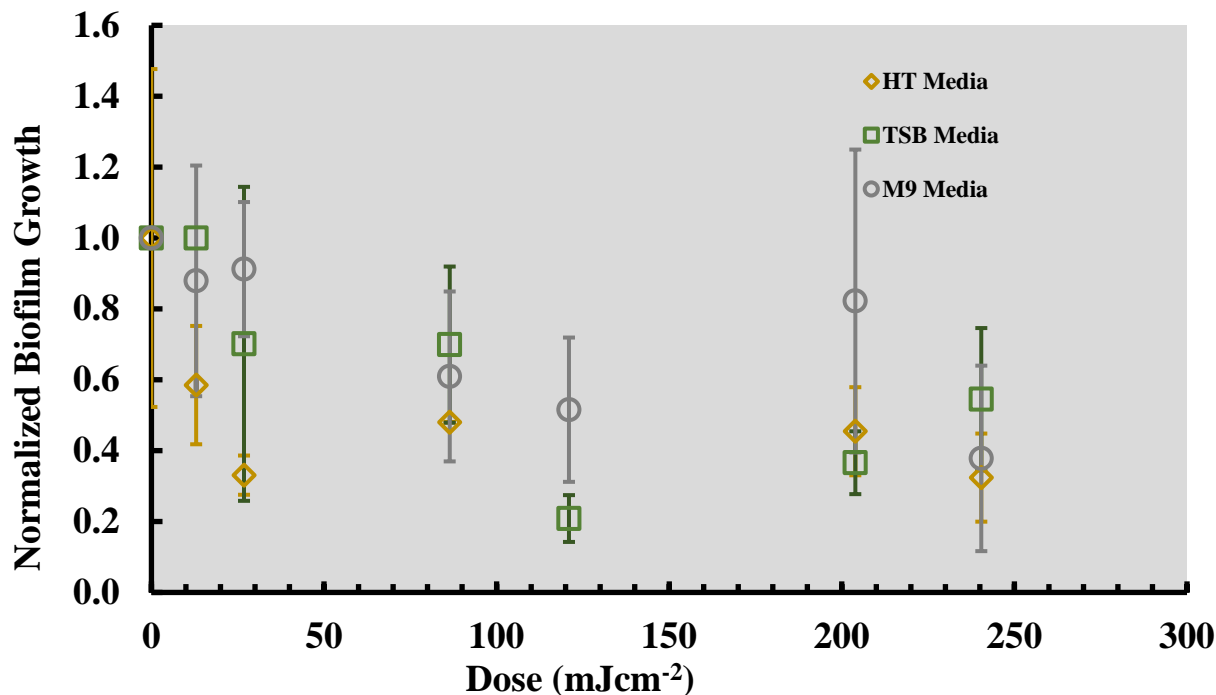


**Figure 31: Normalized biofilm growth as a function of dose for irradiated *E. coli* grown in all media.** Starting *E. coli* concentrations of  $4.73 \pm 0.237 \times 10^8$ ,  $1.77 \pm 0.427 \times 10^9$ , and  $1.33 \pm 0.326 \times 10^8$  CFUmL<sup>-1</sup> were used for HT, TSB, and M9 media respectively. Biofilm growth was quantified using a safranin stain read at 450 nm. A normalized value of 1.0 represents zero growth difference between irradiated and dark controls, and bacteria were irradiated for 24 hr. This Figure is a combination of Figures 31 to 33.

In addition to evaluating the average of the normalized biofilm growth, overall trends were studied by normalizing each irradiated biofilm growth result to an overall dark control average of  $0.257 \pm 0.114$ . These results are shown in Figure 35 where biofilm growth as a function of applied dose is inconclusive. The sporadic nature of these trends is evidenced by a linear fit ( $R^2$ ) of less than 0.6 in all cases. In addition to the poor fit, linear trends also suggest that increasing dose has minimal effect on the overall biofilm growth.



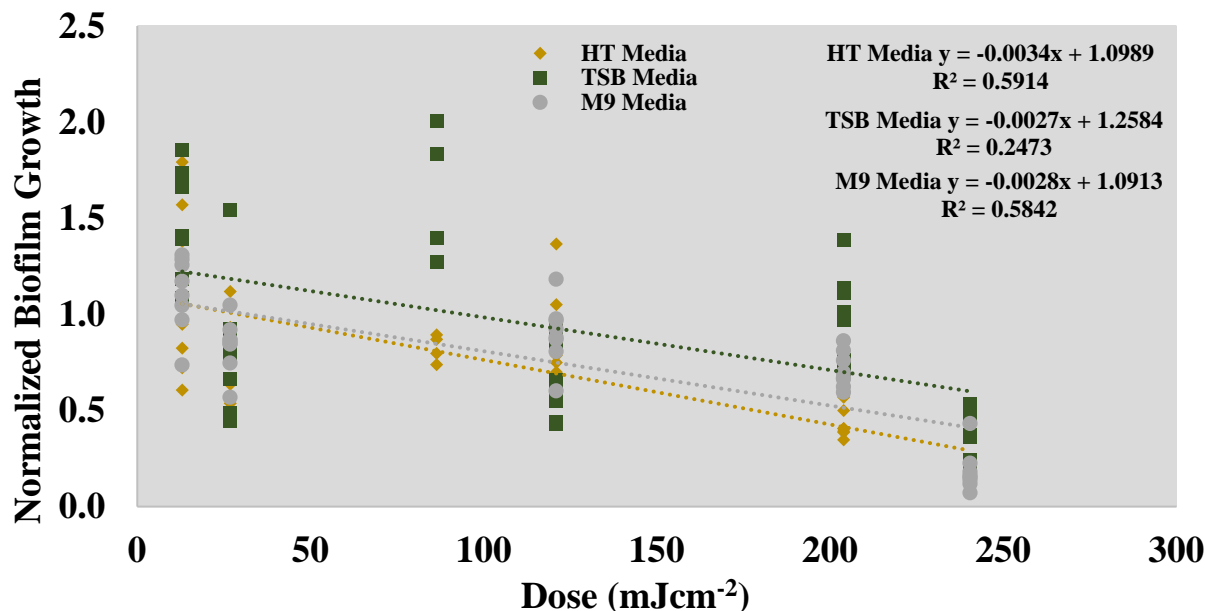


Figure 32: Normalized Biofilm Growth as a function of dose for irradiated *E. coli* grown in all media. Dotted lines represent linear regressions. Starting *E. coli* concentrations of  $4.73 \pm 0.237 \times 10^8$ ,  $1.77 \pm 0.427 \times 10^9$ , and  $1.33 \pm 0.326 \times 10^8$  CFU mL<sup>-1</sup> were used for HT, TSB, and M9 media respectively. Biofilm growth was quantified using a safranin stain read at 450 nm. A normalized value of 1.0 represents zero growth difference between irradiated and dark, and bacteria were irradiated for 24 hr.

Overall, there is little evidence that biofilm formation is affected at the low UVC doses studied here. Only the highest dose studied in HT media resulted in a statistically significant decrease in biofilm formation, 54.5%. This irradiation intensity also resulted in a significant reduction in bacterial growth (Figure 26) and a log removal of  $6.93 \pm 1.54$ . Thus, it is only when planktonic bacteria are significantly compromised that an effect on biofilm formation is observed.

## 5.5. Motility Analysis

### 5.5.1. Swimming Motility

The impact of low-intensity UVC on swimming motility is shown in Figure 36. For normalized results, a value of one represents no change from a dark control conducted during the

same test. In the case of swimming motility, a marked decrease ( $p = 0.0038$ ) in swimming occurred at  $11.23 \text{ mJcm}^{-2}$ , where normalized swimming was  $0.281 \pm 0.141$ . Almost no swimming occurred at a dose of  $203.9 \text{ mJcm}^{-2}$ , where normalized swimming was  $0.026 \pm 0.005$ . Based on these results, it was determined that there is statistical evidence to suggest that swimming motility is decreased even at low intensities of biocidal UV. In all cases, a ( $p < 0.004$ ). Because swimming is the method of transportation bacteria most often utilizes in stagnant conditions to reach a surface, it is postulated that the decrease in motility could aid in the prevention of initial contact between bacteria and the surface.

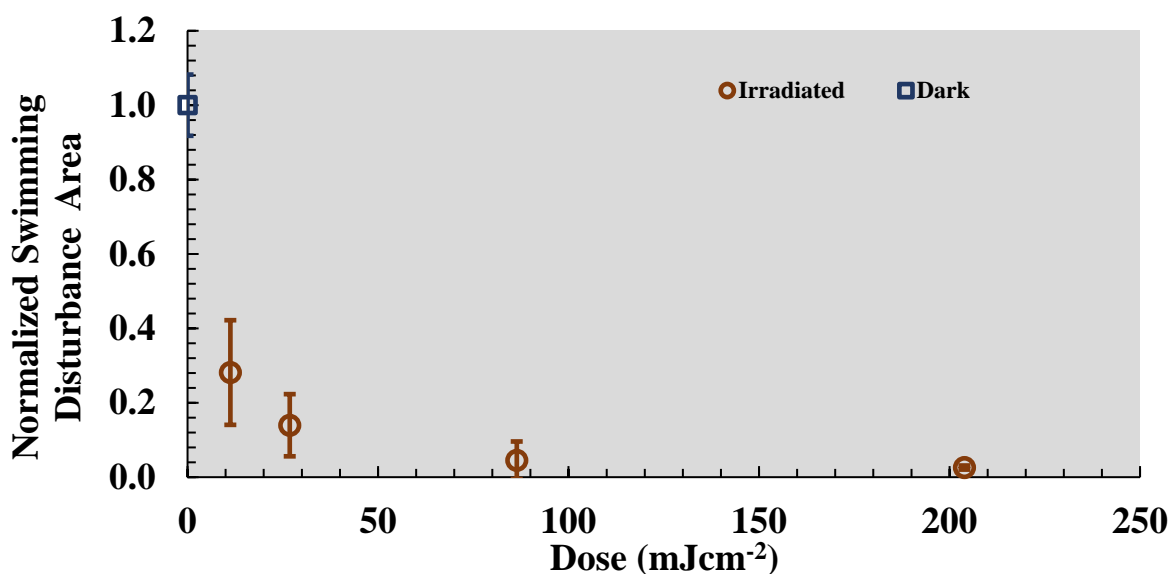


Figure 33: Normalized swim plate growth area results for *E. coli*. (1% tryptone, 0.5% NaCl, and 0.3% agar). Irradiation occurred over 24 hr. Error bars represent the combined standard error of the dark and irradiated values.

### 5.5.2. Swarming Motility

Swarming motility results were quantified by measuring swarm area using in ImageJ. Results were then normalized to a dark control and plotted as a function of applied dose (Figure 37). A value of one represents no change from a dark control. *E. coli* was found to display

featureless swarming [60]. This pattern of swarming in *E. coli* has been well documented [61] [62] and occurs when the outer edge of a swarm colony create a monolayer that is immobile [62].

Swarming motility decreased significantly at an applied dose of 53.64 mJcm<sup>-2</sup> to,  $0.180 \pm 0.085$  and  $0.088 \pm 0.061$  at an applied dose of 407.8 mJcm<sup>-2</sup> ( $p < 0.034 < 0.046$ ).

Increasing intensity after this point appears to have no additional effect on motility ( $p > 0.999$ ) when comparing between irradiated samples. Based on these results, it was determined that swarming motility decreases even at low intensities of biocidal UV. Because swarming is the method of transportation bacteria most often utilizes move across a surface, it is postulated that the decrease in motility could aid in partial prevention of biofilm attachment on a surface.

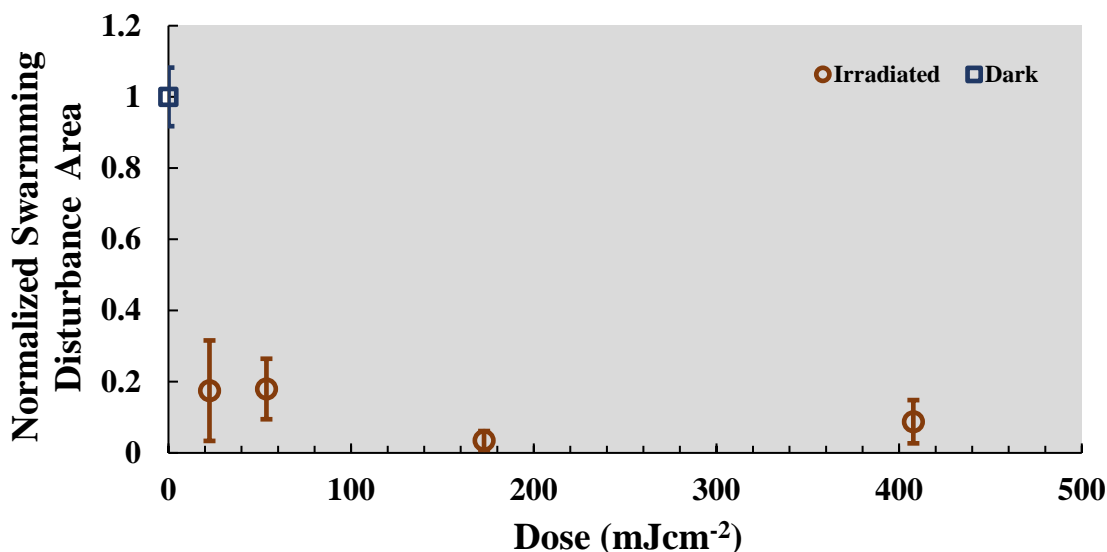


Figure 34: Normalized swarm plate growth area results for *E. coli* (0.5% agar, 8 g/L nutrient broth, and 8 g/L dextrose). Irradiation occurred over 48 hr.

Thus, both swimming and swarming are significantly affected in these tests at even low UVC doses. One must, however, be careful in interpreting these results, as the viability tests (Figure 22) indicate that significant inactivation may occur under these conditions. (However,

bacterial growth tests, Figure 29, indicate otherwise). As the health of the bacteria is in question, it is difficult to determine whether or not bacterial viability or concentration significantly affected the motility results observed. However, although motility tests do seem to indicate that bacteria could have difficulty forming biofilms under these UVC doses, few statistically significant differences in biofilm formation were actually observed (Figure 34).

## 6. Future Work and Recommendations

Although most of these results seem to indicate that biofilm formation is not suppressed at sub-lethal UVC doses, this study has made some interesting findings that warrant further study. The primary purpose of utilizing motility assays in this thesis was to determine an overall change in motility as a function of applied dose. By using confocal laser scanning microscopy, however, a more thorough analysis of the effect of low-intensity UVC irradiation on the mechanisms of motility could be performed. Motility should be more thoroughly quantified by two metrics. First, flagella stains should be utilized to evaluate oxidative damage both under irradiated and dark control conditions [43]. Second, swimming and swarming speeds should be evaluated by the utilization of microscopy and particle tracking [17]. By evaluating swimming and swarming speed, the direct effect of UV can also be evaluated in different media types. This would allow for evaluation of the hypothesis that UV directly, and negatively affects both swimming and swarming motility by causing oxidative damage to the flagella.

Moving forward, an additional recommendation is to better control experimental temperature. A thermostat-equipped space heater in a small lab should be sufficient to maintain a constant temperature during experiment time with the current apparatus or the apparatus could be modified to fit inside an incubator. By stabilizing experimental temperature, the variance in dark controls experienced during this thesis should be reduced. A second recommendation is to determine both initial and final colony counts using a spread plate.

In addition to the above recommendations, if this project is to be applied to the industry further analysis should be conducted. This thesis specifically evaluated the model organism *E. coli* in stagnant conditions. The first analysis that should be conducted would be to evaluate other model organisms, including *Pseudomonas aeruginosa* [45], *B. subtilis*, *Norovirus* [63], and

*Adenovirus* [63] under stagnant conditions. Additionally, for all media and model organisms, UVC irradiation should be evaluated on a flow system [43].

If the research discussed in this thesis is found to be valid, and there does exist a low-intensity dose that, when applied for extended time periods, can reduce biofouling due to planktonic bacteria, then testing should be conducted on different membranes to determine if low-intensity UV caused the same water filtration membrane degradation that high-intensity UV causes. If it is determined that low-intensity UVC does not cause membrane degradation, then pilot-scale testing should be conducted with the end goal being a low-intensity UVC application system for use within membranes. By applying low-intensity UVC to a membrane, and hopefully reducing biofilms, this technology would reduce chemical waste, increase productivity, and prolong membrane life. By augmenting the operations of membrane systems, it would allow for expansion of the use of membrane filtration for treatment of otherwise contaminated water systems. For example, RO technology could be better implemented in small, coastal communities that would otherwise not be capable of facilitating the maintenance costs.

## 7. Conclusions

Due to the rising human population, and the depletion of clean water sources, there is a drinking water crisis on planet earth. This crisis requires novel technologies to remove contaminants of concern and produce potable water. Perhaps the most promising technology for ending the drinking water crisis comes in the form of seawater desalination via the application of membrane technology. The most selective membrane type, reverse osmosis, operates by applying pressure to force water across a semi-permeable membrane and separate seawater into brine and potable water. Membrane technology, however, has a major operational downfall in the form of biofouling. Biofouling occurs when bacteria congregate on a surface and form EPS, a sticky polymer which is difficult to remove. Biofouling decreases productivity and increases operating cost. Additionally, traditional cleaning techniques for biofouling create chemical waste and take the membranes off-line, decreasing overall production.

If RO desalination is to be a viable technology for ending the drinking water crisis, then biofouling needs to be significantly reduced within membrane systems. Research currently focuses on preventing biofilms, including disinfecting the feed water. Due to bacteria's ability to self-replicate, however, if even a single bacterium survives initial biocide treatment, then biofouling can occur. Because of this, if disinfection is going to be applicable for biofouling prevention, then the biocide needs to be applied continuously throughout the treatment process.

The primary objective of this thesis was to determine if low-intensity UVC, when applied continuously over a 24-hour irradiation period, can reduce biofouling on a surface. To accomplish this, a custom-built apparatus was used to irradiate stagnant planktonic bacteria for 24 hours. Bacterial replication was estimated using OD<sub>620</sub> measurements while biofilm growth was quantified using a colorimetric assay. Additionally, the disinfection kinetics of low-intensity

irradiation of *E. coli* was fit to the Chick-Watson and Rennecker-Mariñas models to determine which model was followed. Initial bacterial counts were quantified by utilizing an OD<sub>600</sub> measurement while ending bacterial counts were quantified by utilizing spread plates. Effect of UVC at 254 nm on swimming and swarming motility were quantified by utilizing agar motility assays.

Ultimately, the hypothesis that there exists a sub-lethal dose which decreases biofilm growth was rejected. This rejection is because a statistically significant change in biofilm formation was only measured after the application of a lethal dose.

As part of the above hypothesis, the death kinetics model for planktonic *E. coli* experiencing low-intensity UVC irradiation in three media was evaluated. For all three media (HT, TSB, and M9), it was determined that the system of *E. coli* undergoing UVC irradiation fits the Chick-Watson death kinetics model.

Additionally, bacterial replication was evaluated by measuring the change in OD<sub>620</sub> in irradiated and dark plates. These results were used to evaluate the effect of low-intensity irradiation on bacterial growth. Traditional UV irradiation occurs over short time periods, usually on par with or less than the doubling time of bacteria. Therefore, bacterial replication is not traditionally evaluated as a function of applied dose. For this thesis, it was determined that for *E. coli* in HT medium, bacterial growth is only significantly affected at lethal doses while *E. coli* growth in M9 medium is not significantly affected at any applied dose. *E. coli* growth in TSB medium was sporadically significantly affected by UVC irradiation, but this fact is more likely due to climate variation throughout experimentation. These experiments determined that there exists an applied dose which has no effect on bacterial growth.



Interestingly, these results somewhat contradict the plate count results, indicating that further experiments would need to be carried out to determine the overall health of bacteria under low doses of UVC irradiation.

To further evaluate the primary hypothesis of this thesis, biofilm formation was evaluated at doses including those which had no significant effect on bacterial growth. It was determined, that for both TSB and M9 media, there is no evidence to suggest that biofilm formation is decreased by the application of low-intensity UVC irradiation. For *E. coli* in HT medium, there is only statistical evidence to suggest that biofilm growth is affected by UVC irradiation when a lethal dose, according to plate counts, is applied.

Unlike the primary hypothesis, the secondary hypothesis was verified. It was determined that even under sub-lethal irradiation, swimming and swarming motility are both significantly reduced. As discussed in the future work section, further tests are needed to determine if this relationship is correlated to bacterial death, or if it is directly caused by oxidative injury of flagella due to UVC irradiation.

While the primary hypothesis of this thesis was refuted, this study filled valuable knowledge gaps in the field of UVC application for biofilm prevention. It verified the effect of UVC on motility at low applied intensities, set standard operating procedures for experimentation with low doses of UVC, and identified and eliminated many concerns, such as climate control and contamination. Building upon the work in this thesis, future studies can focus on characterizing bacteria health during low-intensity UVC irradiation, using microscopic techniques to evaluate the effect of UVC on flagella and motility, and evaluating low-intensity UVC on other bacteria strains and at higher applied doses. Although sub-lethal UVC dose does not prevent biofilm prevention, the basic theories evaluated during this thesis could still provide

for a novel approach to biofilm prevention. For instance, a lethal dose of UVC could still potentially be applied within a closed system to prevent biofilm formation.

## 8. Bibliography

- [1] worldometers, "World Population," [Online]. Available:  
<http://www.worldometers.info/world-population/>. [Accessed 9 December 2018].
- [2] M. M. Mekonnen and A. Y. Hoekstra, "Four billion people facing severe water scarcity," *Science Advances*, 2016.
- [3] World Population Review , "Cape Town Population 2018," 2018.  
[Online]. Available: <http://worldpopulationreview.com/world-cities/cape-town-population/>. [Accessed 15 November 2018].
- [4] A. Baker, "What It's Like To Live Through Cape Town's Massive Water Crisis," *TIME*.
- [5] US EPA, "How We Use Water," [Online]. Available:  
<https://www.epa.gov/watersense/how-we-use-water>. [Accessed 9 December 2018].
- [6] M. Williams, "What percent of Earth is water?," Physics.org, 2 December 2014. [Online]. Available: <https://phys.org/news/2014-12-percent-earth.html>.  
[Accessed 14 November 2018].
- [7] A. K. Chapagain and A. Y. Hoekstra , "The global component of freshwater demand and supply: an assessment of virtual water flows between nations as a result of trade in agricultural and industrial products," *Water International*, pp. 19-32, 2008.

- [8] U. Caldera and C. Breyer, "Learning Curve for Seawater Reverse Osmosis Desalination Plants: Capital Cost Trend of the Past, Present, and Future," *Water Resources Research*, 2017.
- [9] General Electric Company, "Africa's Largest Seawater Desalination Plant Eases Water Scarcity for City of Algiers, Algeria," , June 2016. [Online]. Available: <https://www.suezwatertechnologies.com/sites/default/files/documents/CS1338EN.pdf>. [Accessed 14 November 2018].
- [10] Tampa Bay Water, "Tampa Bay Seawater Desalination Plant," [Online]. Available: <https://www.tampabaywater.org/tampa-bay-seawater-desalination-plant>. [Accessed 14 November 2018].
- [11] T. Smedley, "Is the world running out of fresh water?," BBC, 12 April 2017. [Online]. Available: <http://www.bbc.com/future/story/20170412-is-the-world-running-out-of-fresh-water>. [Accessed 15 November 2018].
- [12] H. C. Flemming, G. Schaule, T. Griebel, J. Schmitte and A. Tamachkierow, "Biofouling- the Achilles heel of membrane processes.," *Elsevier*, pp. 215-225, 1997.
- [13] P. Tingpej, R. Tiengtip and S. Kondo, "Decontamination Efficacy of Ultraviolet Radiation Against Biofilms of Common Nosocomial Bacteria," *J Medical Association Tai*, vol. 98, no. 6, 2015.

- [14 J. C. Crittenden, R. R. Trussell, D. W. Hand, K. J. Howe and G.  
] Tchobanoglous, *Water Treatment Principles and Design*, John Wiley and Sons,  
2012.
- [15 T. Nguyen, F. A. Roddick and L. Fam , "Biofouling of Water Treatment  
] Membranes: a Review of Underlying Causes, Monitoring Techniques and Control  
Measures," *Membranes*, pp. 804-840, 2012.
- [16 G. Tragidrdh , "Membrane Cleaning," *Elsevier*, pp. 325-335, 1989.  
]
- [17 T. Atsumi, E. Fujimoto, M. Fuuta and M. Kato, "Effect of gamma-ray  
] Irradiation on Escheria Coli motility," *Central European Journal of Biology*,  
2014.
- [18 E. L. Cates, M. Cho and J.-H. Kim, "Converting Visible Light into UVC:  
] Microbial Inactivation by Pr<sup>3+</sup>-Activated Upconversion Materials,"  
*Environmental Science and Technology*, pp. 3680-3866, 2011.
- [19 L. Li and C. Visvanathan, "Membrane technology for surface water  
] treatment: advancement from microfiltration to membrane bioreactor," *Springer*,  
pp. 737-760, 2017.
- [20 C. Bell , F. W. Brownell, D. R. Case, A. N. Davis , K. A. Ewing and J. O.  
] King, *Environmental Law Handbook*, Bernan Press, 2013.
- [21 K. Zodrow, Artist, [Art]. Montana Tech of the University of Montana.  
]

- [22 H. C. Flemming, "Biofouling in water systems--cases, causes and  
] countermeasures," *Applied Microbiology and Biotechnology*, vol. 59, no. 6, 2002.
- [23 M. Herzberg and M. Elimelech, "Biofouling of reverse osmosis  
] membranes: Role of biofilm-enhanced osmotic pressure," *Journal of Membrane Science*, pp. 11-20, 2007.
- [24 D. Davies, "Understanding Biofilm Resistance to Antibacterial Agents,"  
] *Nature*, pp. 114-122, 2003.
- [25 K. Sauer, A. K. Camper, G. D. Ehrlich, J. W. Costerton and D. G. Davies,  
] "Pseudomonas aeruginosa Displays Multiple Phenotypes during Development as a Biofilm," *Journal of Bacteriology*, pp. 1140-1154, 2002.
- [26 W. Song, C. Zhao, D. Zhang, S. Mu and X. Pan, "Different Resistance To  
] UV-B Radiation of Extracellular Polymeric Substances of Two Cyanobacteria from Contrasting Habitats," *Frontiers in Microbiology*, vol. 7, 2016.
- [27 A. Matin, Z. Khan, S. Zaidi and M. Boyce, "Biofouling in reverse osmosis  
] membranes for seawater desalination: Phenomena and prevention," *Elsevier*, 2003.
- [28 E. D. d. Avila, R. S. d. Molon, C. E. Vergani, F. d. A. Mollo, Jr. and V.  
] Salih, "The relationship between biofilm and physical-chemical properties of implant abutment materials for successful dental implants," *Materials*, pp. 3651-3662, 2014.
- [29 A. sakamoto, Y. Terui, C. Horie, T. Fukui, T. Masuzawa, S. Sugawara, K.  
] Shigets, T. Shigeta, K. Igarashi and K. Kashiwagi, "Antibacterial effects of

protruding and recessed shark skin micropatterned surfaces of polyacrylate plate with a shallow groove," *FEMS Microbiology Letters*, vol. 361, no. 1, pp. 10-16, 2014.

- [30        E. Bar-Zeev, I. Berman-Frank, O. Girshevitz and T. Berman, "Revised  
]        Paradigm of Aquatic Biofilm Formation Facilitated by Microgel Transparent  
Exopolymer Particles," *PNAS*, vol. 109, 2012.
  
- [31        K. Marshall and B. L. Blainey, "ROLE OF BACTERIAL ADDESION IN  
]        BIOFILM FORMATION AND BIOCORROSION," in *International Workshop  
on Industrial Biofouling and Biocorrosion*, Stuttgart, 1990.
  
- [32        J. M. Willey, L. M. Sherwood and C. J. Woolverton , Prescott's  
]        Microbiology, New York : McGraw Hill Companies Inc. , 2014.
  
- [33        A. Amaro-Ortiz, B. Yan and J. A. D'Orazio, "Ultraviolet Radiation,  
]        Aging and the Skin: Prevention of Damage by Topical cAMP Manipulation,"  
*Molecules*, pp. 6202-6219, 2014.
  
- [34        T. Dai, M. S. Vrahas, C. K. Murray and M. R. Hamblin, "Ultraviolet C  
]        irradiation:an alternative antimicrobial approach to localized infections," *National  
Institutes of Health*, pp. 185-195, 2012.
  
- [35        Y.-Y. He and D.-P. Hader, "Involvement of rective oxygen in the UV-B  
]        damage to the cyanobacterium *Anabaena* sp.," *Elsevier*, pp. 73-80, 2002.
  
- [36        D. Monroe, "Looking for Chinks in the Armor of Bacterial Biofilms,"  
]        *PLOS Biology*, vol. 5, no. 11, pp. 2458-2461, 2007.

- [37            L.-Z. Chen , G.-H. Wang, A. Liu, C. Li and Y.-D. Liu, "UV-B Oxidative  
]            Damage and Protective Role of Exopolysaccharides in Desert Cyanobacterium  
             Microcoleus vaginatus," *Journal of integrative Plant Biology*, 2008 .
- [38            M. O. Elasri and R. V. Miller, "Study of the Response of a Biofilm  
]            Bacterial Community to UV Radiation," *Applied and Environmental  
             Microbiology* , 1999.
- [39            N. Redman, C. Good and B. J. Vinci, "Assessing the Utility of Ultraviolet  
]            Irradiation to Reduce Bacterial Biofilms in Fish Hatchery Well Water Supplies,"  
             *Journal of Aquaculture Research and Developement*, vol. 8, no. 7, 2017.
- [40            V. F. Zenoff, F. Sinerix and M. E. Farias, "Diverse Responses to UV-B  
]            Radiation and Repair Meachnaisms of Bacteria Isolated from High-Altitude  
             Aquatic Environments," *Applied and Environmental Microbiology* , pp. 7857-  
             7863, 2006.
- [41            E. Van Donk and D. O. Hessen , "Loss of flagella in the green alga  
]            Chlamydomonas reinhardtii due to in situ UV-exposure," *Scientia Marina*, pp.  
             107-112, 1995.
- [42            S. D. Mora, S. Demers and M. Vernet, The Effects of UV Radiation in the  
]            Marine Environment, Cambridge University Press, 2000.
- [43            P. M. Merritt, T. Danhorn and C. Fuqua, "Motility and Chemotaxis in  
]            Agrobacterium tumefaciens Surface Attachment and Biofilm Formation," *Journal  
             of Bacteriology* , pp. 8005-8014, 2007.



- [44 M. Flethcher, Bacterial Adhesion: Molecular and Ecological Diversity,  
] New York City: John Wiley and Sons, 1996.
- [45 E. Deziel, Y. Comeau and R. Villemur, "Initiation of Biofilm Formation  
] by Pseudomonas aeruginosa 57 RP correlates with Emergence of Hyperppilated  
and Highly Adherent Phenotypic Variants Deficient in Swimming, Swarming,  
and Twitching Motilities," *Journal of Bacteriology* , vol. 183, pp. 1195-1204,  
2001.
- [46 D.-P. Hader and M. Hader, "Effects of Solar and Artificail UV Radiation  
] on Motility and Pigmentation in the Marine Cryptomonas Maculata,"  
*Environmental and experimental botany*.
- [47 N. Morales-Soto, M. E. Anyan, A. E. Mattingly, C. S. Madukoma, C. W.  
] Harvey, M. Alber, E. Deziel, D. B. Kearns and J. D. Shrout, "Preparation,  
Imaging, and Quantification of Bacterial Surface Motility Assays," *Journal of  
Visualized Experiments*, 2015.
- [48 N. Morales-Soto, M. E. Anyan, A. E. Mattingly, C. S. Madukoma, C. W.  
] Harvey, M. Alber, E. Deziel, D. B. Kearns and J. D. Shrout, "Preparation,  
Imaging, and Quantification of Bacterial Surface Motility Assays," *Journal of  
Visualized Experiments*, 2015.
- [49 A. B. T. Semmler, C. B. Whitchurch and J. S. Mattick, "A re-examination  
] of twitching motility in Psuedomonas aeruginosa," *Microbiology*, pp. 2863-2873,  
1999.

- [50] J. R. Bolton and K. G. Linden, "standardization of methods for fluence (uv dose) determination in bench-scale uv experiments.," *journal of environmental engineering*, pp. 209-215, 2003.
- [51] J.-H. Jung, N.-Y. Choi and S.-Y. Lee, "Biofilm formation and exopolysaccharide (EPS) production by *Cronobacter sakazakii* depending on environmental conditions," *Elsevier*, pp. 70-80, 2013.
- [52] H. Torkzadeh, Clemson Univeristy , 2018.
- [53] K. R. Zodrow, J. D. Schiffman and M. Elimelech, "Biodegradable Polymer (PLGA) Coatings Featuring Cinnamaldehyde and Carvacrol Mitigate Biofilm Formation," *Langmuir*, pp. 13993-13999, 2017.
- [54] J. Schindelin, I. Arganda-Carreras and E. Frise, "Fiji: an open-source platform for biological-image analysis," *Nature Methods*, pp. 676-682.
- [55] N. Sauvonnet, P. Gounon and A. P. Pugsley, "PpdD Type IV Pilin of *Escherichia coli* K-12 Can Be Assembled into Pili in *Pseudomonas aeruginosa*," *Journal of Bacteriology* , vol. 182, pp. 848-854, 2000.
- [56] R Core Team 2013, "R: A language and environment for statistical," R Foundation for Statistical Computing, [Online]. Available: <http://www.R-project.org>.
- [57] R. A. Serway and J. W. Jewett, *Physics for Scientists and Engineers* 6th Edition, Thomson Brooks/Cole, 2004.

- [58        B. F. Severin, M. T. Suidan and R. S. Engelbrecht, "Kinetic Modeling of  
]        U.V. Disinfection of Water," *Elsevier*, vol. 17, no. 11, pp. 1669-1678, 1983.
  
- [59        Y. Gilba and E. Friedler, "UV disinfection of RBE-treated light greywater  
]        effluent: Kinetics, survival and regrowth of selected microorganisms," *Elsevier*,  
pp. 1043-1050, 2008.
  
- [60        D. B. Kearns, "A field guide to bacterial swarming motility," *Nature*  
]        *Reviews Microbiology*, pp. 634-644, 2010.
  
- [61        J.-M. swiecicki, O. Sliusarenko and D. B. Weibel, "From swimming to  
]        swarming: Escherichia coli cell motility in two-dimensions," *Integrative Biology*,  
no. 12, 2013.
  
- [62        M. F. Copeland and D. B. Weibel, "Bacterial Swarming: A Model System  
]        for Studying Dynamic Self-assembly," *Soft Matter*, no. 6, 2009.
  
- [63        C. R. Kanna and J. Ottoson, *Inactivation of Viruses in water by*  
]        *chlorination using bacteriophages as model organisms.*, Swedish University of  
Agricultural Sciences, 2015.
  
- [64        L. Hall-Stoodley, J. W. Costerton and P. Stoodley, "Bacterial Biofilm:  
]        from the natural envrionmentl to infection diseases".
  
- [65        B. D. Wilson, MD, M. S. Moon, BS and F. Armstrong, DO,  
]        "Comprehensive Review of Ultraviolet Radiation and the Current Status on  
Sunscreens," *The Journal of Clinical and Aesthetic Dermatology*, vol. 5`, no. 9,  
2012.

- [66] E. Cates and K. Zodrow , "Collaborative REasearch:WRF: Mechanisms an  
] dQuantification of Biofilm Inhibition by Continuous Lethal and Sublethal  
Ultraviolet-A, B, and C Irradiation," 2017.
- [67] Sigma-Aldrich, "Introduction to Microbial Media," [Online]. Available:  
] [https://www.sigmaaldrich.com/technical-documents/articles/biology/microbial-](https://www.sigmaaldrich.com/technical-documents/articles/biology/microbial-media.html)  
media.html. [Accessed 30 December 2018].

## 9. Appendix A – Biofilm Growth ANOVA Code

```
## Analysis of Biofilm Data
```

```
## ANOVA and post hoc Tukey Test
```

```
## Biofilm Assay OD Values
```

```
# Dark Control HT
```

```
y1 = c(0.3094, 0.3704, 0.4056, 0.4216, 0.2709, 0.3297, 0.3709, 0.4815, 0.4738, 0.4252, 0.3826,
0.5111, 0.1540, 0.1138, 0.1188, 0.1751, 0.1612, 0.1054, 0.1773, 0.18510, 0.1554, 0.2472,
0.2617, 0.2085, 0.2814, 0.2953, 0.4135, 0.2995, 0.266875, 0.277875, 0.225175, 0.330675,
0.290375, 0.196575, 0.233475, 0.201575, 0.170025, 0.097225, 0.145425, 0.198025, 0.199825,
0.185225, 0.066725, 0.107925)
```

```
# Irradiated HT September 5, 2018
```

```
y2 = c(0.2294, 0.2234, 0.2046, 0.1897)
```

```
# Dark Control TSB
```

```
y3 = c(0.1518, 0.1637, 0.1693, 0.1978, 0.1021, 0.0927, 0.0678, 0.1844, 0.1235, 0.1378, 0.0751,
0.1333, 0.1712, 0.0574, 0.0867, 0.0513, 0.0534, 0.0747, 0.0807, 0.0447, 0.0555, 0.0302, 0.0377,
0.0430, 0.0271, 0.0312, 0.0371, 0.0279, 0.093675, 0.065175, 0.103275, 0.058675, 0.093475,
0.077775, 0.090775, 0.126375, 0.082025, 0.049725, 0.058125, 0.048125, 0.065925, 0.053725,
0.052325)
```

```
# Irradiated TSB September 5, 2018
```

```
y4 = c(0.1692, 0.1177, 0.1547, 0.1071)
```

```
# Irradiated HT September 7, 2018
```

```
y5 = c(0.1556, 0.2116, 0.2806, 0.3542, 0.4031, 0.4603, 0.2436, 0.1854)
```

```
# Irradiated TSB September 7, 2018
```

```
y6 = c(0.0999, 0.1465, 0.1430, 0.0917, 0.1173, 0.1186, 0.1567, 0.1404)
```

```
# Dark Control M9
```

```
y7 = c(0.3520, 0.3407, 0.3273, 0.3966, 0.4075, 0.4049, 0.5415, 0.4035, 0.2761, 0.3075, 0.2935,
0.3272, 0.3706, 0.3387, 0.4014, 0.3457, 0.4192, 0.2474, 0.1882, 0.6958, 0.6712, 0.4745, 0.5450,
0.4749, 0.328075, 0.274775, 0.412575, 0.499075, 0.268875, 0.329075, 0.029975, 0.120075,
0.087625, 0.135725, 0.261825, 0.113225, 0.058025, 0.130725, 0.134125, 0.361625)
```

```
# Irradiated M9 September 7, 2018
```

```
y8 = c(0.3597, 0.2410, 0.3837, 0.4114, 0.4210, 0.4283, 0.3425, 0.3179)
```

```
# Irradiated HT September 10, 2018
```

```
y9 = c(0.1919, 0.2317, 0.2265, 0.2874, 0.2395, 0.1380, 0.2256, 0.1633)
```



```
# ANOVA for Biofilm Assay Results
data = data.frame(y = y, group = factor(group))
fit <- aov(y ~ group, data)
anova(fit)
```

```
# Tukey Honestly Significant Differences
TukeyHSD(fit)
```

```
# Results for Biofilm Assay Results
```

```
# Fit: aov(formula = y ~ group, data = data)
```

```
# $group
      diff      lwr      upr  p adj
2-1 -0.04501818 -0.2123987360 0.1223623723 0.9999455
3-1 -0.17241469 -0.2411436542 -0.1036857327 0.0000000
4-1 -0.11961818 -0.2869987360 0.0477623723 0.5036162
5-1  0.03000682 -0.0931819341 0.1531955705 0.9999858
6-1 -0.13003068 -0.2532194341 -0.0068419295 0.0269606
7-1  0.07061432  0.0005940087 0.1406346276 0.0456389
8-1  0.10639432 -0.0167944341 0.2295830705 0.1834173
9-1 -0.04380568 -0.1669944341 0.0793830705 0.9981848
10-1 -0.19251818 -0.3157069341 -0.0693294295 0.0000163
11-1  0.01781932 -0.1053694341 0.1410080705 1.0000000
12-1 -0.03183068 -0.1550194341 0.0913580705 0.9999682
13-1 -0.20044318 -0.3236319341 -0.0772544295 0.0000053
14-1  0.03815682 -0.0850319341 0.1613455705 0.9996594
15-1 -0.20939318 -0.3325819341 -0.0862044295 0.0000014
16-1 -0.22373068 -0.3469194341 -0.1005419295 0.0000002
17-1 -0.19614318 -0.3193319341 -0.0729544295 0.0000098
3-2 -0.12739651 -0.2949391777 0.0401461545 0.3883270
4-2 -0.07460000 -0.3012343417 0.1520343417 0.9992766
5-2  0.07502500 -0.1212460973 0.2712960973 0.9958807
6-2 -0.08501250 -0.2812835973 0.1112585973 0.9847393
7-2  0.11563250 -0.0524440262 0.2837090262 0.5737000
8-2  0.15141250 -0.0448585973 0.3476835973 0.3621733
9-2  0.00121250 -0.1950585973 0.1974835973 1.0000000
10-2 -0.14750000 -0.3437710973 0.0487710973 0.4098732
11-2  0.06283750 -0.1334335973 0.2591085973 0.9994854
12-2  0.01318750 -0.1830835973 0.2094585973 1.0000000
13-2 -0.15542500 -0.3516960973 0.0408460973 0.3162102
14-2  0.08317500 -0.1130960973 0.2794460973 0.9877330
15-2 -0.16437500 -0.3606460973 0.0318960973 0.2264184
16-2 -0.17871250 -0.3749835973 0.0175585973 0.1217574
```

17-2 -0.15112500 -0.3473960973 0.0451460973 0.3655875  
 4-3 0.05279651 -0.1147461545 0.2203391777 0.9995774  
 5-3 0.20242151 0.0790125826 0.3258304406 0.0000042  
 6-3 0.04238401 -0.0810249174 0.1657929406 0.9987939  
 7-3 0.24302901 0.1726220603 0.3134359629 0.0000000  
 8-3 0.27880901 0.1554000826 0.4022179406 0.0000000  
 9-3 0.12860901 0.0052000826 0.2520179406 0.0314285  
 10-3 -0.02010349 -0.1435124174 0.1033054406 1.0000000  
 11-3 0.19023401 0.0668250826 0.3136429406 0.0000235  
 12-3 0.14058401 0.0171750826 0.2639929406 0.0097738  
 13-3 -0.02802849 -0.1514374174 0.0953804406 0.9999947  
 14-3 0.21057151 0.0871625826 0.3339804406 0.0000013  
 15-3 -0.03697849 -0.1603874174 0.0864304406 0.9997763  
 16-3 -0.05131599 -0.1747249174 0.0720929406 0.9898877  
 17-3 -0.02372849 -0.1471374174 0.0996804406 0.9999995  
 5-4 0.14962500 -0.0466460973 0.3458960973 0.3836430  
 6-4 -0.01041250 -0.2066835973 0.1858585973 1.0000000  
 7-4 0.19023250 0.0221559738 0.3583090262 0.0107267  
 8-4 0.22601250 0.0297414027 0.4222835973 0.0083451  
 9-4 0.07581250 -0.1204585973 0.2720835973 0.9953795  
 10-4 -0.07290000 -0.2691710973 0.1233710973 0.9970108  
 11-4 0.13743750 -0.0588335973 0.3337085973 0.5413915  
 12-4 0.08778750 -0.1084835973 0.2840585973 0.9791454  
 13-4 -0.08082500 -0.2770960973 0.1154460973 0.9908526  
 14-4 0.15777500 -0.0384960973 0.3540460973 0.2908593  
 15-4 -0.08977500 -0.2860460973 0.1064960973 0.9742374  
 16-4 -0.10411250 -0.3003835973 0.0921585973 0.9093466  
 17-4 -0.07652500 -0.2727960973 0.1197460973 0.9948830  
 6-5 -0.16003750 -0.3202921799 0.0002171799 0.0507289  
 7-5 0.04060750 -0.0835252412 0.1647402412 0.9993293  
 8-5 0.07638750 -0.0838671799 0.2366421799 0.9625047  
 9-5 -0.07381250 -0.2340671799 0.0864421799 0.9725191  
 10-5 -0.22252500 -0.3827796799 -0.0622703201 0.0002835  
 11-5 -0.01218750 -0.1724421799 0.1480671799 1.0000000  
 12-5 -0.06183750 -0.2220921799 0.0984171799 0.9954308  
 13-5 -0.23045000 -0.3907046799 -0.0701953201 0.0001298  
 14-5 0.00815000 -0.1521046799 0.1684046799 1.0000000  
 15-5 -0.23940000 -0.3996546799 -0.0791453201 0.0000522  
 16-5 -0.25373750 -0.4139921799 -0.0934828201 0.0000115  
 17-5 -0.22615000 -0.3864046799 -0.0658953201 0.0001989  
 7-6 0.20064500 0.0765122588 0.3247777412 0.0000064  
 8-6 0.23642500 0.0761703201 0.3966796799 0.0000709  
 9-6 0.08622500 -0.0740296799 0.2464796799 0.8990953  
 10-6 -0.06248750 -0.2227421799 0.0977671799 0.9948784  
 11-6 0.14785000 -0.0124046799 0.3081046799 0.1088675  
 12-6 0.09820000 -0.0620546799 0.2584546799 0.7613334



13-6 -0.07041250 -0.2306671799 0.0898421799 0.9824393  
 14-6 0.16818750 0.0079328201 0.3284421799 0.0288986  
 15-6 -0.07936250 -0.2396171799 0.0808921799 0.9478049  
 16-6 -0.09370000 -0.2539546799 0.0665546799 0.8205892  
 17-6 -0.06611250 -0.2263671799 0.0941421799 0.9906799  
 8-7 0.03578000 -0.0883527412 0.1599127412 0.9998643  
 9-7 -0.11442000 -0.2385527412 0.0097127412 0.1097276  
 10-7 -0.26313250 -0.3872652412 -0.1389997588 0.0000000  
 11-7 -0.05279500 -0.1769277412 0.0713377412 0.9872776  
 12-7 -0.10244500 -0.2265777412 0.0216877412 0.2486211  
 13-7 -0.27105750 -0.3951902412 -0.1469247588 0.0000000  
 14-7 -0.03245750 -0.1565902412 0.0916752412 0.9999627  
 15-7 -0.28000750 -0.4041402412 -0.1558747588 0.0000000  
 16-7 -0.29434500 -0.4184777412 -0.1702122588 0.0000000  
 17-7 -0.26675750 -0.3908902412 -0.1426247588 0.0000000  
 9-8 -0.15020000 -0.3104546799 0.0100546799 0.0946834  
 10-8 -0.29891250 -0.4591671799 -0.1386578201 0.0000001  
 11-8 -0.08857500 -0.2488296799 0.0716796799 0.8772816  
 12-8 -0.13822500 -0.2984796799 0.0220296799 0.1851523  
 13-8 -0.30683750 -0.4670921799 -0.1465828201 0.0000000  
 14-8 -0.06823750 -0.2284921799 0.0920171799 0.9871276  
 15-8 -0.31578750 -0.4760421799 -0.1555328201 0.0000000  
 16-8 -0.33012500 -0.4903796799 -0.1698703201 0.0000000  
 17-8 -0.30253750 -0.4627921799 -0.1422828201 0.0000000  
 10-9 -0.14871250 -0.3089671799 0.0115421799 0.1034757  
 11-9 0.06162500 -0.0986296799 0.2218796799 0.9956003  
 12-9 0.01197500 -0.1482796799 0.1722296799 1.0000000  
 13-9 -0.15663750 -0.3168921799 0.0036171799 0.0633854  
 14-9 0.08196250 -0.0782921799 0.2422171799 0.9319001  
 15-9 -0.16558750 -0.3258421799 -0.0053328201 0.0347300  
 16-9 -0.17992500 -0.3401796799 -0.0196703201 0.0120205  
 17-9 -0.15233750 -0.3125921799 0.0079171799 0.0831230  
 11-10 0.21033750 0.0500828201 0.3705921799 0.0008983  
 12-10 0.16068750 0.0004328201 0.3209421799 0.0485741  
 13-10 -0.00792500 -0.1681796799 0.1523296799 1.0000000  
 14-10 0.23067500 0.0704203201 0.3909296799 0.0001269  
 15-10 -0.01687500 -0.1771296799 0.1433796799 1.0000000  
 16-10 -0.03121250 -0.1914671799 0.1290421799 0.9999994  
 17-10 -0.00362500 -0.1638796799 0.1566296799 1.0000000  
 12-11 -0.04965000 -0.2099046799 0.1106046799 0.9996583  
 13-11 -0.21826250 -0.3785171799 -0.0580078201 0.0004272  
 14-11 0.02033750 -0.1399171799 0.1805921799 1.0000000  
 15-11 -0.22721250 -0.3874671799 -0.0669578201 0.0001791  
 16-11 -0.24155000 -0.4018046799 -0.0812953201 0.0000418  
 17-11 -0.21396250 -0.3742171799 -0.0537078201 0.0006414  
 13-12 -0.16861250 -0.3288671799 -0.0083578201 0.0280328

14-12	0.06998750	-0.0902671799	0.2302421799	0.9834481
15-12	-0.17756250	-0.3378171799	-0.0173078201	0.0144284
16-12	-0.19190000	-0.3521546799	-0.0316453201	0.0045597
17-12	-0.16431250	-0.3245671799	-0.0040578201	0.0379508
14-13	0.23860000	0.0783453201	0.3988546799	0.0000567
15-13	-0.00895000	-0.1692046799	0.1513046799	1.0000000
16-13	-0.02328750	-0.1835421799	0.1369671799	1.0000000
17-13	0.00430000	-0.1559546799	0.1645546799	1.0000000
15-14	-0.24755000	-0.4078046799	-0.0872953201	0.0000222
16-14	-0.26188750	-0.4221421799	-0.1016328201	0.0000047
17-14	-0.23430000	-0.3945546799	-0.0740453201	0.0000880
16-15	-0.01433750	-0.1745921799	0.1459171799	1.0000000
17-15	0.01325000	-0.1470046799	0.1735046799	1.0000000
17-16	0.02758750	-0.1326671799	0.1878421799	0.9999999

## 10. Appendix B- Bacterial Growth ANOVA Code

```
## Analysis of Bacterial Growth HT
```

```
## ANOVA and post hoc Tukey Test
```

```
## Biofilm Assay OD Values
```

```
# Dark Control HT
```

```
y1 = c(0.6863, 0.6246, 0.6287, 0.6342, 0.5361, 0.5936, 0.586, 0.5741, 0.5705, 0.5635,  
0.5616, 0.5576, 0.5361, 0.5936, 0.586, 0.5741, 0.5705, 0.5635, 0.5616, 0.5576, 0.4513, 0.4143,  
0.4354, 0.4504, 0.4442, 0.4381, 0.4346, 0.4531, 0.553, 0.5514, 0.5487, 0.5484, 0.519, 0.5107,  
0.5174, 0.5194, 0.6138, 0.6043, 0.5992, 0.5889, 0.6113, 0.5853, 0.5522, 0.5607, 0.549202273,  
0.061974678)
```

```
# Irradiated HT 24
```

```
y2 = c(0.7109, 0.6796, 0.6653, 0.6518)
```

```
# Irradiated Ht 3.6
```

```
y3 = c(0.7866, 0.7595, 0.7325, 0.7036, 0.6977, 0.6983, 0.6687, 0.6943)
```

```
# Irradiated HT 7.45
```

```
y4 = c(0.5700, 0.5739, 0.5673, 0.5698, 0.5600, 0.5494, 0.5525, 0.5562)
```

```
# Irradiated HT 33.6
```

$y5 = c(0.4789, 0.504, 0.4626, 0.4561, 0.4554, 0.4452, 0.4531, 0.4507)$

# Irradiated HT 56.64

$y6 = c(0.4645, 0.4331, 0.441, 0.4232, 0.4249, 0.4102, 0.4111, 0.398)$

# Irradiated HT 66.72

$y7 = c(0.421, 0.4003, 0.4088, 0.4247, 0.4236, 0.4086, 0.4153, 0.4176)$

# Dark Control TSB

$y8 = c(0.5615, 0.7293, 0.7609, 0.7011, 1.6185, 1.7116, 1.7376, 1.7653, 1.7703, 1.7904, 1.7649, 1.778, 1.6185, 1.7116, 1.7376, 1.7653, 1.7703, 1.7904, 1.7649, 1.778, 1.4484, 1.4755, 1.4631, 1.4567, 1.4754, 1.4667, 1.4989, 1.5075, 1.544, 1.5436, 1.5191, 1.6436, 1.6133, 1.633, 1.6058, 1.6292, 1.5512, 1.5531, 1.5534, 1.551, 1.5536, 1.552, 1.5518, 1.5706, 1.536056818)$

# Irradiated TSB 24

$y9 = c(1.761, 1.7885, 1.7801, 1.7799, 1.7716, 1.7775, 1.7698, 1.7533)$

# Irradiated TBS 86.4

$y10 = c(1.6657, 1.6736, 1.6698, 1.7077)$

# Irradiated TSB 7.45

$y_{11} = c(1.761, 1.7885, 1.7801, 1.7799, 1.7716, 1.7775, 1.7698, 1.7533)$

# Irradiated TSB 33.6

$y_{12} = c(1.6514, 1.6284, 1.6247, 1.6266, 1.6206, 1.6258, 1.6287, 1.626)$

# Irradiated TSB 56.64

$y_{13} = c(1.6438, 1.5317, 1.53, 1.5203, 1.5031, 1.5063, 1.5107, 1.484)$

# Irradiated TSB 66.78

$y_{14} = c(1.478, 1.4518, 1.4504, 1.4372, 1.4379, 1.4267, 1.437, 1.4212)$

# Irradiated M9 Dark Control

$y_{15} = c(0.5149, 0.6392, 0.6561, 0.6113, 0.6867, 0.6672, 0.6111, 0.635, 0.5149, 0.6392,$   
 $0.6561, 0.6113, 0.6867, 0.6672, 0.6111, 0.635, 0.3278, 0.3614, 0.4573, 0.4609, 0.4184, 0.4573,$   
 $0.4485, 0.5081, 0.4966, 0.5607, 0.6428, 0.6227, 0.6369, 0.6211, 0.6395, 0.7112, 0.714, 0.7083,$   
 $0.7058, 0.6654, 0.7039, 0.6738, 0.594352632)$

# Irradiated M9 24

$y_{16} = c(0.4015, 0.4757, 0.4927, 0.4721, 0.4987, 0.515, 0.4909, 0.4848)$

# Irradiated M9 7.45

$y_{17} = c(0.4015, 0.4757, 0.4927, 0.4721, 0.4987, 0.515, 0.4909, 0.4848)$



15, 15, 15, 15, 15, 16, 16, 16, 16, 16, 16, 16, 16, 17, 17, 17, 17, 17, 17, 17, 17, 18, 18, 18, 18, 18,  
18, 18, 18)

```
# ANOVA for Biofilm Assay Results
```

```
data = data.frame(y = y, group = factor(group))
```

```
fit <- aov(y ~ group, data)
```

```
anova(fit)
```

```
# Tukey Honestly Significant Differences
```

```
TukeyHSD(fit)
```

```
Fit: aov(formula = y ~ group, data = data)
```

```
$`group`
```

	diff	lwr	upr	p adj
2-1	-0.0450181818	-0.209147113	0.1191107494	0.9999850
3-1	-0.1724146934	-0.239808489	-0.1050208978	0.0000000
4-1	-0.1196181818	-0.283747113	0.0445107494	0.4986815
5-1	0.0300068182	-0.090788804	0.1508024408	0.9999969
6-1	-0.1300306818	-0.250826304	-0.0092350592	0.0202940
7-1	0.0706143182	0.001954260	0.1392743761	0.0361433

8-1 0.1063943182 -0.014401304 0.2271899408 0.1660809  
 9-1 -0.0438056818 -0.164601304 0.0769899408 0.9991104  
 10-1 -0.1925181818 -0.313313804 -0.0717225592 0.0000062  
 11-1 0.0178193182 -0.102976304 0.1386149408 1.0000000  
 12-1 -0.0318306818 -0.152626304 0.0889649408 0.9999920  
 13-1 -0.2004431818 -0.321238804 -0.0796475592 0.0000018  
 14-1 0.0381568182 -0.082638804 0.1589524408 0.9998727  
 15-1 -0.1418056818 -0.262601304 -0.0210100592 0.0056470  
 16-1 -0.1716931818 -0.292488804 -0.0508975592 0.0001272  
 17-1 -0.0242681818 -0.145063804 0.0965274408 0.9999999  
 18-1 -0.2093931818 -0.330188804 -0.0885975592 0.0000004  
 19-1 -0.2237306818 -0.344526304 -0.1029350592 0.0000000  
 20-1 -0.1961431818 -0.316938804 -0.0753475592 0.0000035  
 3-2 -0.1273965116 -0.291684406 0.0368913822 0.3765179  
 4-2 -0.0746000000 -0.296831623 0.1476316234 0.9996941  
 5-2 0.0750250000 -0.117433231 0.2674832314 0.9977059  
 6-2 -0.0850125000 -0.277470731 0.1074457314 0.9896713  
 7-2 0.1156325000 -0.049178883 0.2804438829 0.5734225  
 8-2 0.1514125000 -0.041045731 0.3438707314 0.3490595  
 9-2 0.0012125000 -0.191245731 0.1936707314 1.0000000  
 10-2 -0.1475000000 -0.339958231 0.0449582314 0.3992248  
 11-2 0.0628375000 -0.129620731 0.2552957314 0.9997942  
 12-2 0.0131875000 -0.179270731 0.2056457314 1.0000000



13-2 -0.1554250000 -0.347883231 0.0370332314 0.3011341  
 14-2 0.0831750000 -0.109283231 0.2756332314 0.9919556  
 15-2 -0.0967875000 -0.289245731 0.0956707314 0.9598474  
 16-2 -0.1266750000 -0.319133231 0.0657832314 0.6904388  
 17-2 0.0207500000 -0.171708231 0.2132082314 1.0000000  
 18-2 -0.1643750000 -0.356833231 0.0280832314 0.2091228  
 19-2 -0.1787125000 -0.371170731 0.0137457314 0.1060142  
 20-2 -0.1511250000 -0.343583231 0.0413332314 0.3526370  
 4-3 0.0527965116 -0.111491382 0.2170844055 0.9998363  
 5-3 0.2024215116 0.081409990 0.3234330337 0.0000014  
 6-3 0.0423840116 -0.078627510 0.1633955337 0.9994462  
 7-3 0.2430290116 0.173989823 0.3120682003 0.0000000  
 8-3 0.2788090116 0.157797490 0.3998205337 0.0000000  
 9-3 0.1286090116 0.007597490 0.2496205337 0.0240092  
 10-3 -0.0201034884 -0.141115010 0.1009080337 1.0000000  
 11-3 0.1902340116 0.069222490 0.3112455337 0.0000092  
 12-3 0.1405840116 0.019572490 0.2615955337 0.0066756  
 13-3 -0.0280284884 -0.149040010 0.0929830337 0.9999990  
 14-3 0.2105715116 0.089559990 0.3315830337 0.0000004  
 15-3 0.0306090116 -0.090402510 0.1516205337 0.9999959  
 16-3 0.0007215116 -0.120290010 0.1217330337 1.0000000  
 17-3 0.1481465116 0.027134990 0.2691580337 0.0027723  
 18-3 -0.0369784884 -0.157990010 0.0840330337 0.9999220

19-3 -0.0513159884 -0.172327510 0.0696955337 0.9935535  
 20-3 -0.0237284884 -0.144740010 0.0972830337 0.9999999  
 5-4 0.1496250000 -0.042833231 0.3420832314 0.3715914  
 6-4 -0.0104125000 -0.202870731 0.1820457314 1.0000000  
 7-4 0.1902325000 0.025421117 0.3550438829 0.0073917  
 8-4 0.2260125000 0.033554269 0.4184707314 0.0056147  
 9-4 0.0758125000 -0.116645731 0.2682707314 0.9973811  
 10-4 -0.0729000000 -0.265358231 0.1195582314 0.9984158  
 11-4 0.1374375000 -0.055020731 0.3298957314 0.5389502  
 12-4 0.0877875000 -0.104670731 0.2802457314 0.9852446  
 13-4 -0.0808250000 -0.273283231 0.1116332314 0.9942543  
 14-4 0.1577750000 -0.034683231 0.3502332314 0.2749141  
 15-4 -0.0221875000 -0.214645731 0.1702707314 1.0000000  
 16-4 -0.0520750000 -0.244533231 0.1403832314 0.9999879  
 17-4 0.0953500000 -0.097108231 0.2878082314 0.9652704  
 18-4 -0.0897750000 -0.282233231 0.1026832314 0.9812265  
 19-4 -0.1041125000 -0.296570731 0.0883457314 0.9221826  
 20-4 -0.0765250000 -0.268983231 0.1159332314 0.9970542  
 6-5 -0.1600375000 -0.317178988 -0.0028960121 0.0405870  
 7-5 0.0406075000 -0.081113773 0.1623287731 0.9997198  
 8-5 0.0763875000 -0.080753988 0.2335289879 0.9712433  
 9-5 -0.0738125000 -0.230953988 0.0833289879 0.9797951  
 10-5 -0.2225250000 -0.379666488 -0.0653835121 0.0001389

11-5 -0.0121875000 -0.169328988 0.1449539879 1.00000000  
 12-5 -0.0618375000 -0.218978988 0.0953039879 0.9974147  
 13-5 -0.2304500000 -0.387591488 -0.0733085121 0.0000592  
 14-5 0.0081500000 -0.148991488 0.1652914879 1.00000000  
 15-5 -0.1718125000 -0.328953988 -0.0146710121 0.0164179  
 16-5 -0.2017000000 -0.358841488 -0.0445585121 0.0011497  
 17-5 -0.0542750000 -0.211416488 0.1028664879 0.9995436  
 18-5 -0.2394000000 -0.396541488 -0.0822585121 0.0000219  
 19-5 -0.2537375000 -0.410878988 -0.0965960121 0.0000042  
 20-5 -0.2261500000 -0.383291488 -0.0690085121 0.0000943  
 7-6 0.2006450000 0.078923727 0.3223662731 0.0000022  
 8-6 0.2364250000 0.079283512 0.3935664879 0.0000306  
 9-6 0.0862250000 -0.070916488 0.2433664879 0.9122687  
 10-6 -0.0624875000 -0.219628988 0.0946539879 0.9970512  
 11-6 0.1478500000 -0.009291488 0.3049914879 0.0937749  
 12-6 0.0982000000 -0.058941488 0.2553414879 0.7723077  
 13-6 -0.0704125000 -0.227553988 0.0867289879 0.9878737  
 14-6 0.1681875000 0.011046012 0.3253289879 0.0218987  
 15-6 -0.0117750000 -0.168916488 0.1453664879 1.00000000  
 16-6 -0.0416625000 -0.198803988 0.1154789879 0.9999912  
 17-6 0.1057625000 -0.051378988 0.2629039879 0.6512756  
 18-6 -0.0793625000 -0.236503988 0.0777789879 0.9581858  
 19-6 -0.0937000000 -0.250841488 0.0634414879 0.8336512

20-6 -0.0661125000 -0.223253988 0.0910289879 0.9941296  
 8-7 0.0357800000 -0.085941273 0.1575012731 0.9999565  
 9-7 -0.1144200000 -0.236141273 0.0073012731 0.0945875  
 10-7 -0.2631325000 -0.384853773 -0.1414112269 0.0000000  
 11-7 -0.0527950000 -0.174516273 0.0689262731 0.9916126  
 12-7 -0.1024450000 -0.224166273 0.0192762731 0.2316354  
 13-7 -0.2710575000 -0.392778773 -0.1493362269 0.0000000  
 14-7 -0.0324575000 -0.154178773 0.0892637731 0.9999904  
 15-7 -0.2124200000 -0.334141273 -0.0906987269 0.0000003  
 16-7 -0.2423075000 -0.364028773 -0.1205862269 0.0000000  
 17-7 -0.0948825000 -0.216603773 0.0268387731 0.3665234  
 18-7 -0.2800075000 -0.401728773 -0.1582862269 0.0000000  
 19-7 -0.2943450000 -0.416066273 -0.1726237269 0.0000000  
 20-7 -0.2667575000 -0.388478773 -0.1450362269 0.0000000  
 9-8 -0.1502000000 -0.307341488 0.0069414879 0.0804661  
 10-8 -0.2989125000 -0.456053988 -0.1417710121 0.0000000  
 11-8 -0.0885750000 -0.245716488 0.0685664879 0.8908484  
 12-8 -0.1382250000 -0.295366488 0.0189164879 0.1678015  
 13-8 -0.3068375000 -0.463978988 -0.1496960121 0.0000000  
 14-8 -0.0682375000 -0.225378988 0.0889039879 0.9914993  
 15-8 -0.2482000000 -0.405341488 -0.0910585121 0.0000080  
 16-8 -0.2780875000 -0.435228988 -0.1209460121 0.0000002  
 17-8 -0.1306625000 -0.287803988 0.0264789879 0.2511317

18-8 -0.3157875000 -0.472928988 -0.1586460121 0.0000000  
 19-8 -0.3301250000 -0.487266488 -0.1729835121 0.0000000  
 20-8 -0.3025375000 -0.459678988 -0.1453960121 0.0000000  
 10-9 -0.1487125000 -0.305853988 0.0084289879 0.0886951  
 11-9 0.0616250000 -0.095516488 0.2187664879 0.9975249  
 12-9 0.0119750000 -0.145166488 0.1691164879 1.0000000  
 13-9 -0.1566375000 -0.313778988 0.0005039879 0.0518175  
 14-9 0.0819625000 -0.075178988 0.2391039879 0.9435626  
 15-9 -0.0980000000 -0.255141488 0.0591414879 0.7752326  
 16-9 -0.1278875000 -0.285028988 0.0292539879 0.2875169  
 17-9 0.0195375000 -0.137603988 0.1766789879 1.0000000  
 18-9 -0.1655875000 -0.322728988 -0.0084460121 0.0267881  
 19-9 -0.1799250000 -0.337066488 -0.0227835121 0.0083737  
 20-9 -0.1523375000 -0.309478988 0.0048039879 0.0697583  
 11-10 0.2103375000 0.053196012 0.3674789879 0.0004900  
 12-10 0.1606875000 0.003546012 0.3178289879 0.0387003  
 13-10 -0.0079250000 -0.165066488 0.1492164879 1.0000000  
 14-10 0.2306750000 0.073533512 0.3878164879 0.0000578  
 15-10 0.0507125000 -0.106428988 0.2078539879 0.9998260  
 16-10 0.0208250000 -0.136316488 0.1779664879 1.0000000  
 17-10 0.1682500000 0.011108512 0.3253914879 0.0217917  
 18-10 -0.0168750000 -0.174016488 0.1402664879 1.0000000  
 19-10 -0.0312125000 -0.188353988 0.1259289879 0.9999999

20-10 -0.0036250000 -0.160766488 0.1535164879 1.00000000  
 12-11 -0.0496500000 -0.206791488 0.1074914879 0.9998722  
 13-11 -0.2182625000 -0.375403988 -0.0611210121 0.0002175  
 14-11 0.0203375000 -0.136803988 0.1774789879 1.00000000  
 15-11 -0.1596250000 -0.316766488 -0.0024835121 0.0418256  
 16-11 -0.1895125000 -0.346653988 -0.0323710121 0.0036017  
 17-11 -0.0420875000 -0.199228988 0.1150539879 0.9999897  
 18-11 -0.2272125000 -0.384353988 -0.0700710121 0.0000841  
 19-11 -0.2415500000 -0.398691488 -0.0844085121 0.0000172  
 20-11 -0.2139625000 -0.371103988 -0.0568210121 0.0003391  
 13-12 -0.1686125000 -0.325753988 -0.0114710121 0.0211804  
 14-12 0.0699875000 -0.087153988 0.2271289879 0.9886663  
 15-12 -0.1099750000 -0.267116488 0.0471664879 0.5782637  
 16-12 -0.1398625000 -0.297003988 0.0172789879 0.1527902  
 17-12 0.0075625000 -0.149578988 0.1647039879 1.00000000  
 18-12 -0.1775625000 -0.334703988 -0.0204210121 0.0102281  
 19-12 -0.1919000000 -0.349041488 -0.0347585121 0.0028969  
 20-12 -0.1643125000 -0.321453988 -0.0071710121 0.0295239  
 14-13 0.2386000000 0.081458512 0.3957414879 0.0000240  
 15-13 0.0586375000 -0.098503988 0.2157789879 0.9986983  
 16-13 0.0287500000 -0.128391488 0.1858914879 1.00000000  
 17-13 0.1761750000 0.019033512 0.3333164879 0.0114859  
 18-13 -0.0089500000 -0.166091488 0.1481914879 1.00000000

19-13 -0.0232875000 -0.180428988 0.1338539879 1.00000000  
 20-13 0.0043000000 -0.152841488 0.1614414879 1.00000000  
 15-14 -0.1799625000 -0.337103988 -0.0228210121 0.0083470  
 16-14 -0.2098500000 -0.366991488 -0.0527085121 0.0005146  
 17-14 -0.0624250000 -0.219566488 0.0947164879 0.9970880  
 18-14 -0.2475500000 -0.404691488 -0.0904085121 0.0000086  
 19-14 -0.2618875000 -0.419028988 -0.1047460121 0.0000016  
 20-14 -0.2343000000 -0.391441488 -0.0771585121 0.0000387  
 16-15 -0.0298875000 -0.187028988 0.1272539879 1.00000000  
 17-15 0.1175375000 -0.039603988 0.2746789879 0.4471070  
 18-15 -0.0675875000 -0.224728988 0.0895539879 0.9923905  
 19-15 -0.0819250000 -0.239066488 0.0752164879 0.9437965  
 20-15 -0.0543375000 -0.211478988 0.1028039879 0.9995362  
 17-16 0.1474250000 -0.009716488 0.3045664879 0.0963639  
 18-16 -0.0377000000 -0.194841488 0.1194414879 0.9999983  
 19-16 -0.0520375000 -0.209178988 0.1051039879 0.9997479  
 20-16 -0.0244500000 -0.181591488 0.1326914879 1.00000000  
 18-17 -0.1851250000 -0.342266488 -0.0279835121 0.0053320  
 19-17 -0.1994625000 -0.356603988 -0.0423210121 0.0014258  
 20-17 -0.1718750000 -0.329016488 -0.0147335121 0.0163354  
 19-18 -0.0143375000 -0.171478988 0.1428039879 1.00000000  
 20-18 0.0132500000 -0.143891488 0.1703914879 1.00000000  
 20-19 0.0275875000 -0.129553988 0.1847289879 1.00000000

## 11. Appendix C- Swim Plate ANOVA Code

```
## Analysis swimming motility
```

```
## ANOVA and post hoc Tukey Test
```

```
## Swimming Motility Tests
```

```
# Dark Control Swim
```

```
y1 = c(0.547, 0.55, 0.691, 0.547, 0.55, 0.984, 0.691, 0.465, 0.641, 0.547, 0.55, 0.672,  
0.847, 0.672, 0.672, 0.847, 1.395, 1.504)
```

```
# Irradiated 11.232
```

```
y2 = c(0.177, 0.213, 0.113)
```

```
# Irradiated 203.904
```

```
y3 = c(0.014, 0.013, 0.018, 0.012)
```

```
# Irradiated 26.82
```

```
y4 = c(0.192, 0.058, 0.115, 0.043)
```

```
# Irradiated 86
```

```
y5 = c(0.015, 0.029, 0.043)
```



```
# PDA
```

```
# Combine all observations for all samples into one vector
```

```
y = c(y1, y2, y3, y4, y5)
```

```
# Assign a group to each observation
```

```
group = c(1, 1, 1, 1, 1, 1, 1, 1, 1, 1, 1, 1, 1, 1, 1, 1, 1, 1, 2, 2, 2, 3, 3, 3, 3, 4, 4, 4, 4, 5, 5,
```

5)

```
# ANOVA for Contact Angle Measurements
```

```
data = data.frame(y = y, group = factor(group))
```

```
fit <- aov(y ~ group, data)
```

```
anova(fit)
```

```
# Tukey Honestly Significant Differences
```

```
TukeyHSD(fit)
```

```
# Results for Contact Angle
```

```
# Fit: aov(formula = y ~ group, data = data)
```

```
$`group`
```

```
diff    lwr    upr    p adj
```

2-1 -0.57522222 -0.9956120 -0.1548324 0.0037619

3-1 -0.72863889 -1.1012746 -0.3560031 0.0000420

4-1 -0.64088889 -1.0135246 -0.2682531 0.0002579

5-1 -0.71388889 -1.1342787 -0.2934991 0.0003049

## 12. Appendix D- Swarm Plate ANOVA Code

```
## Analysis of Solar MD Data
```

```
## ANOVA and post hoc Tukey Test
```

```
## swarm plate
```

```
# Control
```

```
y1 = c(0.35, 0.828, 0.263, 0.55, 0.547, 0.55, 0.984, 0.691, 0.117, 0.132, 0.195, 0.298,  
0.276, 0.199, 0.121, 0.117, 0.173, 0.205, 0.353)
```

```
# 22.464
```

```
y2 = c(0.044, 0.026)
```

```
# 407.808
```

```
y3 = c(0.013, 0.01, 0.023, 0.019)
```

```
# 53.64
```

```
y4 = c(0.029, 0.043, 0.03, 0.026)
```

```
# 172.8
```

```
y5 = c(0.013, 0.011, 0.024, 0.019)
```

```
# PDA
```

```
# Combine all observations for all samples into one vector
```

```
y = c(y1, y2, y3, y4, y5)
```

```
# Assign a group to each observation
```

```
group = c(1, 1, 1, 1, 1, 1, 1, 1, 1, 1, 1, 1, 1, 1, 1, 1, 1, 1, 1, 1, 2, 2, 3, 3, 3, 3, 4, 4, 4, 4, 5, 5, 5,
```

5)

```
# ANOVA for Contact Angle Measurements
```

```
data = data.frame(y = y, group = factor(group))
```

```
fit <- aov(y ~ group, data)
```

```
anova(fit)
```

```
# Tukey Honestly Significant Differences
```

```
TukeyHSD(fit)
```

```
# Results for Contact Angle
```

```
# Fit: aov(formula = y ~ group, data = data)
```

```
# $group
```

```
# diff      lwr      upr    p adj
```

2-1 -0.3307368 -0.7762735 0.114799865 0.2231092  
3-1 -0.3494868 -0.6791897 -0.019783945 0.0336592  
4-1 -0.3337368 -0.6634397 -0.004033945 0.0461793  
5-1 -0.3489868 -0.6786897 -0.019283945 0.0340035  
3-2 -0.0187500 -0.5377846 0.500284557 0.9999704  
4-2 -0.0030000 -0.5220346 0.516034557 1.0000000  
5-2 -0.0182500 -0.5372846 0.500784557 0.9999734  
4-3 0.0157500 -0.4080399 0.439539941 0.9999668  
5-3 0.0005000 -0.4232899 0.424289941 1.0000000  
5-4 -0.0152500 -0.4390399 0.408539941 0.9999708

## 13. Appendix E- Average and Standard Deviation Used for Normalization

### 13.1. E.1- Bacterial Growth

**Table I: Averages and standard deviations for bacterial growth normalization.**

Medium Type	Applied Dose (mJcm <sup>-2</sup> )	Average	Standard Deviation
HT	12.96	0.568	0.018
	26.82	0.568	0.018
	86.40	0.643	0.029
	120.96	0.574	0.013
	203.90	0.534	0.018
	240.41	0.589	0.023
TSB	12.96	1.742	0.056
	26.82	1.742	0.056
	86.40	1.640	0.037
	120.96	1.628	0.022
	203.90	1.591	0.048
	240.41	1.555	0.007
M9	12.96	0.628	0.053
	26.82	0.628	0.053
	120.96	0.489	0.031
	203.90	0.597	0.057
	240.41	0.690	0.027

### 13.2. E.2- Biofilm Growth

**Table II: Averages and standard deviations for biofilm growth normalization.**

Medium Type	Applied Dose (mJcm <sup>-2</sup> )	Average	Standard Deviation
HT	12.96	0.287	0.082
	26.82	0.309	0.048
	86.40	0.317	0.050
	120.96	0.036	0.075
	203.90	0.253	0.044
	240.41	0.146	0.047
TSB	12.96	0.000	0.038
	26.82	0.092	0.055
	86.40	0.111	0.020
	120.96	0.465	0.010
	203.90	0.089	0.020
	240.41	0.059	0.011
M9	12.96	0.278	0.067
	26.82	0.301	0.022
	86.40	0.186	0.041
	120.96	0.524	0.181
	203.90	0.283	0.141
	240.41	0.160	0.094

### 13.3. E.3-Swimming Motility

**Table III: Averages and standard deviations for swimming motility normalization.**

Applied Dose (mJcm <sup>-2</sup> )	Average	Standard Deviation
12.96	0.596	0.082
26.82	0.730	0.101
86.40	1.105	0.407
203.90	0.551	0.072

### 13.4. E.4-Swarming Motility

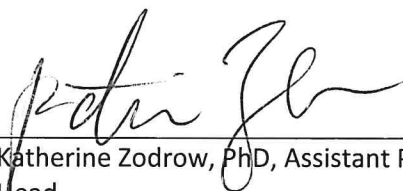
Table IV: Averages and standard deviations for swarming motility normalization.

Applied Dose (mJcm <sup>-2</sup> )	Average	Standard Deviation
25.92	0.596	0.251
53.64	0.730	0.065
172.80	1.105	0.078
407.81	0.551	0.082



## SIGNATURE PAGE

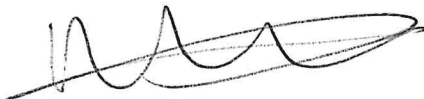
This is to certify that the thesis prepared by Student Name entitled "Utilization of Continuous, Sub-Lethal Ultraviolet Irradiation for Biofilm Prevention" has been examined and approved for acceptance by the Department of Environmental Engineering, Montana Technological University, on this 14th day of December, 2018.



---

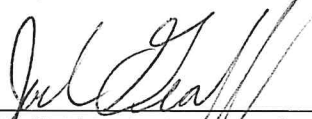
Katherine Zodrow, PhD, Assistant Professor and Interim Department Head

Department of Environmental Engineering  
Chair, Examination Committee



---

Daqian Jiang, PhD, Assistant Professor  
Department of Environmental Engineering  
Member, Examination Committee



---

Joel Graff, PhD, Assistant Professor  
Department of Biological Sciences  
Member, Examination Committee



---

Akua Oppong-Anane, PhD, Assistant Professor  
Department of Freshman Engineering  
Member, Examination Committee